

AFWAL-TR-84-3062

62



AD-A176 292

**NONLINEAR FLYING QUALITIES
CRITERIA FOR LARGE-AMPLITUDE MANEUVERS**

**F.J. SERNA
A.R. MITCHELL**

THE ANALYTIC SCIENCES CORPORATION
One Jacob Way
Reading, Massachusetts 01867

DECEMBER 1984

**FINAL REPORT FOR PERIOD:
JULY 1982—MARCH 1984**

SELECTED
FEB 3 1987
A

APPROVED FOR PUBLIC RELEASE; DISTRIBUTION UNLIMITED

DTIC FILE COPY

**FLIGHT DYNAMICS LABORATORY
AIR FORCE WRIGHT AERONAUTICAL LABORATORIES
AIR FORCE SYSTEMS COMMAND
WRIGHT-PATTERSON AIR FORCE BASE, OHIO 45433**

87

2

2

086

NOTICE

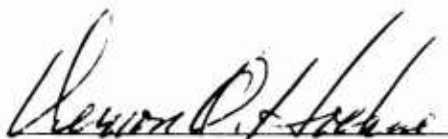
When Government drawings, specifications, or other data are used for any purpose other than in connection with a definitely related Government procurement operation, the United States Government thereby incurs no responsibility nor any obligation whatsoever; and the fact that the government may have formulated, furnished, or in any way supplied the said drawings, specification, or other data, is not to be regarded by implication or otherwise as in any manner licensing the holder or any other person or corporation, or conveying any rights or permission to manufacture use, or sell any patent invention that may in any way be related thereto.

This report has been reviewed by the Office of Public Affairs (ASD/PA) and is releasable to the National Technical Information Service (NTIS). At NTIS, it will be available to the general public, including foreign nations.

This technical report has been reviewed and is approved for publication.



Charles F. Suchomel
Project Engineer
Control Dynamics Branch



Vernon O. Hoehne, Chief
Controls Dynamics Branch
Flight Control Division

FOR THE COMMANDER



Frank A. Scarpino, Chief
Flight Control Division
Flight Dynamics Laboratories

If your address has changed, if you wish to be removed from our mailing list, or if the addressee is no longer employed by your organization please notify AFWAL/FIGC, W-PAFB, OH 45433-6553 to help us maintain a current mailing list.

Copies of this report should not be returned unless return is required by security considerations, contractual obligations, or notice on a specific document.

UNCLASSIFIED

SECURITY CLASSIFICATION OF THIS PAGE

REPORT DOCUMENTATION PAGE

1a. REPORT SECURITY CLASSIFICATION Unclassified			1b. RESTRICTIVE MARKINGS	
2a. SECURITY CLASSIFICATION AUTHORITY			3. DISTRIBUTION/AVAILABILITY OF REPORT Approved for Public Release; Distribution Unlimited	
2b. DECLASSIFICATION/DOWNGRADING SCHEDULE				
4. PERFORMING ORGANIZATION REPORT NUMBER(S)			5. MONITORING ORGANIZATION REPORT NUMBER(S) AFWAL-TR-84-3062	
6a. NAME OF PERFORMING ORGANIZATION The Analytic Sciences Corp		6b. OFFICE SYMBOL (If applicable)	7a. NAME OF MONITORING ORGANIZATION Air Force Wright Aeronautical Laboratories Flight Dynamics Laboratory, AFWAL/FIGC	
6c. ADDRESS (City, State and ZIP Code) One Jacob Way Reading MA 01867			7b. ADDRESS (City, State and ZIP Code) Air Force Systems Command Wright Patterson AFB OH 45433-6553	
8a. NAME OF FUNDING/SPONSORING ORGANIZATION		8b. OFFICE SYMBOL (If applicable) AFWAL/FIGC	9. PROCUREMENT INSTRUMENT IDENTIFICATION NUMBER F33615-82-C-3606	
8c. ADDRESS (City, State and ZIP Code)			10. SOURCE OF FUNDING NOS.	
			PROGRAM ELEMENT NO.	PROJECT NO.
			61102F	2307
11. TITLE (Include Security Classification) Nonlinear Flying Qualities for Large-Amplitude Maneuvers (U)			TASK NO.	WORK UNIT NO.
			K1	03
12. PERSONAL AUTHOR(S) Frank J. Serra and Alan R. Mitchell				
13a. TYPE OF REPORT Final		13b. TIME COVERED FROM Jul 82 TO Mar 84	14. DATE OF REPORT (Yr, Mo., Day) 1984 December	
15. PAGE COUNT 193				
16. SUPPLEMENTARY NOTATION				
<p style="text-align: right;">Approved</p>				
17. COSATI CODES			18. SUBJECT TERMS (Continue on reverse if necessary and identify by block number)	
FIELD	GROUP	SUB. GR.		
01	03		Flying Qualities; Handling Qualities	
23	01		Fighter Aircraft; Nonlinear System Theory	
			Combat Maneuvers; Equivalent Systems	
19. ABSTRACT (Continue on reverse if necessary and identify by block number)				
<p>→ The Nonlinear Flying Qualities (NFQ) for Large-Amplitude Maneuvers Program examined promising techniques from nonlinear analysis and nonlinear system theory which are pertinent to the formation of a nonlinear flying qualities methodology. This report surveys nonlinear system theory and describes the development of an applied flying qualities methodology based on a canonical system theory and using research in relative controllability/observability. The applied flying qualities formulation is implemented in a numerical procedure and coupled with a six degree-of-freedom simulation to yield a flying qualities criteria of a multivariable time-varying representation of the aircraft dynamics. Results for representative classes of canonical systems for aircraft in both steady flight and large-amplitude maneuvers are presented. The relationship with current flying qualities formulations is also discussed. <i>Keywords: Flight dynamics</i></p>				
20. DISTRIBUTION/AVAILABILITY OF ABSTRACT UNCLASSIFIED/UNLIMITED <input type="checkbox"/> SAME AS RPT <input checked="" type="checkbox"/> DTIC USERS <input type="checkbox"/>			21. ABSTRACT SECURITY CLASSIFICATION Unclassified	
22a. NAME OF RESPONSIBLE INDIVIDUAL CHARLES F. SUCHOMEL			22b. TELEPHONE NUMBER (Include Area Code) (513) 255-8496	22c. OFFICE SYMBOL AFWAL/FIGC

TABLE OF CONTENTS

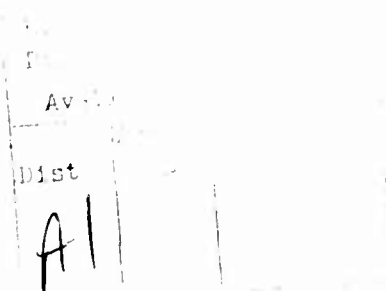
	<u>Page</u>
1. INTRODUCTION	1
1.1 Background	1
1.2 Program Overview	3
1.3 Summary of Results	5
1.3.1 Literature Search	5
1.3.2 NFQ Formulation	6
1.3.3 NFQ Test and Evaluation	9
1.4 Recommendations	11
1.5 Report Organization	12
2. CANONICAL SYSTEM THEORY AND RELATIVE CONTROLLABILITY FOR FLYING QUALITIES ANALYSIS	13
2.1 Canonical System Theory	13
2.1.1 Canonical System Theory: Definition	16
2.1.2 Second-Order Canonical System Example	18
2.1.3 Canonical Systems and Trajectory Equivalence	26
2.2 Relative Controllability	31
2.3 NFQ Analysis Formulation	33
2.3.1 Step One: Selecting a Canonical System Structure	34
2.3.2 Step Two: Correlating the Intrinsic and Extrinsic Flying Qualities Criteria	36
2.3.3 Step Three: Computing the Canonical System Match and the Relative Controllability Measure	37
3. NONLINEAR FLYING QUALITIES NUMERICAL RESULTS AND EVALUATION	39
3.1 Nonlinear Flying Qualities Analysis Process	39
3.2 Canonical System Candidates	42
3.2.1 Class I: Upper Triangular	42
3.2.2 Classes II and III: Decoupled, Two Block Longitudinal-Lateral	45
3.2.3 Class IV: Four Block Diagonal, Longitudinal-Lateral	48
3.2.4 Class V: Fully Diagonal	51

TABLE OF CONTENTS (Concluded)

	<u>Page</u>
3.3 Numerical Results	55
3.3.1 Sample Maneuver Description	56
3.3.2 Maneuver I Canonical System Analysis	62
3.3.3 Maneuver II Canonical System Analysis	71
3.4 Concluding Remarks	75
4. REVIEW OF RELEVANT TECHNIQUES IN NONLINEAR SYSTEM THEORY	79
4.1 Overview of Nonlinear Systems Theory	79
4.1.1 Categorization of Nonlinear System Theory	80
4.1.2 Classes of Nonlinear Systems	81
4.2 Nonlinear Reachability, Observability, and Realization	90
4.2.1 Nonlinear Reachability/Controllability	91
4.2.2 Nonlinear Observability/Reconstructability	98
4.3 Relative (Robustness of) Controllability for Nonlinear Systems	98
4.3.1 Theorem Statement	99
4.3.2 Outline of Proof	104
4.3.3 Computation of the Relative Controllability Index	107
5. CONCLUSIONS AND RECOMMENDATIONS	113
5.1 Summary	113
5.2 Conclusions	114
5.3 Recommendations	116
APPENDICES:	
A AFTI/F-16 Six-Degree-of-Freedom Simulation Overview	118
B Canonical System Evaluator (CASE) Software	153
C Review of Underlying Mathematical Concepts	171
REFERENCES	185
GLOSSARY	192

LIST OF ILLUSTRATIONS

<u>Figure</u>		<u>Page</u>
1.2-1	Large Amplitude AFTI-16 Maneuvers	4
2.1-1	Second-Order Example: Response to Initial Conditions	23
2.3-1	Linear, Piecewise-Time-Invariant Description of the Aircraft Dynamics	38
3.1-1	Canonical System Analysis Process	40
3.2-1	Canonical System Block Diagram: Classes II and III	47
3.2-2	Canonical System Block Diagram: Class IV	50
3.2-3	Canonical System Block Diagram: Class V	54
3.3-1	Maneuver I: Wind-Up Turn (First 20 Seconds)	57
3.3-2	Maneuver II: Rolling Reversal	63
3.3-3	Maneuver I: Class III Canonical System Analysis	68
3.3-4	Maneuver I: Class IV Canonical System Analysis	69
3.3-5	Maneuver II: Class III Canonical System Analysis	72
3.3-6	Maneuver II: Class IV Canonical System Analysis	73
4.1-1	Nonlinear System Theory Overview	82
4.1-2	Bilinear System Block Diagram	87



1.

INTRODUCTION

1.1 BACKGROUND

Flying qualities requirements for military aircraft are currently specified in MIL-F-8785C, "Military Specification - Flying Qualities of Piloted Airplanes." The principal tenet of MIL-F-8785C is that the dynamics of the overall aircraft system -- as perceived by the pilot during controlled flight -- can be described and evaluated in terms of simplified dynamic models. The specification does not discuss the principles of aircraft design nor does it describe how the designer ensures that the specification be met. Conventional aircraft typically have simple dynamic descriptions which match those used in MIL-F-8785C. However, the advent of highly-augmented and control-configured aircraft have brought a dramatic change in the potential complexity required of a full dynamic description.

Highly-augmented and control-configured aircraft differ from conventional aircraft in the number (order) of dynamic modes that are present. Highly-augmented aircraft introduce pre-filters and flexible mode filters which add modes to the closed loop response. Verification that an aircraft complies with the requirements on dynamics is performed principally through equivalent system matching (exceptions are the time-domain roll-sideslip coupling and roll performance requirements on the actual response of the aircraft). The equivalent systems methodology produces an equivalent of the augmented aircraft dynamics by matching the actual high-order system to a low-order system like those in the specification. Flying

qualities are then evaluated in terms of this equivalent low-order system.

A serious restriction of the methodology used in MIL-F-8785C is that only motions about steady-trimmed flight, based on linear equations of motion, can be considered. The low-order systems in the specification are only valid for perturbations about equilibrium flight of that aircraft. Large-amplitude combat maneuvers can not be adequately specified because of an inadequate dynamic representation of the aircraft in such maneuvers; the nonlinear, time-varying character of the full aircraft equations of motion causes these difficulties.

Another restriction of MIL-F-8785C is that only single-input/single-output dynamics are described, such as longitudinal control stick force relative to normal acceleration. However, in many critical situations of flight the pilot is commanding multiple inputs and the aircraft is responding with multiple outputs in its natural dynamics of translation and rotation.

This program researched innovative methods for analytically assessing the flying qualities of aircraft under any controllable maneuver. The research was in response to the two principal limitations of MIL-F-8785C noted above. The research effort pursued those results in nonlinear system theory and analysis that would accommodate the full nonlinear six-degree-of-freedom equations of motion and could lead to a flying qualities formulation for the overall multivariable aircraft system in any maneuver. As is outlined in the remainder of this chapter and detailed in this final technical report, the Nonlinear Flying Qualities (NFQ) research effort led to two main results:

- A technique analogous to the equivalent systems methodology (herein called canonical systems theory) which overcomes two major limitations of equivalent systems: the restrictions of single-input, single-output and of time-invariance
- A generic criterion for characterizing aircraft dynamic behavior in any maneuver through the use of a nonlinear relative controllability theorem.

Together, the two results are combined into a methodology that can provide the basis of a new flying qualities specification for aircraft performance in unsteady large amplitude maneuvers, with respect to multiple-input, multiple-output time-varying dynamic models.

1.2 PROGRAM OVERVIEW

The research goal was to extend the current flying qualities formulation of MIL-F-8785C to:

- Include unsteady, large-amplitude flight maneuvers (e.g., air combat maneuver profiles)
- Include multiple-input, multiple-output dynamics (e.g., simultaneous pitch and roll pilot inputs to the vehicle normal acceleration and roll response)
- Include the current flying qualities formulation as a special case
- Obtain a practical, numerically computable formulation.

Once a preferred formulation was found, the NFQ program tested the research product in a simulation of a highly

augmented, control-configured fighter/attack aircraft; a non-linear, six-degree-of-freedom (6-DOF) aeropropulsive model of the AFTI-16 aircraft was provided by the Flight Dynamics Laboratory for the applications test and evaluation. Figure 1.2-1 illustrates AFTI-16 maneuvers which are typical of those used in the 6-DOF simulation analysis.

The research objectives emphasize the development of an applied flying qualities formulation which would provide numerical results that encompass, as a limiting case, the current formulation of MIL-F-8785C. Hence, computability and compatibility with MIL-F-8785C were driving factors in both the literature search and the formulation tasks.

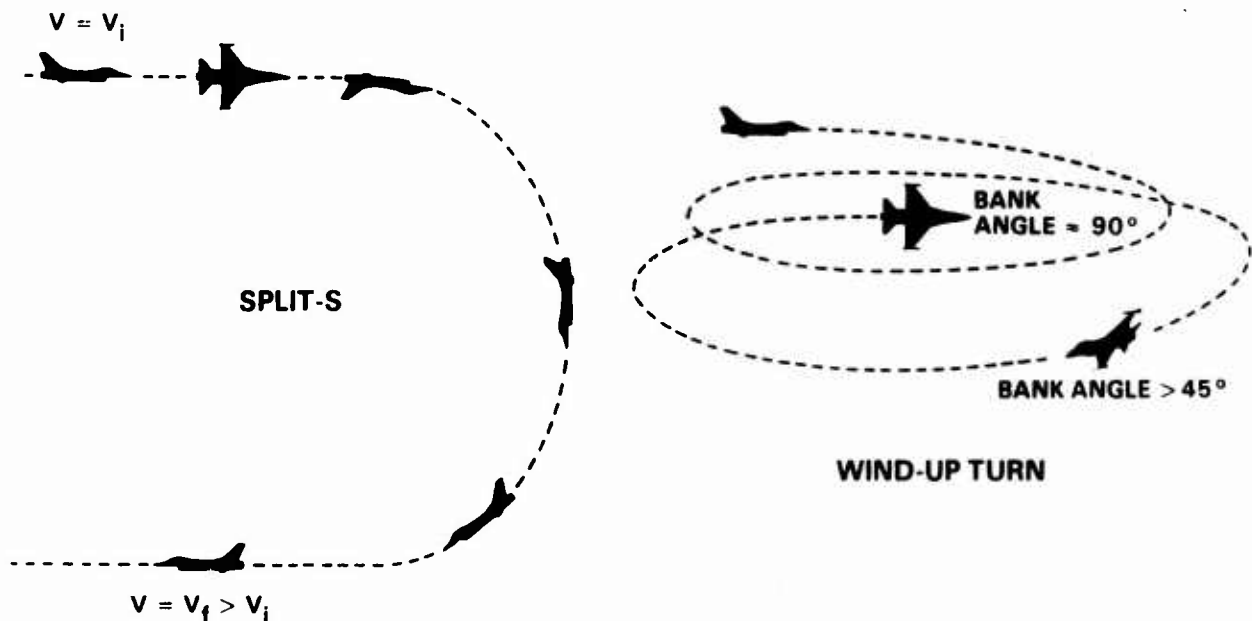


Figure 1.2-1 Large Amplitude AFTI-16 Maneuvers

1.3 SUMMARY OF RESULTS

This section provides a summary of results in terms of each of the three NFQ program objectives: literature search, formulation and evaluation.*

1.3.1 Literature Search

A review of the literature in nonlinear system theory focused on three general areas:

- Local Theory (i.e., linearized systems)
- Global Theory (i.e., differential geometry and topology)
- Functional Analysis (e.g., Volterra series).

In general, global theory was found to ask different questions than posed by NFQ. Global theory does not investigate the fine quantitative structure of stability and control, but instead searches for large-scale descriptions of dynamic behavior (e.g., the number and character of bifurcations). Mathematically speaking, global theory is invariant under the action of diffeomorphisms[†] on the state space or the control space. In other words a restructuring of the aircraft modes, e.g., exchanging the lateral and longitudinal modes, would produce the same global results but would certainly not meet with pilot approval.

*Definitions of the mathematical terms that will be introduced can be found in a glossary at the end of this report and in Appendix C.

†Differentiable functions from a space into itself, with a differentiable left and right inverse. See Ref. 42 for a comprehensive definition.

Functional analysis techniques, such as Volterra series expansions, were found to be computationally immature. However, such techniques are very promising from a purely theoretical point-of-view. Therefore, many functional analysis techniques merit further basic research to develop practical computational methods. Additional detail on the literature research in global theory and functional analysis is contained in Chapter 4.

As a result of the above findings, the NFQ research program focused on local (linearized) theory. (Nevertheless, as reported in Chapter 2, local theory does include somewhat specialized nonlinear analysis results.) Only the local theory was found to offer a mathematical basis which today is mature enough to be consistent with the latter two requirements listed in Section 1.2: inclusion of the current flying qualities formulation and computability.

1.3.2 NFQ Formulation

Table 1.3-1 presents the basic viewpoint of the reported research, in which any flying qualities formulation is seen as consisting of five sequential characteristics. The current effort only involves the first four characteristics; the final characteristic must be investigated in future programs through unmanned and manned (pilot-in-the-loop) simulation as well as through actual flight tests.

The reference flight path of MIL-F-8785C is restricted to be steady, equilibrium flight, whereas the NFQ formulation applies to any maneuver that can be realized through control inputs. Both formulations refer to a local (linearized) perturbation of the reference flight path, but the resulting mathematical structure of NFQ permits the full linearized, time-varying dynamics to be considered.

TABLE 1.3-1
CHARACTERISTICS OF A FLYING QUALITIES FORMULATION

FORMULATION CHARACTERISTICS	CURRENT	NFQ
Reference Flight Path	Steady, Equilibrium Flight: $\dot{\phi} = \dot{p} = \dot{q} = \dot{r} = \dot{V} = \dot{\gamma} = 0$	General Large Amplitude Maneuvers
Perturbed Flight Path	Linear, Constant Coefficient, Single Input/Multiple Output Dynamics and Modal character- istics	Linear, Time-Varying Coefficient, Multiple Input/Multiple Output Dynamics
Mathematical Structure	Low Order, Single Input Approximation, mostly in Laplace or Frequency Domain ("Equivalent System")	Low Order, Multiple Input/ Multiple Output Approximation in Time Domain ("Canonical System")
Intrinsic Flying Qualities Parameters	Equivalent System Parameters (Poles, Zeros, Time Delay), Roll-Sideslip Coupling, and Roll Response	Functions and Functionals of Canonical System Parameters (Grammian Singular Values and Eigenvectors; etc)
Extrinsic Flying Qualities Parameters	Pilot Opinion (Cooper-Harper Rating), Pilot-Vehicle Performance, and Pilot Workload	Pilot Opinion; Combat Effective- ness; Terrain-Following Capability; etc

The two formulations, within their mathematical structure of perturbed dynamics, define intrinsic flying qualities to be parameters that describe a simplified or idealized subset of mathematical structures. For example, the current formulation includes the following equivalent system of longitudinal control stick to pitch rate dynamics (Ref. 1, p. 3):

$$T(s) = K \frac{(s+a)e^{-\tau s}}{s^2 + 2\zeta\omega s + \omega^2} \quad (1.3-1)$$

An idealization of the response of an unaugmented aircraft which is only one of a great many possible simplifications of an actual, higher order transfer function of a current fighter

aircraft. Only research into the fifth characteristic (pilot opinion) has justified the particular five-parameter version of Eq. 1.3-1 (Ref. 2). Such research has led to correlations between these parameters and Cooper-Harper pilot ratings, as presented in MIL-F-8785C.

On the other hand, the NFQ formulation reported here considers the full perturbed dynamics described by the vector equation

$$\dot{\underline{x}} = \underline{F}\underline{x} + \underline{G}\underline{u} \quad (1.3-2)$$

where \underline{F} and \underline{G} , as well as \underline{x} and \underline{u} are in general time-varying as a result of multiply-perturbed control inputs about those that generated the reference flight path. One possible simplification (i.e., a candidate canonical system) has \underline{G} as block diagonal and \underline{F} as block upper triangular such that stability lateral-directional dynamics are decoupled, i.e., the roll mode is decoupled from the dutch roll and spiral modes. One candidate measure of intrinsic flying qualities is the relative controllability index of Eq. 1.3-2 (as detailed in Chapter 2). This index is a measure of the margin of controllability enjoyed by a pilot fortunate enough to fly such an idealized aircraft, and furthermore, indicates the extent to which the approximated dynamics, e.g., decoupled roll, dutch roll, and spiral, represent the true aircraft dynamics.

Like the equivalent system of Eq. 1.3-1, any trial definition of a canonical system structure only attains transcendent importance when further research into extrinsic flying qualities demonstrates three conditions:

- Canonical system structures with specified parameters can be made to represent

aircraft dynamics that pilots prefer, i.e., the canonical system would receive a low Cooper-Harper rating

- Aircraft dynamics which cannot be approximated by any of the specified canonical systems are generally perceived by pilots to perform poorly, i.e., the aircraft receives a high Cooper-Harper rating
- Good modern aircraft (highly augmented and control-configured) can be made to approximate the canonical simulation model.

Because experiments with pilot-in-the-loop simulation were not performed, this effort only provides a NFQ formulation of generic applicability to any trial definition of canonical system structure and subsequent measure of intrinsic flying qualities within the perturbed dynamics of Eq. 1.3-2. Several examples of large amplitude maneuvers, of canonical systems and of intrinsic flying qualities measures were defined to conduct a test and evaluation of computability, and thereby to demonstrate generic applicability.

1.3.3 NFQ Test and Evaluation

The NFQ formulation was tested and evaluated with a nonlinear 6-DOF simulation and with special numerical procedures to solve the canonical system and relative controllability parameters. The goal of this evaluation was to demonstrate the flexibility and numerical reliability of the numerical procedures, not to characterize the flying qualities of the aircraft modeled in the simulation. Preliminary assessment of the value of these metrics for quantifying flying qualities is the recommended next step.

Two principal maneuvers were considered: a wind-up turn and a rolling reversal. The canonical systems methodology was applied to time-spaced linearizations of the aircraft dynamics during each of the maneuvers. The criteria investigated included:

- $||\Delta F||$ and $||\Delta G||$; the L_2 norms of the differences between the true-linearized and closest-canonical matrices for differential equations of the form of Eq. 1.3-2
- εC_0 ; the relative controllability measure which is computed using the relative controllability theorem of Sastry and Desoer (described in Section 4.3).

The norms $||\Delta F||$ and $||\Delta G||$ measure the closeness of the fit between the true perturbed dynamics and a given member from the chosen canonical system class, and thus can be used in a gradient procedure to find the closest canonical system. This is analogous to the current practice of finding the closest equivalent system (in the Laplace domain) to the true constant coefficient, single input linearized dynamics. If pilots like simulated aerospace vehicles that fly exactly like the canonical systems and do not like quite different dynamic behavior, then $||\Delta F||$ and $||\Delta G||$ could also be used as intrinsic flying qualities measures with, one expects, strong correlations with pilot opinion.

The intrinsic flying qualities parameter εC_0 is, in a very general sense, analogous to a stability margin such as the equivalent system parameter ζ of Eq. 1.3-1. In fact, εC_0 is a controllability margin. It is conjectured that strong correlations exist between εC_0 and extrinsic flying qualities such as pilot opinion and close-in combat effectiveness.

The NFQ test and evaluation investigated the relative performance of various canonical system structures in terms of $||\Delta F||$, $||\Delta G||$ and εC_0 over time, from F upper triangular to pure diagonal. The different canonical system structures were examined to discover the best approximation to the time-varying dynamics during the maneuver.

1.4 RECOMMENDATIONS

The NFQ test and evaluation revealed that the canonical systems methodology is a tractable and useful approach to characterizing aircraft behavior based on time-varying multi-variable descriptions of the aircraft. The next step is to apply the tools that have been developed to calibrate the intrinsic flying qualities (e.g., εC_0) against extrinsic flying qualities such as pilot opinion and combat effectiveness. This correlation of intrinsic and extrinsic flying qualities can form the basis for the next generation military specification. However, to avoid the high cost of pilot-in-the-loop simulation or flight test, the NFQ formulation can be initially applied to an aircraft in an autonomous flight mode. The primary recommendations are thus:

- An initial approach to calibrating the canonical system-parameters to extrinsic flying qualities should be pursued through the analysis of autonomous flying modes, e.g., automatic landing, terrain-following, in which the vehicle performance can be quantitatively evaluated without pilot opinion
- In a parallel investigation, the canonical systems can be flown while adjusting the control and guidance algorithms, to yield an ideal system structure that provides the best performance in a given mission.

1.5 REPORT ORGANIZATION

This report is divided into five chapters and three appendices which document the research effort and describe the flying qualities analysis tools developed to date. Although the literature search was the first task, it is felt that the detailed results are of interest only to the basic researcher; to permit a simple, unbroken exposition of the NFQ formulation, results from the literature search are delayed until Chapter 4. Chapter 2 provides an overall account of the NFQ formulation: canonical systems theory, its derivation, its relevance to flying qualities, and the procedure for numerically computing a canonical system match. Chapter 2 also includes a detailed exposition of the relative controllability theorem used to define one intrinsic measure of flying qualities. Chapter 3 details the numerical results obtained with the canonical systems technique and the evaluation of relative controllability. Canonical system candidates and the rationale for the specific choices are also documented in Chapter 3. Furthermore, Chapter 3 presents simulation traces of the true and matched canonical systems in the selected large amplitude maneuvers. Finally, Chapter 5 summarizes this report and provides the conclusions and recommendations of the NFQ research.

Appendices A and B provide comprehensive descriptions of the numerical procedures developed during the program. Appendix A documents the 6-DOF simulation and the specific aircraft model employed. Appendix B documents the Canonical System Evaluator (CASE) procedure which implements the methodology discussed in Chapter 2. Appendix C contains a review of underlying mathematical concepts, i.e., induced norms and the controllability Grammian, which are mentioned frequently throughout this report. Finally, there is a glossary of the mathematical symbols used.

2.

CANONICAL SYSTEM THEORY AND RELATIVE
CONTROLLABILITY FOR FLYING QUALITIES ANALYSIS

Canonical system theory is the basis for the applied flying qualities formulation developed in the NFQ program. Although similar to the equivalent systems methodology currently applied in flying qualities analysis, canonical systems theory admits multivariable time-varying descriptions of the aircraft dynamics. Furthermore, like the equivalent systems methodology, canonical systems are produced by computing closest approximations to the true aircraft dynamics. This chapter contains a description of the canonical systems theory and the general methodology with which it is applied to the aircraft flying qualities analysis problem. Section 2.1 defines canonical system theory and describes the specific form that the NFQ analysis employs. Section 2.2 describes how relative controllability can be used as a flying qualities criterion. Finally, Section 2.3 describes the overall process in which the canonical systems technique would be used.

2.1 CANONICAL SYSTEM THEORY

Canonical system theory can best be understood through a discussion of its similarities with realization theory, decomposition, canonical forms (e.g., Jordan matrix), structure and parameter identification, and the equivalent systems methodology. Note that the first three techniques mentioned are direct methods, i.e., can be solved in closed form, whereas the last three involve approximations and estimation theory. Canonical system theory is primarily an approximation method

that lies in between the two extremes of approximation and estimation. The discussion of these related techniques begins with the equivalent systems methodology.

In flying qualities analysis using the equivalent systems methodology, the problem being resolved has the following elements:

- Given that modern aircraft differ significantly in their mathematical models and in control augmentation and control surface configurations, a common aircraft dynamic model is required which is representative of most aircraft and yet maintains simplicity
- Once an ideal (low-order) or desired aircraft dynamic model has been determined, the free parameters of the ideal (low-order) system must be adjusted such that the ideal system best approximates the true aircraft dynamics with respect to an intrinsic criterion or norm; furthermore, the acceptable values of these parameters must be correlated with extrinsic flying qualities criteria (e.g., pilot opinion).

A final obstacle to employing equivalent systems in flying qualities analysis is that the norm implied in the second problem element may be very large, hence, suggesting that the equivalent system is a poor representative of the true aircraft dynamics. What constitutes a poor match, and when to conclude that a poor match is all that can be accomplished, have been discussed at some length (Refs. 1-12) but definitive answers seem not to have been found -- though a feeling emerges that a bad match indicates poor flying qualities.

The preceding problem statement, i.e., taking an ideal system model and matching it to the true dynamics, could

describe numerous mathematical techniques. The phrase -- equivalent systems methodology -- refers to the current practice in flying qualities analysis of employing a Laplace variable transfer function as the mathematical structure for the ideal model and adjusting its parameter (i.e., zero, pole, and delay) values such that the ideal frequency response matches the frequency response of the true aircraft. This process is, therefore, similar to the general concept of decomposition (specifically order-reduction) in which excess modes are discarded and the true dynamics are recast into a lower-order model. Furthermore, this method also includes elements of parameter identification (where measurements are considered to be perfect).

The fundamental limitation of equivalent systems resides in the use of frequency response data of the true dynamics and not in the general concept. The use of frequency response data forces the flying qualities analyst to consider only steady, equilibrium flight conditions. The frequency response cannot include time-varying and transient phenomenon thereby excluding most maneuvers from the equivalent systems approach.

The basic tenets of equivalent systems, i.e., creating an idealized system, can be accomplished through a number of techniques. For example, parameter identification can be used to identify the unknown parameters of an ideal model, regardless of whether the model is linear, time-invariant or time-varying, or nonlinear. Similarly, as exemplified by Section 4.2 nonlinear forms of realization theory exist. Thus it is not necessary to work with the frequency response alone; the time-domain data can be used. Nevertheless, the fundamental concept of equivalent systems is an excellent starting point for numerous problems. Canonical systems expands the basic tenet

of equivalent systems by extending the classes of ideal systems to time-varying, multivariable state-space forms. The methodologies for matching the ideal system in canonical systems theory, however, is markedly different, because of the different form of the ideal system and the use of system-theoretic properties, e.g., controllability.

The closest canonical system is that system which is closest to the original system in the norm sense and maintains the controllability properties of the original system. The relative controllability measure of the canonical system reflects how well the canonical system approximates the original nonlinear system. Consequently, canonical systems surpasses the equivalent systems methodology because they are matched to the original nonlinear system through controllability, unlike equivalent systems which are matched to a linear frequency response representation of the aircraft dynamics.

2.1.1 Canonical System Theory: Definition

A canonical system is a class of systems that approximates the original system model for a particular solution and (ideally) maintains desired properties of the original system. For a linear time-varying system, with a desired property (e.g., controllability)

$$\dot{\underline{x}}(t) = F(t)\underline{x} + G(t)\underline{u} \quad (2.1-1)$$

the canonical systems consist of those systems described by

$$\dot{\underline{x}} = F_e(t)\underline{x} + G_e(t)\underline{u} \quad (2.1-2)$$

which satisfies the desired property(s) with

$$F_e(t) \triangleq F(t) - \Delta F \quad (2.1-3)$$

$$G_e(t) \triangleq G(t) - \Delta G \quad (2.1-4)$$

where

$$||\Delta F||_i \leq \varepsilon_f \quad (2.1-5)$$

$$||\Delta G||_i \leq \varepsilon_g \quad (2.1-6)$$

are the induced norm of the maps $F(t): R^n \rightarrow R^n$, $G(t): R^m \rightarrow R^n$.^{*}

The closest canonical system is that member of a canonical system class, F_e or G_e ,[†] that minimizes the induced norm, viz,

$$F_c = \min ||F_e - F(t)||_i \quad (2.1-7)$$

$$G_c = \min ||G_e - G(t)||_i \quad (2.1-8)$$

Similar canonical system classes can be developed for nonlinear equations of the form

$$\dot{\underline{x}} = f(\underline{x}, \underline{u}, t) \quad (2.1-9)$$

where the canonical system class satisfies

$$f_c = \min_{[0, T]} ||f_e(\underline{x}, \underline{u}, t) - f(\underline{x}, \underline{u}, t)||_i \quad 0 \leq t \leq T \quad (2.1-10)$$

Note that this induced norm is performed on infinite dimensional spaces, i.e., Eq. 2.1-10 is a functional optimization

^{*}See Appendix C for a discussion of induced norms.

[†]For convenience, the dependence of F_e and G_e on time will be dropped from this point on in the discussion.

problem, and hence, would require a much more complicated numerical procedure than the parameter optimization problem of Eqs. 2.1-7 and 2.1-8.

In accord with the philosophy stressed throughout the NFQ program, the linear time-varying form of canonical system theory, Eqs. 2.1-2 to 2.1-8 will be pursued because of its real-time computational ease over the nonlinear form, Eqs. 2.1-9 and 2.1-10.* Furthermore, the key property that will be enforced in a canonical system class will be controllability, hence, the emphasis on the relative controllability theorem of Sastry and Desoer in Chapter 4.

2.1.2 Second-Order Canonical System Example

The canonical system definition just outlined can be applied to a full aircraft state equation with 12 or more states or to simple systems. As an example consider a second-order system

$$\dot{\underline{x}} = \begin{bmatrix} Z_w & Z_q \\ M_w & M_q \end{bmatrix} \underline{x} + \begin{bmatrix} Z_{\delta_H} & Z_{\delta_{TEF}} \\ M_{\delta_H} & M_{\delta_{TEF}} \end{bmatrix} \underline{u} \quad (2.1-11)$$

Equation 2.1-11 is a short-period dynamics approximation where

$$\underline{x} \triangleq [w, q]^T \quad (2.1-12)$$

*The relative controllability is useful in both the linear and nonlinear canonical systems forms, however, the linear piecewise time-invariant computation procedure of Section 4.3 justifies the use of linear canonical systems theory.

includes normal velocity and pitch rate and

$$\underline{u} \triangleq [\delta_H, \delta_{TEF}] \quad (2.1-13)$$

are the elevator and flap deflections. One canonical system class which has a simpler structure is

$$\dot{\underline{x}} = \begin{bmatrix} f_1 & f_2 \\ 0 & f_3 \end{bmatrix} \underline{x} + \begin{bmatrix} 0 & g_2 \\ g_1 & 0 \end{bmatrix} \underline{u} \quad (2.1-14)$$

where f_i and g_i represent free parameters of the canonical system that will be selected to minimize $||\Delta F||_i$ and $||\Delta G||_i$, which were defined in Eqs. 2.1-3 and 2.1-4. The induced norm for the problem in Eqs. 2.1-11 and 2.1-14 is the L_2 norm,[†] defined for an arbitrary $m \times n$ matrix A as

$$||A||_{L_2} = \max_i \sqrt{\lambda_i(AA^*)} \quad i=1,n \quad (2.1-15)$$

where A^* is the conjugate transpose of A and λ_i is the i^{th} eigenvalue of the product (AA^*) . (Note that the right hand side of Eq. 2.1-15 is equivalent to the maximum singular value of A . Reliable numerical procedures for computing the singular values of a matrix are readily available.)[§]

The minimization defined in Eqs. 2.1-7 and 2.1-8 for finding the closest canonical system requires a numerical optimization algorithm (see Appendix B). Solving for the second-order example of Eqs. 2.1-11 and 2.1-12 where the numerical

[†]A thorough discussion of L_p and ℓ_p spaces and their respective norms is contained in Ref. 13, Chapter 2, Ref. 14, Section 2.10, or Appendix C.

[§]See Ref. 13 or Appendix C for a derivation of the L_2 norm of a matrix as the maximum singular value.

values for F are representative of the AFTI/F-16 in steady-trimmed flight at 829 ft/sec,

$$F = \begin{bmatrix} -2.24 & 829 \\ -0.241 & -10.15 \end{bmatrix} \quad (2.1-16)$$

the closest canonical dynamic matrix is

$$F_c = \begin{bmatrix} -2.20 & 828.6 \\ 0 & -10.10 \end{bmatrix} \quad (2.1-17)$$

where F_c (and subsequently G_c) were computed with the numerical procedure described in Appendix B. The final L_2 norm of the canonical system match is

$$||\Delta F||_{L_2} = .047, ||F||_{L_2} = 828. \quad (2.1-18)$$

Although the L_2 norm of the difference between the dynamics matrices are quite small (relative to $||F||$) their eigenvalues are distinctly different. Because F_c is upper triangular the eigenvalues are simply the diagonal values

$$\lambda(F_c) = -2.2, -10.1 \quad (2.1-19)$$

The eigenvalues of the true dynamics can be readily computed.

$$\lambda(F) = -6.2 \pm 2.1 i \quad (2.1-20)$$

Not only are the magnitudes different but the canonical system has two real poles while the true system has a complex pair. However, the principal tenet of canonical systems theory is, if $||\Delta F||$ and $||\Delta G||$ are small, the true and canonical systems will share the same properties. One of the most

important shared properties is trajectory equivalence, i.e., the property that the solutions of the true and canonical systems are within a prescribed tolerance. This property can also be expressed mathematically as,

$$||\Delta \underline{x}|| \leq \varepsilon \quad (2.1-21)$$

where

$$||\Delta \underline{x}|| \triangleq ||\underline{x}(t) - \underline{x}_c(t)|| \quad (2.1-22)$$

For the second-order example being considered, the solutions are, according to the variation of constants formula (see Ref. 15).

$$\underline{x}(t) = e^{F(t-t_0)} \underline{x}(t_0) \quad (2.1-23)$$

where the state transition matrix is the matrix exponential $e^{F(t-t_0)}$ and

$$\underline{x}_c(t) = e^{F_c(t-t_0)} \underline{x}(t_0) \quad (2.1-24)$$

The second-order system is sufficiently uncomplicated to permit the analytical computation of the matrix exponential, hence, ($\Delta t = t - t_0$)

$$e^{F\Delta t} = \left[\begin{array}{c|c} e^{-6.2\Delta t} \begin{pmatrix} 1.89 \sin 2.1\Delta t \\ + \cos 2.1\Delta t \end{pmatrix} & e^{-6.2\Delta t} (595.2 \sin 2.1\Delta t) \\ \hline e^{-6.2\Delta t} (.0116 \sin 2.1\Delta t) & e^{-6.2\Delta t} \begin{pmatrix} 1.89 \sin 2.1\Delta t \\ + \cos 2.1\Delta t \end{pmatrix} \end{array} \right] \quad (2.1-25)$$

and for the canonical system

$$e^{F_c \Delta t} = \left[\begin{array}{c|c} e^{-2.2\Delta t} & 104.9(e^{-10.1\Delta t} - e^{-2.2\Delta t}) \\ \hline 0 & e^{-10.1\Delta t} \end{array} \right] \quad (2.1-26)$$

Although the transition matrices in Eqs. 2.1-25 and 2.1-26 appear significantly different, the fact that $||\Delta F||$ is small, will cause the solutions generated with Eqs. 2.1-23 and 2.1-24 to lie within a tolerance governed by $||\Delta F||$. The bounds on the magnitude of $\Delta \underline{x}(t)$ (i.e., the difference between $\underline{x}(t)$ and $\underline{x}_c(t)$) will be derived in the following section. The trajectory equivalence of the second-order system under consideration can be demonstrated by computing Eqs. 2.1-23 and 2.1-24 using the solutions of the transition matrices just given in Eqs. 2.1-25 and 2.1-26.

Figure 2.1-1 contains the time responses of the true and canonical systems of Eqs. 2.1-23 and 2.1-24, with respect to identical initial conditions. Notice that only the true system trajectory exhibits a second-order (i.e., damped sinusoidal) response in pitch rate. This phenomenon reflects Eqs. 2.1-25 and 2.1-26 which show that the canonical system transition matrix has no sinusoidal functions. The difference in responses truly originates from the complex eigenvalues of the true system, whereas the canonical system has real eigenvalues and hence, produces only first-order responses. The reason the canonical system does not have complex eigenvalues is the structure itself.

The triangular canonical system structure of Eq. 2.1-24 will not admit complex eigenvalues. This arises because only real-valued matrices are deemed appropriate for the canonical

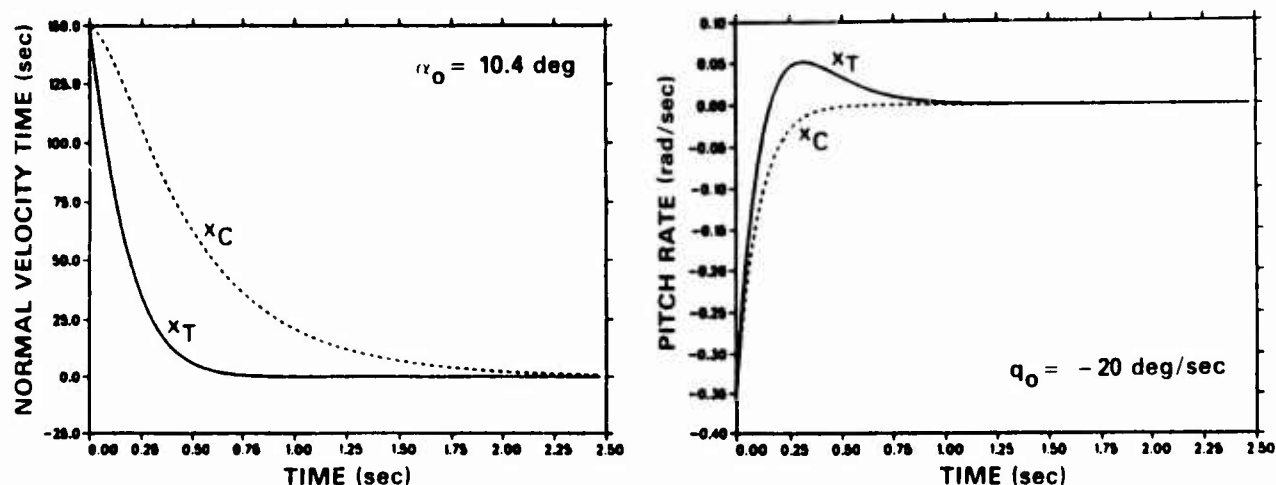


Figure 2.1-1 Second-Order Example: True and Canonical Responses to Initial Conditions

systems which are employed to model physical systems,^{*} e.g., aircraft dynamics. The dynamics matrix in Eq. 2.1-14 is upper triangular, hence its eigenvalues are the diagonal elements, thus it can have only real eigenvalues. The canonical system for this second-order example is inadequate because, regardless of how the match is computed, F_c can only have real eigenvalues, f_1 and f_3 . Yet, it is typically the case that the short-period mode of an aircraft is composed of a complex pair of eigenvalues. Later, in Chapter 3, in the discussion of canonical system classes for 6-DOF aircraft dynamics, the issue of creating structures which admit complex eigenvalues is addressed. Let it suffice to say that if the canonical dynamics matrix or a submatrix is upper (or lower) triangular, diagonal, or in Jordan form, then the eigenvalues of that matrix or submatrix will only be real and thus, may not represent the ideal dynamic structure desired.

^{*}Although complex-valued differential equations do arise in mathematical physics, the classical mechanics description of the aircraft equations has coefficients which represent physical quantities such as mass, or are elements of a direction cosine matrix.

The analysis just presented can be extended to include the canonical control matrix. For the numerical example under consideration (for the same trim point used earlier),

$$G = \begin{bmatrix} -3.52 & -7.99 \\ -.571 & -.394 \end{bmatrix} \quad (2.1-27)$$

The closest canonical control matrix (for the class defined in Eq. 2.1-14) is

$$G_c = \begin{bmatrix} 0 & -7.99 \\ -.571 & 0 \end{bmatrix} \quad (2.1-28)$$

where

$$||\Delta G|| = 3.52, ||G|| = 8.75 \quad (2.1-29)$$

The comparison of the trajectory for the inhomogeneous canonical system (where the control inputs \underline{u} are non zero) versus the inhomogeneous true system is easily accomplished with the variation of constants formula (Ref. 15) viz,

$$\underline{x}(t) = e^{F(t-t_o)} \underline{x}(t_o) + \int_{t_o}^t e^{F(t-\tau)} G \underline{u}(\tau) d\tau \quad (2.1-30)$$

for the true system (Eq. 2.1-11) and

$$\underline{x}_c(t) = e^{F_c(t-t_o)} \underline{x}(t_o) + \int_{t_o}^t e^{F_c(t-\tau)} G \underline{u}(\tau) d\tau \quad (2.1-31)$$

for the canonical system (Eq. 2.1-14). An analysis of the trajectories is straightforward using the same transition matrices defined in Eqs. 2.1-25 and 2.1-26.

The most significant concept illustrated by the previous example is that, like equivalent systems, the canonical systems methodology tries to minimize a distance measure between a true and ideal system by adjusting the parameters of the ideal system. The ideal of the second-order example just presented was that the dynamics matrix should be upper triangular and the controls decoupled. This example is not especially useful in light of the fact that the true short-period dynamics did not necessarily require simplification. But consider the case when there is a control augmentation system with an integrator in the forward loop. Equation 2.1-11 then becomes

$$\dot{\underline{x}} = \begin{bmatrix} Z_w & Z_q & Z_I \\ M_w & M_q & M_I \\ I_w & I_q & I_I \end{bmatrix} \underline{x} + \begin{bmatrix} Z_{\delta_H} & Z_{\delta_{TEF}} \\ M_{\delta_H} & M_{\delta_{TEF}} \\ I_{\delta_H} & I_{\delta_{TEF}} \end{bmatrix} \underline{u} \quad (2.1-32)$$

A candidate canonical system may then be one which decouples the integrator state from the short-period dynamics and controls. Hence,

$$\dot{\underline{x}}_c = \begin{bmatrix} f_1 & f_2 & 0 \\ f_3 & f_4 & 0 \\ 0 & 0 & f_5 \end{bmatrix} \underline{x}_c + \begin{bmatrix} g_1 & g_2 \\ g_3 & g_4 \\ 0 & 0 \end{bmatrix} \underline{u} \quad (2.1-33)$$

Furthermore, f_5 may be arbitrarily forced to zero. The form of the canonical system in Eq. 2.1-33 yields a system in which the augmentation is completely decoupled, i.e., an implicit model reduction has been enforced where a low-order system approximates the augmented dynamics. Thus the submatrices formed by $f_1 - f_4$ and $g_1 - g_4$ should yield the second-order approximation to the dynamics in Eq. 2.1-32.

2.1.3 Canonical Systems and Trajectory Equivalence

The mathematical basis for canonical system theory is derived from functional analysis and the theory of differential equations. Fundamentally the problem of linear canonical system theory is to demonstrate that a perturbation in $F(t)$ or $G(t)$, i.e., $\Delta F(t)$ or $\Delta G(t)$ where

$$||\Delta F(t)|| \leq \varepsilon_f \quad (2.1-34)$$

$$||\Delta G(t)|| \leq \varepsilon_g \quad (2.1-35)$$

produces a perturbed solution that lies in the neighborhood of the nominal solution, viz,

$$||\Delta\phi(t)|| \leq \varepsilon_\phi \quad (2.1-36)$$

where $\Delta\phi(t)$ is the difference between the solutions of the differential equations (a vector), Eqs. 2.1-1 and 2.1-2. For example, Ref. 13 uses the criterion of matrix measure (not a true norm) to bound the solutions of a linear time-varying differential equation. The theorem is as follows (Ref. 13, p. 35): given

$$\dot{\underline{x}}(t) = F(t) \underline{x}(t) \quad (2.1-37)$$

where the solution of Eq. 2.1-14 is

$$\underline{x}(t) = \exp \left\{ \int_{t_0}^t F(\tau) d\tau \right\} \underline{x}(t_0)^* \quad (2.1-38)$$

*Equation 2.1-38 holds for any $F(t)$ that commutes with itself over time, see Ref. 15 and Appendix C.

Then Eqs. 2.1-37 and 2.1-38 satisfy the inequalities

$$\begin{aligned} |\underline{x}(t_0)| \exp \left\{ - \int_{t_0}^t \mu[-F(\tau)] d\tau \right\} &\leq |x(t)| \\ &\leq |\underline{x}(t_0)| \exp \left\{ \int_{t_0}^t \mu[F(\tau)] d\tau \right\} \end{aligned} \quad (2.1-39)$$

where $\mu\{F(t)\}$ is the matrix measure of F ,

$$\mu(F) \triangleq \lim_{\phi \downarrow 0} (||I + \phi F|| - 1)/\phi \quad (2.1-40)$$

where F may be constant or time-varying. (See Ref. 13, p. 30 for proof of the existence of the limit in Eq. 2.1-40.) Note that the matrix measure is not a norm because $\mu(F) = 0$ does not imply that $F = 0$. The following properties of the matrix measure will be of use in the ensuing discussion:

$$\mu(I) = 1 \quad , \quad \mu(-I) = -1 \quad (2.1-41)$$

$$\mu(0) = 0 \quad (2.1-42)$$

$$- ||F|| \leq -\mu(-F) \leq \mu(F) \leq ||F|| \quad (2.1-43)$$

$$\mu[\lambda F_1 + (1-\lambda)F_2] \leq \lambda\mu(F_1) + (1-\lambda)\mu(F_2) \quad (2.1-44)$$

i.e., $\mu: C^{n \times n} \rightarrow R$ is convex

$$- \mu(-F)|x| \leq |Fx| \quad (2.1-45)$$

and

$$|\mu(F_1) - \mu(F_2)| \leq |\mu(F_1 - F_2)| \leq ||F_1 - F_2|| \quad (2.1-46)$$

Using Eqs. 2.1-41 to 2.1-46; Eq. 2.1-39 can be recast into an inequality based on the norms of F , albeit a less tight inequality,

$$\begin{aligned}
 |x(t_0)| \exp \left\{ - \int_{t_0}^t ||F(\tau)|| d\tau \right\} &\leq |x(t)| \\
 &\leq |x(t_0)| \exp \left\{ \int_{t_0}^t ||F(\tau)|| d\tau \right\}
 \end{aligned} \tag{2.1-47}$$

The proof follows from

$$D^+ n(t) \leq \mu(F(t)) x(t) \tag{2.1-48}$$

$$D^+ n(t) \leq ||F(t)|| n(t) \tag{2.1-49}$$

where $n(t) = |x(t)|$, Eq. 2.1-49 follows from the relationship between the matrix measure and norm in Eq. 2.1-43. Assuming $x(t)$ is a nonzero solution of the differential equation, Eq. 2.1-38, then Eq. 2.1-49 becomes

$$D^+ n(t)/n(t) = ||F(t)|| \tag{2.1-50}$$

Integrating Eq. 2.1-50 yields the right hand inequality of Eq. 2.1-47. A similar argument with $n(t) = -|x(t)|$ can be used to prove the left-hand inequality of Eq. 2.1-47.

The techniques above can be used to show that the bounds of $\Delta \underline{x}$, the difference in the true and canonical system trajectories is governed by the norm of ΔF . First note that the true and canonical differential equations are

$$\dot{\underline{x}}_T = F \underline{x}_T \quad (2.1-51)$$

$$\dot{\underline{x}}_C = (F - \Delta F) \underline{x}_C \quad (2.1-52)$$

Subtracting Eq. 2.1-52 from Eq. 2.1-51 and defining

$$\Delta \underline{x} = \underline{x}_T - \underline{x}_C \quad (2.1-53)$$

yields

$$\Delta \dot{\underline{x}} = F \Delta \underline{x} + \Delta F \underline{x}_C \quad (2.1-54)$$

which can be further manipulated to yield

$$\Delta \dot{\underline{x}} = (F - \Delta F) \Delta \underline{x} + \Delta F \underline{x}_T \quad (2.1-55)$$

The second term on the right hand side of Eq. 2.1-55, $\Delta F \underline{x}_T$, which is a function of the true trajectory, is a driving term of the $\Delta \underline{x}$ differential equation. Hence, the solution of Eq. 2.1-55 using the variation of constants formula is

$$\begin{aligned} \Delta \underline{x}(t) = & e^{(F-\Delta F)(t-t_o)} \Delta \underline{x}(t_o) \\ & + \int_{t_o}^t e^{(F-\Delta F)\tau} (\Delta F \underline{x}_T(\tau)) d\tau \end{aligned} \quad (2.1-56)$$

According to the definition of the canonical system, the true and canonical systems have the same initial condition,

$$\Delta \underline{x}(t_o) = \underline{0} \quad (2.1-57)$$

Thus,

$$\Delta \underline{x}(t) = \int_{t_o}^t e^{(F-\Delta F)\tau} (\Delta F \underline{x}_T(\tau)) d\tau \quad (2.1-58)$$

Equation 2.1-58 yields the difference between the true and canonical system trajectories as a function of time. As expected, if ΔF approaches 0 which implies that $||\Delta F||$ approaches 0 then $\Delta \underline{x}(t)$ is zero for all time; the true and canonical system trajectories are equivalent. Our goal, however, is to find the bounds on Eq. 2.1-58 using the techniques elaborated in the beginning of Section 2.2. This analysis yields the following inequality

$$||\Delta F|| \exp(-||F-\Delta F||) \left(- \int_t^{t_0} |x(t)| \right)^{-1} \leq |\Delta x(t)|$$

$$\leq ||\Delta F|| \exp(||F-\Delta F||) \left(\int_t^{t_0} |x(t)| \right)^{-1} \quad (2.1-59)$$

where ΔF and F are assumed to be piecewise constant matrices.*

Equation 2.1-59 provides bounds on acceptable perturbations to the true dynamics matrix such that the solution to the perturbed solution lies within a neighborhood of the original solution. Thus, Eq. 2.1-59 supplies a basis for the linear canonical system theory of Eqs. 2.1-2 to 2.1-9, where the property of interest is that the solution of canonical system class, $\underline{x}_c(t)$, lie within some neighborhood of $\underline{x}_T(t)$. The property of interest that is being maintained is a common trajectory. Hence, one can consider a closest canonical system which maintains the trajectory property only, to be a time-domain version of equivalent systems. A further distinction is that the canonical system classes can include multivariable and time-varying systems. Although two alternatives for bounding the

*The extension to the case where the true and canonical systems are inhomogeneous is straightforward.

closest canonical system have been presented, where the one based on matrix measure is the tighter bound, only the norm based criterion is amenable to the final numerical solution technique. This choice was made because the matrix measure $\mu(A)$ on L_2 is only numerically defined for square matrices,[†] hence it cannot generally be used to find the canonical control matrix G_c .

The relationship between the generic canonical system theory presented thus far and other systems theory concepts (e.g., controllability) arises when one considers the application of canonical system theory to flying qualities analysis. As implied in the previous discussion, a class of canonical systems can be chosen for maintaining a number of properties rather than just one. A second property, which the NFQ research has concluded to be essential, is the controllability of the true aircraft dynamics model. However, as is documented in Chapter 4, controllability and/or reachability are typically presented as binary results, a system is either controllable or not. Hence, the detailed exposition of the relative controllability theorem in Section 4.3. Section 2.2 of this chapter describes how relative controllability is employed to derive a closest canonical system which maintains the trajectory and controllability properties of the true system.

2.2 RELATIVE CONTROLLABILITY

The use of the relative controllability theorem arises naturally in the context of linear canonical system theory. If the canonical system matrices differ from the true system matrices,

$$\dagger \mu_{L_2}(A) = \max_i \lambda_i(\tfrac{1}{2}(A+A^*)) \text{ whereas } ||A||_{L_2} = \max_i \lambda_i(AA^*).$$

$$\Delta F = F - F_c \quad (2.2-1)$$

$$\Delta G = G - G_c \quad (2.2-2)$$

then the differential equation of the canonical system becomes

$$\dot{\underline{x}} = F\underline{x} + G\underline{u} - \Delta F\underline{x} - \Delta G\underline{u} \quad (2.2-3)$$

The last two terms of Eq. 2.1-30 can be interpreted as,

$$\varepsilon h(\underline{x}, \underline{u}) = -\Delta F\underline{x} - \Delta G\underline{u} \quad (2.2-4)$$

Thus, Eq. 2.1-30 becomes

$$\dot{\underline{x}} = F\underline{x} + G\underline{u} + \varepsilon h(\underline{x}, \underline{u}) \quad (2.2-5)$$

The form of Eq. 2.2-5 is identical to that of Eq. 4.3-9 in Section 4.3. Consequently, the relative controllability theorem can be used to determine under what conditions does Eq. 2.2-5 maintain the controllability properties of the true system, Eq. 2.1-1. Controllability is ensured by computing ε as a function of $||\Delta F||$ and $||\Delta G||$, the differences between the canonical and true, system and control matrices. Squaring Eq. 2.2-4 gives

$$\begin{aligned} (\varepsilon h(\underline{x}, \underline{u}))^2 &= \underline{x}^T \Delta F^T \Delta F \underline{x} + 2\underline{x}^T \Delta F^T \Delta G \underline{u} \\ &\quad + \underline{u}^T \Delta G^T \Delta G \underline{u} \end{aligned} \quad (2.2-6)$$

In Section 4.3 it is established that the relative controllability theorem requires that $h(\underline{x}, \underline{u})$ satisfy a Lipschitz condition, then taking norms of Eq. 2.2-6 yields,

$$\begin{aligned} \varepsilon^2 C_0^2 \leq & ||\Delta F||^2 \underline{x}^T \underline{x} + ||\Delta G||^2 \underline{u}^T \underline{u} \\ & + 2 ||\Delta F||^2 (\underline{x} \cdot \underline{x}) ||\Delta G||^2 (\underline{u} \cdot \underline{u}) \end{aligned} \quad (2.2-7)$$

which can be simplified further to yield

$$\varepsilon^2 C_0^2 \leq (||\Delta F|| ||\underline{x}|| + ||\Delta G|| ||\underline{u}||)^2 \quad (2.2-8)$$

$$\varepsilon C_0 \leq ||\Delta F|| ||\underline{x}|| + ||\Delta G|| ||\underline{u}|| \quad (2.2-9)$$

Finally, to guarantee that the canonical system satisfies the controllability properties of the true-linearized, εC_0 must satisfy

$$- \varepsilon_0 C_0 \leq \varepsilon C_0 \leq \varepsilon_0 C_0 \quad (2.2-10)$$

where $\varepsilon_0 C_0$ represents the maximum perturbation of the true system, computed according to the relative controllability theorem of Sastry and Desoer. In Chapter 4, Eq. 4.3-12 contains an explicit formula for computing the maximum perturbation, $\varepsilon_0 C_0$. Later, in Section 4.3, the relative controllability theorem and the techniques for computing the controllability measure, $\varepsilon_0 C_0$, are presented in detail. Chapter 3 of this report discusses the use of the elements of canonical systems theory as intrinsic flying qualities criteria.

2.3 NFQ ANALYSIS FORMULATION

In the preceding sections two major themes have been developed: the use of canonical systems theory to determine an idealized (low-order) aircraft dynamics representation and the use of relative controllability as a flying qualities criterion. This section will describe how these two concepts provide the basis for an applied nonlinear flying qualities formulation.

The role of canonical systems theory and relative controllability becomes clear when one expands upon the analogy with the equivalent system approach. If the canonical system structure (e.g., block diagonal) is embodied in a new specification, then the free parameters of this structure and its relative controllability would be specified to correspond with desired pilot workload and pilot/aircraft performance in specific combat maneuvers and mission profiles. Hence, the second step involves calibrating the canonical system parameters (i.e., intrinsic flying qualities) through correlation with pilot opinion (i.e., extrinsic flying qualities parameters) in simulation and flight test. Then in application of the NFQ formulation, the canonical system structure could be matched with the true aircraft dynamics to verify compliance with the specification. Verifying compliance involves three subtasks: verifying that the magnitude of $||\Delta F||$ and $||\Delta G||$ are within a range to permit a useful match, verifying that the relative controllability measure lies within the specified tolerance, and verifying that the parameters of the matched canonical system lie within the tolerance prescribed.

2.3.1 Step One: Selecting a Canonical System Structure

The selection of a canonical system structure truly requires a process in which all three steps of the NFQ analysis are performed iteratively until a useful canonical system structure is found. The iterative process is performed until a canonical system structure is found that satisfies three objectives:

- The canonical system structure is reasonable enough to permit an adequate canonical system matching to take place, i.e., matches can be found for which $||\Delta F||$ and $||\Delta G||$ are small (relative to the conditions set forth in Section 2.1.3)

- The canonical system structure must contain recognizable parameters that can be related to flying qualities so as to quantitatively determine the specification
- Finally, the canonical system must nominally be controllable and must provide a sensitive relative controllability measure, i.e., a change in the canonical system should cause changes in the relative controllability.

Meeting the first objective simply requires that the canonical system maintain certain properties generic to the aircraft dynamics. For example, if one chose a block-diagonal F matrix for the canonical system structure, then those blocks should correspond to dynamics modes that are approximately decoupled, e.g., one block contains the longitudinal modes, the other lateral-directional for maneuvers in the vertical plane.

The second objective is an extension of the first and also provides compatibility with the current flying qualities specification. The third-order example depicted in Eq. 2.1-33 reflects how elements of the canonical F and G matrices correspond to particular modes of the aircraft dynamics. For example, the parameters f_1 through f_4 correspond to the linear equation coefficients Z_w , Z_q , M_w , M_q . Another example would be a diagonal canonical system F matrix. In that case the diagonal elements correspond to the modal inverse time constants present in the aircraft dynamics. In either example, the parameters of the canonical system correspond to measurable parameters in the true aircraft dynamics. Hence, quantitative specification of the parameters can be determined from the true aircraft data.

The third objective is obviously necessary if the relative controllability measure is to be of any use. However,

the key point of the third objective is to search for a canonical system structure which leads to a sensitive controllability measure. Thus, the NFQ analysis can be used to detect small changes in the controllability of an aircraft as it executes a maneuver or is modified through the addition and jetison of stores or the consumption of fuel.

Note that experiments in execution of Step One of the NFQ formulation -- selection of a canonical system structure -- are documented in Chapter 3 of this report where five canonical system structures are developed. Further discussion can be found in Section 3.2, where the rationale for selecting the canonical system structures with regard to the first two objectives above is explored.

2.3.2 Step Two: Correlating the Intrinsic and Extrinsic Flying Qualities Criteria

Correlating the intrinsic and extrinsic flying qualities is a step that necessarily involves pilot-in-the-loop simulation and/or flight test. Although the resources of the NFQ research effort did not permit any experimentation in this area, it is envisioned that, as is the case of MIL-F-8785, Revisions B and C (Ref. 2), pilot-in-the-loop simulations will be a major source of data. However, some analytical specification (i.e., without pilot opinion) of the intrinsic/extrinsic flying qualities can be determined for simulated-pilot flight modes in which an analytic model of a pilot is used and the performance of the aircraft can be quantitatively measured, e.g., the rms acceleration and altitude in terrain following. Further discussion concerning the application of the NFQ analysis to autonomous can be found in the recommendations for further research in Chapter 5.

2.3.3 Step Three: Computing the Canonical System Match and the Relative Controllability Measure

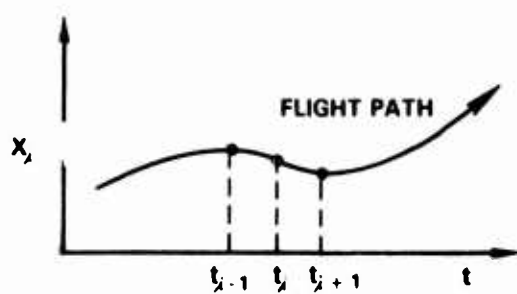
The presentation of the canonical systems theory and the relative controllability imply that the actual use of these concepts requires little additional work. However, a number of issues must be resolved regarding the form of true dynamics that are to be used (e.g., closed-form nonlinear equations?) in the computation of the closest canonical system. Furthermore, a strategy regarding the representation of the time-varying components of the true and canonical systems is required.

The two aforementioned issues were resolved by:

- Choosing a six-degree-of-freedom simulation with table look-up of the aerodynamic data and automated linearization as the tool which supplies the true dynamic description of the aircraft
- Adopting piecewise time-invariant descriptions for the method of representing the time-varying components of the true and canonical systems.

Figure 2.3-1 depicts the process by which the time-varying nonlinear dynamics are decomposed into piecewise linear time-invariant dynamics, valid over the interval $[t_i, t_{i+1}]$. Since each of the F_i and G_i are linear, the true system dynamics are compatible with the linear canonical system theory described in Section 2.1 and the relative controllability theorem described in Sections 2.2 and 4.3.

The canonical system matching procedure then becomes the process of matching each F_i, G_i pair independently at each



$$\dot{\underline{x}} = \underline{f}(\underline{x}, \underline{u}, t)$$

OBTAIN LINEARIZATION ON VARIOUS INTERVALS

$$\Delta t_i = (t_{i+1} - t_i), \quad i = 1, n$$

$$F_i = \left. \frac{\partial \underline{f}(\underline{x}, \underline{u}, t)}{\partial \underline{x}} \right|_{t_i}, \quad G_i = \left. \frac{\partial \underline{f}(\underline{x}, \underline{u}, t)}{\partial \underline{u}} \right|_{t_i}$$

Figure 2.3-1 Linear, Piecewise-Time-Invariant Description of the Aircraft Dynamics

time increment. The collection of linear time-invariant canonical systems F_{c_i} , G_{c_i} can then be taken as a group to represent a linear piecewise time-invariant representation of the aircraft dynamics. Further details concerning the specific computation that must take place can be found in Appendix B, which describes the Canonical System Evaluator (CASE) software and in Subsection 4.3.3 which describes the computation of the relative controllability index for the linear, piecewise-time-invariant dynamics. The linear, piecewise-time-invariant representation is a discrete-time approximation to the original continuous dynamics. The discrete-time approximation simplifies the required numerical computation and furthermore, is the basis of all simulation, (i.e., all numerical integration involves approximating continuous integration as a sequence of discrete-time computations).

In the next chapter, candidate canonical systems classes will be described and computation of the closest canonical system and the relative controllability measure for sample large amplitude maneuvers will be presented.

3.

NONLINEAR FLYING QUALITIES NUMERICAL RESULTS AND EVALUATION

The test and evaluation of the NFQ formulation presented in Chapter 2 was conducted with a nonlinear six-degree-of-freedom (6-DOF) aircraft model with fully-coupled aerodynamic data. The AFTI/F-16 aircraft was obtained and subsequently implemented in a generic 6-DOF simulation as the test vehicle. The simulation is used as an integral part of the canonical system analysis results that are presented in this chapter. Section 3.1 describes the overall canonical system analysis process and explains the role of each tool developed: the 6-DOF simulation and the canonical system evaluator. Section 3.2 documents the canonical system classes (candidate structures) employed in the flying qualities analysis experiments. Section 3.3 contains highlights of the numerical results and the criteria produced for two sample maneuvers. Finally, Section 3.4 concludes the chapter with an examination of the relationship between the equivalent systems and canonical systems methodologies, and speculates on the potential of using previously collected pilot opinion data.

3.1 NONLINEAR FLYING QUALITIES ANALYSIS PROCESS

The canonical systems based flying qualities analysis entails: the use of an accurate aircraft model and 6-DOF simulation, the generation of control histories for large-amplitude maneuvers, the coordination of the simulation and the canonical systems numerical procedure, and the computation of appropriate candidate flying qualities criteria. Figure 3.1-1 depicts the

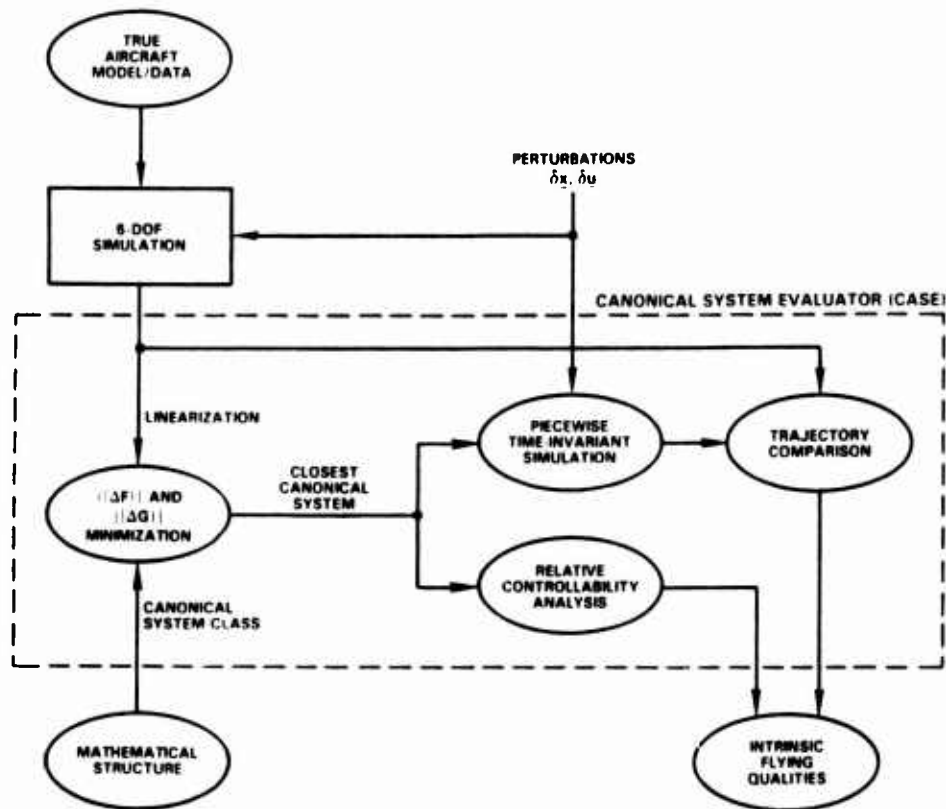


Figure 3.1-1 Canonical System Analysis Process

overall flying qualities analysis process and the relationship of the two major software tools: the 6-DOF simulation, described in Appendix A, and the CANonical System Evaluator (CASE), described in Appendix B.

The generation of large-amplitude maneuver control histories is an integral part of the 6-DOF simulation. An optimal control procedure was initially considered for generating the maneuvers. Initialization of the optimization procedure, however, required an initial trajectory which was of the same form as the final desired maneuver, e.g., wind-up turn. Consequently, once the initial maneuver was generated (via a guidance law in the 6-DOF simulation) the refinement of that trajectory was felt to be unnecessary. Using the 6-DOF simulation to generate maneuvers did mandate the addition of normal acceleration and roll

attitude autopilots, to augment the unstable open-loop AFTI/F-16 aircraft. This augmentation was necessary to permit the use of the acceleration and roll attitude command guidance laws used to generate the maneuver control histories. The guidance laws are more fully described in Section 3.3.

The linearization depicted in Fig. 3.1-1 is performed by the 6-DOF simulation at points in the trajectory specified at run time. The linearized data, contained in the $\frac{\partial \underline{f}}{\partial \underline{x}}$ and $\frac{\partial \underline{f}}{\partial \underline{u}}$ matrices are then used by the canonical system evaluator to compute the closest canonical system.

The lower left element of Fig. 3.1-1, "Mathematical Structure", is the step in which one selects the canonical system class, i.e., the free parameters of the system matrices F_e and G_e which are to be matched to the true linearized matrices computed in the 6-DOF simulation. Section 3.2 of this chapter describes the rationale for selecting a canonical system class through the description of five canonical system classes which have been permanently implemented in the CASE software.

Once the linearized matrices have been obtained and the canonical system class selected, the parameters of the canonical system class are optimized to produce the closest canonical system, i.e., matrices F_c and G_c . The closest canonical system matrices and the respective norms $||\Delta F||$ and $||\Delta G||$ are then used to evaluate the intrinsic flying qualities, which per Chapter 2 are the relative controllability index and the norms $||\Delta F||$ and $||\Delta G||$. As a final appraisal the true trajectory and a perturbed trajectory generated with the canonical system are compared. This comparison establishes the performance of the closest canonical system in achieving a trajectory which lies within a neighborhood of the original trajectory.

3.2 CANONICAL SYSTEM CANDIDATES

The canonical system candidates are representative canonical system classes chosen for the numerical investigation of flying qualities. In accordance with the philosophy described in Chapter 2, the classes are chosen for simplicity, faithfulness to the aircraft model, and the facility to yield flying/handling qualities criteria. The structures presented in this section satisfy these constraints and range from the purely virtual, i.e., the canonical system represents a non-existent, ideal structure, to the aircraft specific, in which decoupling of lateral and longitudinal motion is enforced. Each of the classes mentioned in this section has been implemented in the CASE software and can be selected by the user via input flags (see Appendix B).

3.2.1 Class I: Upper Triangular

The upper triangular canonical system class has an upper triangular system matrix. It is attractive because the matrix diagonal contains the system eigenvalues and each state is less coupled than its forerunner until finally the last state is independent. The generic form for Class I is thus

$$\dot{\underline{x}} = \begin{bmatrix} F_{1,1} & F_{1,2} & \cdot & \cdot & \cdot & \cdot & \cdot & F_{1,12} \\ & F_{2,2} & & & & & & \cdot \\ & & F_{3,3} & & & & & \cdot \\ & & & \cdot & \cdot & \cdot & & \cdot \\ 0 & & & & \cdot & & & \cdot \\ & & & & & \cdot & & \cdot \\ & & & & & & F_{12,12} & \cdot \end{bmatrix} \underline{x} + G_e \underline{u} \quad (3.2-1)$$

Note that the specification of this canonical system class says little about the nature of G_e . The specification of G_e requires knowledge of the available control surfaces for the aircraft under investigation. Furthermore, the specification of G_e is sensitive to the nature of the specific states in the state vector. G_e for Class I was formed for the AFTI/F-16 model employed in the current investigation and reflects the control surface configuration of the aircraft. Hence, G_e is

$$G_e = \begin{bmatrix} g_1 & g_2 & g_3 & g_4 & g_5 & g_6 & g_7 & g_8 & g_9 \\ 0 & 0 & g_{10} & g_{11} & 0 & 0 & 0 & 0 & 0 \\ g_{12} & g_{13} & 0 & 0 & 0 & 0 & g_{14} & g_{15} & g_{16} \\ 0 & 0 & 0 & 0 & 0 & 0 & 0 & 0 & 0 \\ 0 & 0 & 0 & 0 & 0 & 0 & 0 & 0 & 0 \\ 0 & 0 & 0 & 0 & 0 & 0 & 0 & 0 & 0 \\ 0 & 0 & g_{17} & g_{18} & g_{19} & g_{20} & 0 & 0 & 0 \\ g_{21} & g_{22} & 0 & 0 & 0 & 0 & g_{23} & 0 & 0 \\ 0 & 0 & g_{24} & g_{25} & g_{26} & g_{27} & 0 & 0 & 0 \\ 0 & 0 & 0 & 0 & 0 & 0 & 0 & 0 & 0 \\ 0 & 0 & 0 & 0 & 0 & 0 & 0 & 0 & 0 \end{bmatrix} \quad (3.2-2)$$

where the state and control vectors consist of,

$$\underline{x} \triangleq [u, v, w, x, y, z, p, q, r, \phi, \theta, \psi]^T \quad (3.2-3)$$

and

$$\underline{u} \triangleq [\delta_{TEF}, \delta_{LEF}, \delta_{VC}, \delta_R, \delta_{FA}, \delta_{HA}, \delta_H, \delta_{SP}, \delta_{SB}]^T \quad (3.2-4)$$

The definition of the state and control variables in Eqs. 3.2-3 and 3.2-4 can be found in Appendix A. The form of G_e , however, will be different if the state ordering implied by Eq. 3.2-3 is changed.

The state order has profound implications for the form of F_e as well. The upper triangular form implies substantially different dynamics if x_1, \dots, x_{12} represent different physical quantities, e.g., body axis velocities u, v, w . Although the free parameters of F_e are adjusted such that F_c best approximates the true-linear dynamics, the closest upper triangular form will necessarily differ for various state orderings. Thus far, the state ordering found to produce the most rapid convergence to the closest canonical system is:

$$\underline{x} \triangleq [u, v, w, p, q, r, x, y, z, \phi, \theta, \psi]^T \quad (3.2-5)$$

Hence, the final form of G_e is topographically different than that presented in Eq. 3.2-2, although mathematically equivalent.*

A final item to note is that for Class I, F_e contains $n(n+1)/2$ or 78 free parameters and G_e has 28 free parameters. Furthermore, the number of free parameters for both F_e and G_e increase if control augmentation or flexible body mode states are added to the state vector. Two methods predominate in the selection of the canonical system classes; either additional diagonal parameters are added to form an $n+m$ dimension matrix, or the additional rows and columns are set to zero.

*Appendix B discusses the state and control reordering and the transformation of the true linearized state and control matrices.

3.2.2 Classes II and III: Decoupled, Two Block Longitudinal-Lateral

The Two Block Longitudinal-Lateral Canonical System class more closely represents an approximation of aircraft dynamics than Class I. The decomposition of the dynamics matrix into two 6x6 block diagonal matrix recognizes one of the common simplifications of aircraft dynamics. In addition, the Class II and III control effectiveness matrices also apply longitudinal-lateral decoupling: the free parameters are arranged such that a control deflection can affect either the longitudinal or lateral dynamic states, but not both. The generic mathematical form for Classes II and III is;

$$\dot{\underline{x}} = \begin{bmatrix} F_{\text{long}} & | & 0 \\ - & - & - \\ 0 & | & F_{\text{lat}} \end{bmatrix} \underline{x} + G_e \underline{u} \quad (3.2-6)$$

where F_{long} and F_{lat} are 6x6 matrices with 36 free parameters each. The nominal state vector constituents (i.e., ordering) for Eq. 3.2-6 are:

$$\underline{x} \triangleq [u, w, q, \theta, z, x, v, p, r, \phi, \psi, y]^T \quad (3.2-7)$$

The control effectiveness matrix for Classes II and II is a 13 x 9 matrix and has the generic form;

$$G_e = \left[\begin{array}{ccccc|cccc} 0 & 0 & 0 & g_1 & g_2 & & & & \\ g_3 & g_4 & g_5 & 0 & 0 & & & & \\ 0 & 0 & g_6 & 0 & 0 & & & & \\ 0 & 0 & 0 & 0 & 0 & & & & \\ 0 & 0 & 0 & 0 & 0 & & & & \\ 0 & 0 & 0 & 0 & 0 & & & & \\ \hline & & & & & g_7 & 0 & 0 & g_8 \\ & & & & & 0 & g_9 & g_{10} & 0 \\ & & & & & g_{11} & 0 & 0 & g_{12} \\ & & & & & 0 & 0 & 0 & 0 \\ & & & & & 0 & 0 & 0 & 0 \\ & & & & & 0 & 0 & 0 & 0 \\ \hline & & 0 & & & 0 & 0 & 0 & 0 \end{array} \right] \quad (3.2-8)$$

where the 13th row represents the pitch augmentation state and the control vector constituents are:

$$\underline{u} \triangleq [\delta_{TEF}, \delta_{LEF}, \delta_H, \delta_{SP}, \delta_{SB}, \delta_{VC}, \delta_{HA}, \delta_{FA}, \delta_R]^T \quad (3.2-9)$$

The form of G_e in Eq. 3.2-8 and state and the control vector constituents defined in Eqs. 3.2-7 and 3.2-9 imply that the 12 free parameters of G_e correspond to the 12 most significant aerodynamic coefficients for the control surfaces. For example, g_5 can be defined as

$$g_5 \approx \frac{QS}{m} C_{z_{\delta_H}} \Big|_{M, \alpha} \quad (3.2-10)$$

In the next section of this chapter, the numerical results will reveal that the form of G_e in Eq. 3.2-8 produces very close canonical system matches for the two maneuvers investigated. The dynamics however, still represent a departure from traditional dynamics. Although longitudinal-lateral decoupling is present, the all nonzero nature of F_{lat} and F_{long} can produce a closest canonical system which is quite different than conventional linear dynamics. The possibility that each of the longitudinal state derivatives can be a function of all the longitudinal states and similarly, each of the lateral states can be a function of all the lateral states is depicted by the symbolic block diagram in Fig. 3.2-1. Note however, that Fig. 3.2-1 does not imply that all the state derivatives can be functions of the control forces and moments, Eq. 3.2-8 limits those possibilities.

Classes II and III do differ in the treatment of additional control augmentation states. The Class II canonical systems simply adds additional rows and columns that are all zero. Class III provides additional free parameters in the

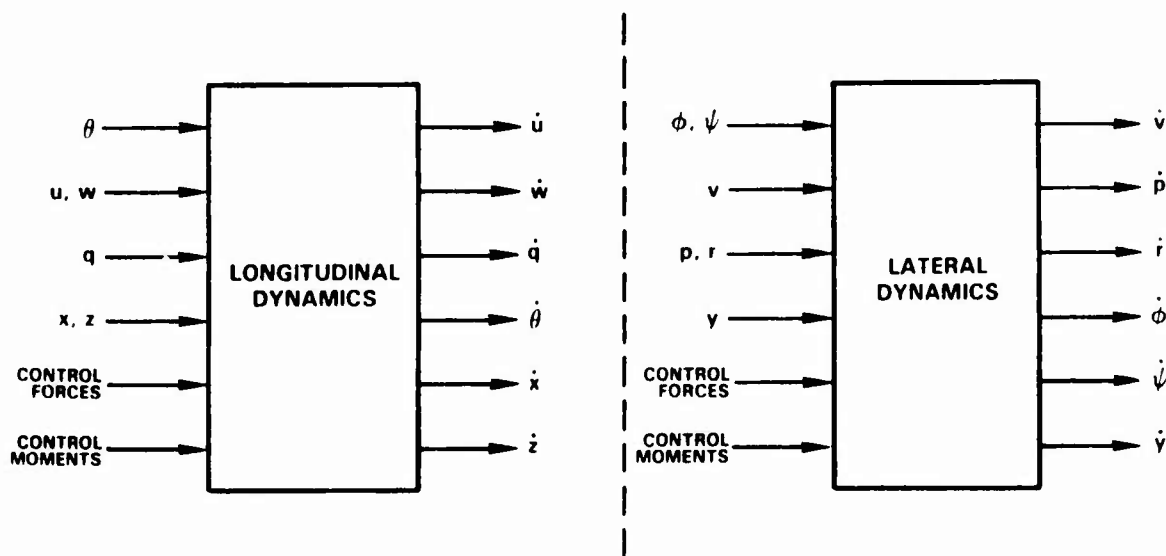


Figure 3.2-1 Canonical System Block Diagram:
Classes II and III

dynamics matrix F_e for each control augmentation (or flexible body mode) state. However, in the subsequent controllability analysis, the additional rows and columns of the Class II canonical system matrices must be ignored otherwise the Class II system would always be uncontrollable.

What is being described is an order reduction technique in which the canonical system, although it takes on the state dimensions of the full nonlinear model, is only significant in the fundamental twelve kinematic states. Consequently, the Class III approximations for two very different aircraft, e.g., one with high-order stability augmentation and one without, hence with two different total number of states would have the same number of free parameters in the Class III approximation. The flying qualities criteria, e.g., relative controllability, for the two aircraft would only be computed on the twelve kinematic states of the respective canonical system matches.

3.2.3 Class IV: Four Block Diagonal, Longitudinal-Lateral

The 4-Block Diagonal, Longitudinal-Lateral Canonical System contains a refinement of the Classes II and III canonical systems. Classes II and III were refined through the removal of free parameters in F_{lat} and F_{long} that are not physically present. Thus, Class IV more closely represents the traditional linear aircraft dynamics (e.g., Eqs. 5.13,18 to 5.13,20 in Ref. 55). The major advantage of the Class IV canonical systems is the small number of free parameters in the dynamics matrix; 25 when there are no free parameters for the augmentation states. The generic mathematical form for the Class IV canonical system is

$$\dot{\underline{x}} = \begin{bmatrix} F_1 & & & 0 \\ & F_2 & & \\ & & F_3 & \\ 0 & & & F_4 \end{bmatrix} \underline{x} + G_e \underline{u} \quad (3.2-11)$$

where

$$F_1 = \begin{bmatrix} f_1 & f_2 & 0 & f_3 \\ f_4 & f_5 & f_6 & 0 \\ f_7 & f_8 & f_9 & 0 \\ 0 & 0 & 1 & 0 \end{bmatrix} \quad (3.2-12)$$

$$F_2 = \begin{bmatrix} f_{10} & 0 \\ 0 & f_{11} \end{bmatrix} \quad (3.2-13)$$

$$F_3 = \begin{bmatrix} f_{12} & f_{13} & f_{14} & f_{15} \\ f_{16} & f_{17} & f_{18} & 0 \\ f_{19} & f_{20} & f_{21} & 0 \\ 0 & f_{22} & f_{23} & 0 \end{bmatrix} \quad (3.2-14)$$

and

$$F_4 = \begin{bmatrix} f_{24} & 0 \\ 0 & f_{25} \end{bmatrix} \quad (3.2-15)$$

The state constituents are defined as,

$$\underline{x} \triangleq [u, w, q, \theta, x, z, v, p, r, \phi, \psi, y]^T \quad (3.2-16)$$

The canonical control effectiveness matrix and the control vector constituents are identical to those for Classes II and III (cf., Eqs. 3.2-8 and 3.2-9).

The symbolic diagram in Fig. 3.2-2 illustrates the functional dependence of the state derivatives on the other states and controls. The body velocity and rotation state derivatives are formed by equations similar to the full force

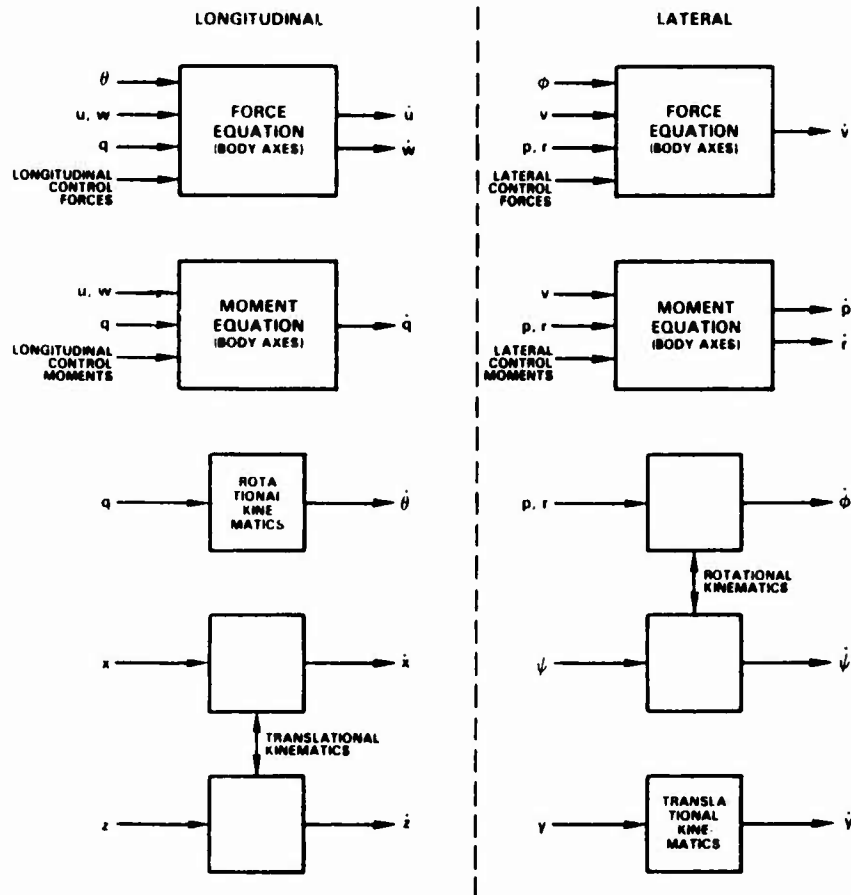


Figure 3.2-2 Canonical System Block Diagram: Class IV

and moment equations of the 6-DOF dynamics (e.g., Eq. B.2-1 and B.2-3 in Appendix B). The euler angles and inertial position state derivatives also take on a functional dependence similar to the 6-DOF equations (e.g., Eqs. B.2-2 and B.2-4 in Appendix B). As in the case of Class III, control augmentation states in Class IV are treated as additional free parameters on the diagonal of F_e .

The diagonal submatrices F_2 and F_4 when combined with the canonical control matrix structure, produce a uncontrollable canonical system regardless of the parameter values. This fact is borne out by Fig. 3.2-2 wherein it is apparent that the states, x , z , ϕ , and ψ are not affected by the controls. Nevertheless, the Class IV canonical can be used in the controllability analysis when the submatrices F_1 and F_3 alone are evaluated. Thus, the longitudinal and lateral subsystems formed by submatrices F_1 and F_3 represent the dynamics used in the computation of the relative controllability criterion to be presented in Section 3.3.

3.2.4 Class V: Fully Diagonal

One of the most appealing canonical system classes is the pure diagonal system, a system characterized by a pure diagonal dynamics matrix. Each mode (pole) in the Class V canonical system is independent and decoupled, hence representing an ideal aircraft dynamic (from a theoretical control configuration viewpoint) in which every mode can be independently adjusted. The generic form for the Class V canonical system is:

$$\dot{\underline{x}} = \begin{bmatrix} F_{kin} & | & 0 \\ \hline 0 & | & F_{aug} \end{bmatrix} \underline{x} + G_e \underline{u} \quad (3.2-17)$$

where F_{kin} is a 12×12 diagonal matrix of the kinematic states,

$$F_{kin} \triangleq \begin{bmatrix} f_1 & & & & & & & & & & & \\ & f_2 & & & & & & & & & & \\ & & f_3 & & & & & & & & & \\ & & & f_4 & & & & & & & & \\ & & & & f_5 & & & & & & & \\ & & & & & \cdot & & & & & & \\ & 0 & & & & & \cdot & & & & & \\ & & & & & & & \cdot & & & & \\ & & & & & & & & \cdot & & & \\ & & & & & & & & & f_{12} & & \end{bmatrix} \quad (3.2-18)$$

and F_{aug} is an $m \times m$ diagonal matrix of the m control augmentation states,

$$F_{aug} \triangleq \begin{bmatrix} a_1 & & & & 0 \\ & \cdot & & & \\ & & \cdot & & \\ & & & \cdot & \\ 0 & & & & \cdot \\ & & & & & a_n \end{bmatrix} \quad (3.2-19)$$

The order of the twelve kinematic states within \underline{x} is unimportant because of the independence of each mode. The control effectiveness matrix for Class V canonic system is as simple a control matrix conceivable, yet still providing controllability of the overall system. The concept is to ensure that a controllable system would ensue if the diagonal parameters (and hence eigenvalues) of the closest Class V canonical system are nonzero.* Although a diagonal control effectiveness would be ideal, the non-square matrix for the AFTI/F-16 model (12×9

*Ensuring that $G_e G_e^T$ is a diagonal matrix of the free parameters is also required.

without augmentation) precludes that possibility. The generic form finally selected is:

$$G_e = \begin{bmatrix} 0 & 0 & 0 & 0 & 0 & 0 & 0 & g_1 & g_2 \\ 0 & 0 & g_3 & g_4 & 0 & 0 & 0 & 0 & 0 \\ g_5 & g_6 & 0 & 0 & 0 & 0 & g_7 & 0 & 0 \\ g_8 & g_9 & 0 & 0 & 0 & 0 & 0 & 0 & 0 \\ g_{10} & g_{11} & 0 & 0 & 0 & 0 & 0 & 0 & 0 \\ g_{12} & g_{13} & 0 & 0 & 0 & 0 & 0 & 0 & 0 \\ 0 & 0 & 0 & 0 & g_{14} & g_{15} & 0 & 0 & 0 \\ 0 & 0 & 0 & 0 & 0 & 0 & g_{16} & 0 & 0 \\ 0 & 0 & g_{17} & g_{18} & 0 & 0 & 0 & 0 & 0 \\ 0 & 0 & 0 & 0 & g_{19} & g_{20} & 0 & 0 & 0 \\ 0 & 0 & 0 & 0 & 0 & 0 & g_{21} & 0 & 0 \\ 0 & 0 & g_{22} & g_{23} & 0 & 0 & 0 & 0 & 0 \end{bmatrix} \quad (3.2-20)$$

where the state vector constituents are (as for Class I)

$$\underline{x} \triangleq [u, v, w, x, y, z, p, q, r, \phi, \theta, \psi]^T \quad (3.2-21)$$

and the control vector constituents are (also as for Class I)

$$\underline{u} \triangleq [\delta_{TEF}, \delta_{LEF}, \delta_{VC}, \delta_R, \delta_{FA}, \delta_{HA}, \delta_H, \delta_{SP}, \delta_{SB}]^T \quad (3.2-22)$$

The Class V control effectiveness matrix conventionally models the control surfaces as pure force and moment generators (i.e., driving accelerations). However, unconventional terms are included in which the flaps (δ_{TEF} , δ_{LEF}) drive velocities and

the moment generating surfaces (δ_{VC} , δ_R , δ_{FA} , δ_{HA}) also generate rotation rates. Figure 3.2-3 depicts the relationships of the states and state derivatives of the Class V canonical system. The diagram reveals why it is necessary to create non-physical control coefficients to drive the inertial velocity and Euler angle rates. If these were not driven, the Class V system would always be uncontrollable, regardless of the closest canonical system match, hence, precluding the use of the relative controllability measure.

In summary the Class V, purely diagonal canonical system exemplifies an abstract system structure almost completely lacking a physical basis. However, it is easily the most tractable of all the canonical system classes considered thus far,

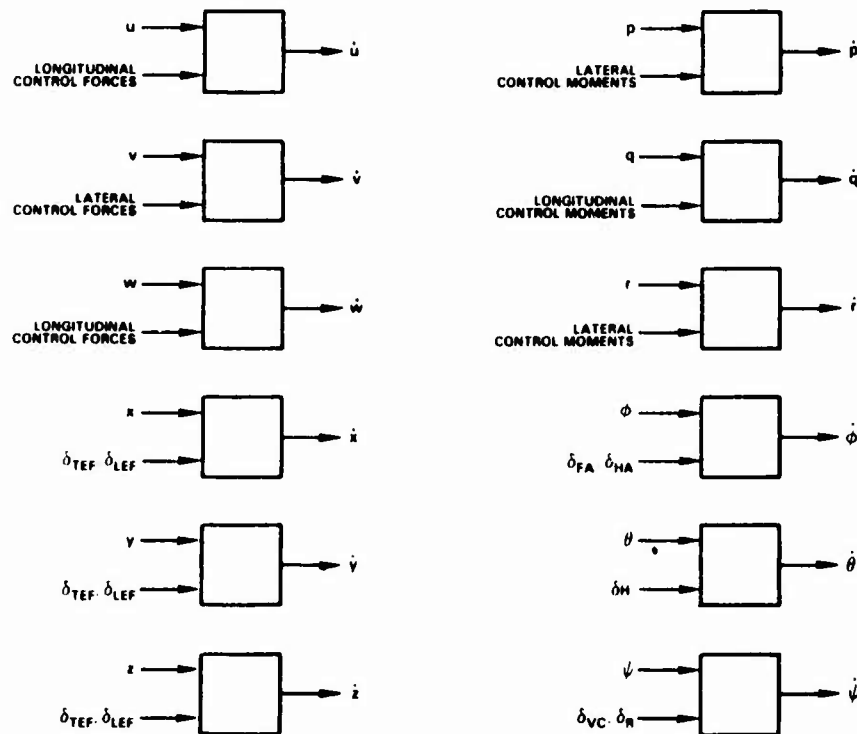


Figure 3.2-3 Canonical System Block Diagram: Class V

with only 12 (plus nonzero augmentation) parameters in the dynamics matrix and 23 parameters in the control effectiveness matrix. The relatively few parameters enhances the potential for flying qualities criteria directly based on the free parameters of F_e . Nevertheless, the ultimate usefulness of Class V depends on its ability to match a given, true-linearized dynamics matrix. The comparative performance of the candidate canonical system classes in matching the true dynamics is the subject of the succeeding section.

3.3 NUMERICAL RESULTS

The numerical results presented in this section pertain to two large-amplitude maneuvers. The canonical systems analysis methodology was applied to each maneuver and evaluated for:

- Performance of the closest canonical system with regard to the norms $||\Delta F||$ and $||\Delta G||$ and the perturbed trajectory, $\underline{f}(\underline{x}, \underline{u} + \delta \underline{u}, t)$
- Sensitivity of the relative controllability index over the trajectory and the correlation with the quality of canonical system match.

The criterion evaluates the effectiveness of the closest canonical system and its distance from the linearized system. The closest canonical system is considered a good match if the trajectory of $\underline{x}(\underline{f}(\underline{x}, \underline{u} + \delta \underline{u}, t))$ lies within a neighborhood of $\underline{x}(\underline{f}(\underline{x}, \underline{u}, t))$ for identical initial conditions. The relative controllability index is then computed and its correlation with the magnitudes of $||\Delta F||$ and $||\Delta G||$ and the difference in the true and perturbed trajectory ($\delta \underline{x}(\delta \underline{u})$) evaluated. The goal was to observe how well the relative controllability index gauged the canonical system approximation of the true dynamics.

3.3.1 Sample Maneuver Description

The sample maneuvers which were employed in the numerical evaluation were:

- A wind-up turn at approximately Mach .9 and 10,000 feet altitude, evaluated for 30 seconds
- A rolling-reversal at Mach .9 and 10,000 feet altitude evaluated for 7 seconds.

The wind-up turn was generated by commanding a normal acceleration,

$$a_n = g \cos \gamma / \cos \phi \quad (3.3-1)$$

which maintains a turn in the horizontal plane. The effective turn rate is,

$$\dot{\zeta} = a_n \sin \phi / v_m \quad (3.3-2)$$

As v_m decreases, the required angle of attack continues to increase: a non-steady flight trajectory. Graphs of significant variables of the first 20 seconds of the wind-up turn, from here on labeled maneuver I, are contained in Fig. 3.3-1. The angle of attack is not increasing in this trajectory because a steady-state error in the acceleration autopilot prevents the aircraft from achieving the acceleration stipulated by Eq. 3.3-1. Thus, the turn is beginning to degenerate into a spiral dive, the attendant increase in negative flight path angle reducing the normal acceleration required to maintain the turn.

The second maneuver investigated, Maneuver II, is a rolling reversal. At $t=1$ second the aircraft begins a rapid

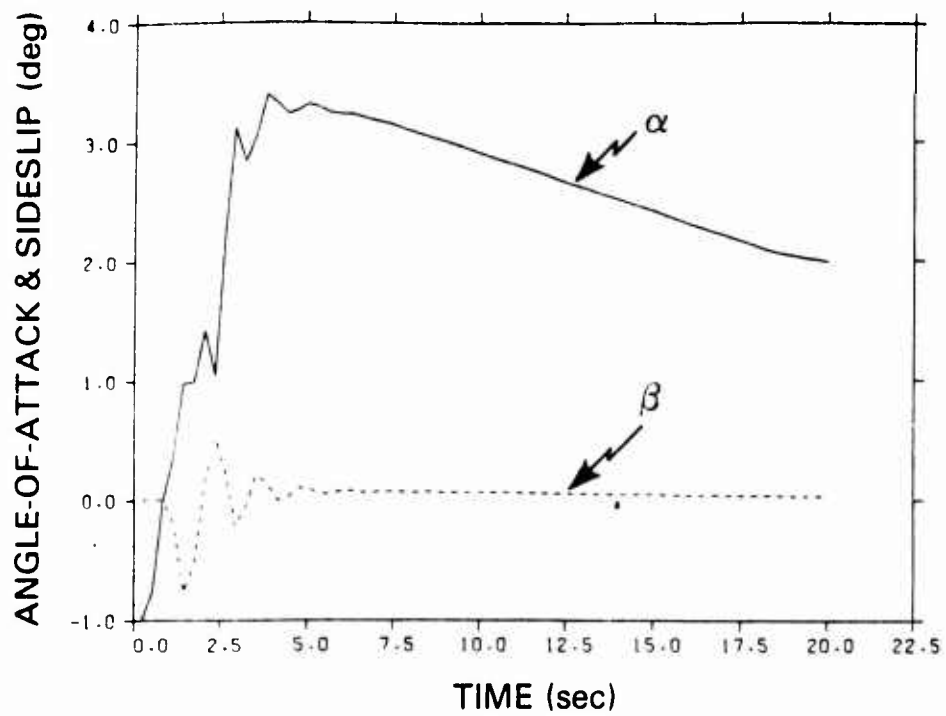
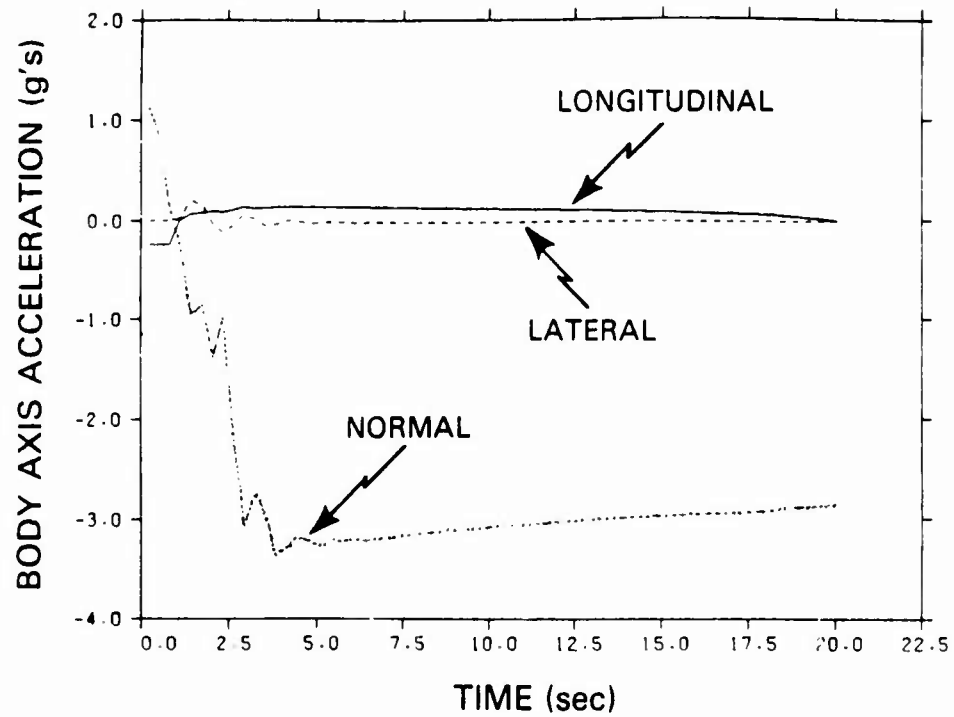


Figure 3.3-1 Maneuver I: Wind-Up Turn
(First 20 seconds)

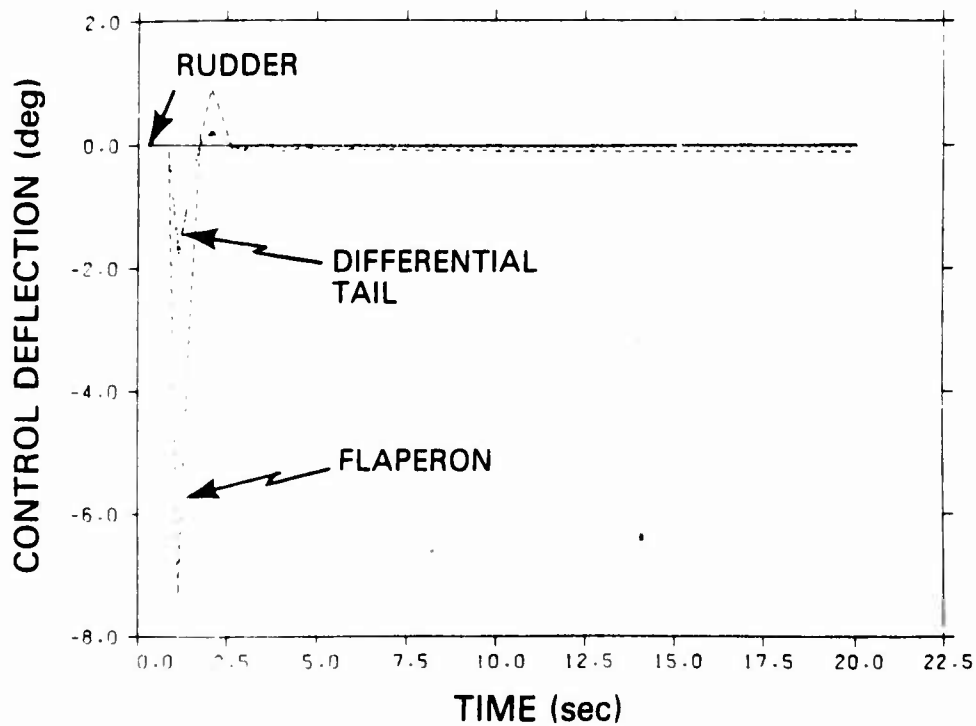
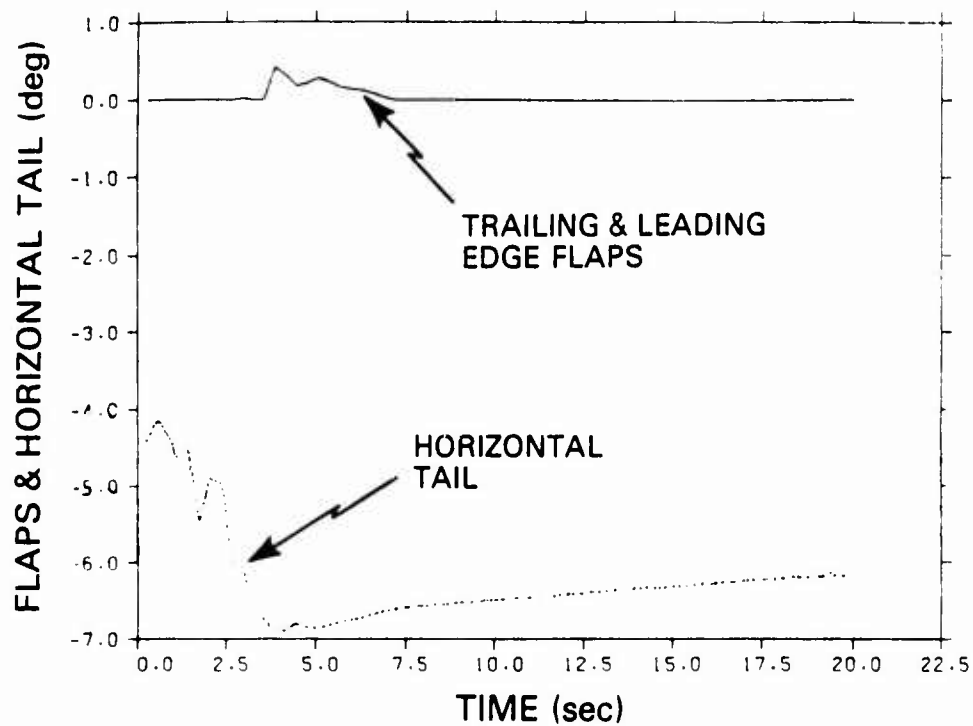


Figure 3.3-1 Maneuver I: Wind-Up Turn
(First 20 seconds) (Continued)

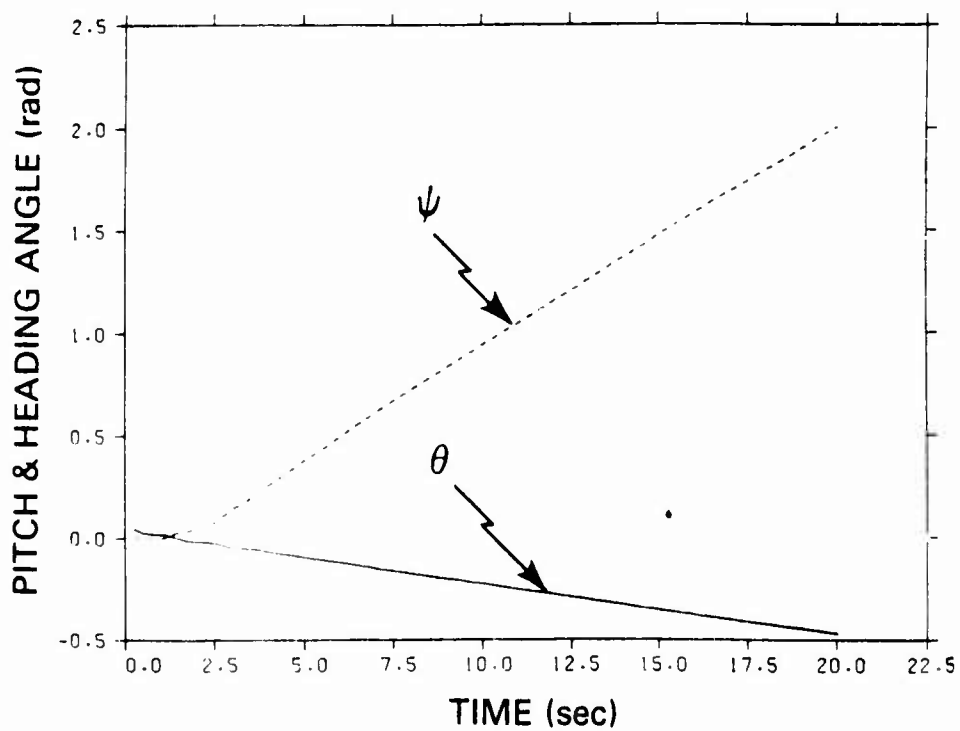
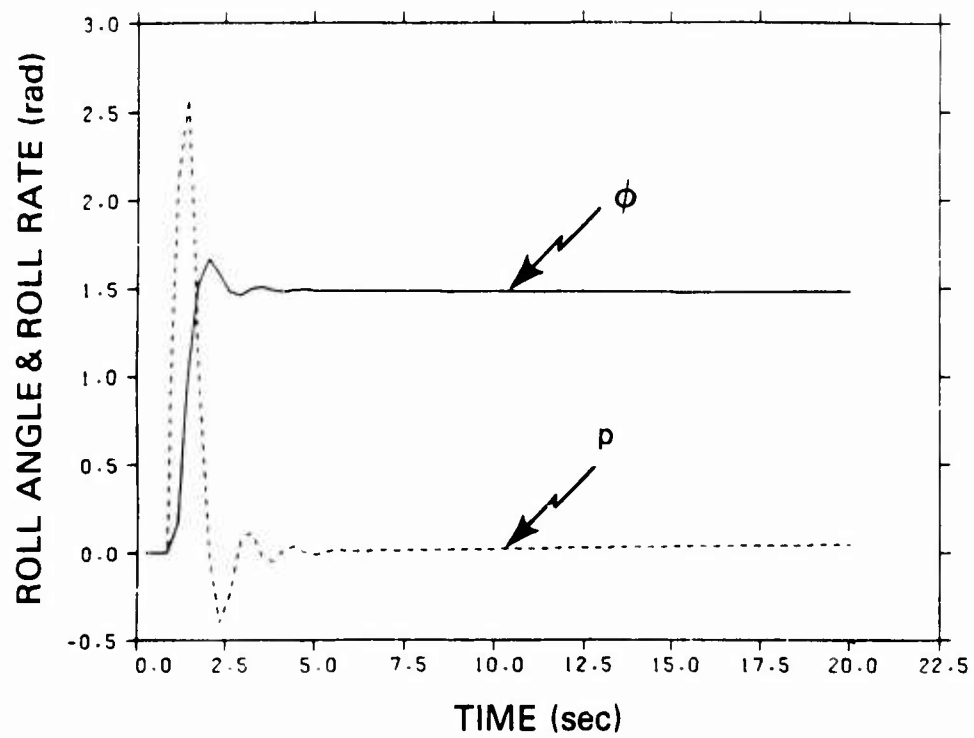


Figure 3.3-1 Maneuver I: Wind-Up Turn
(First 20 seconds) (Continued)

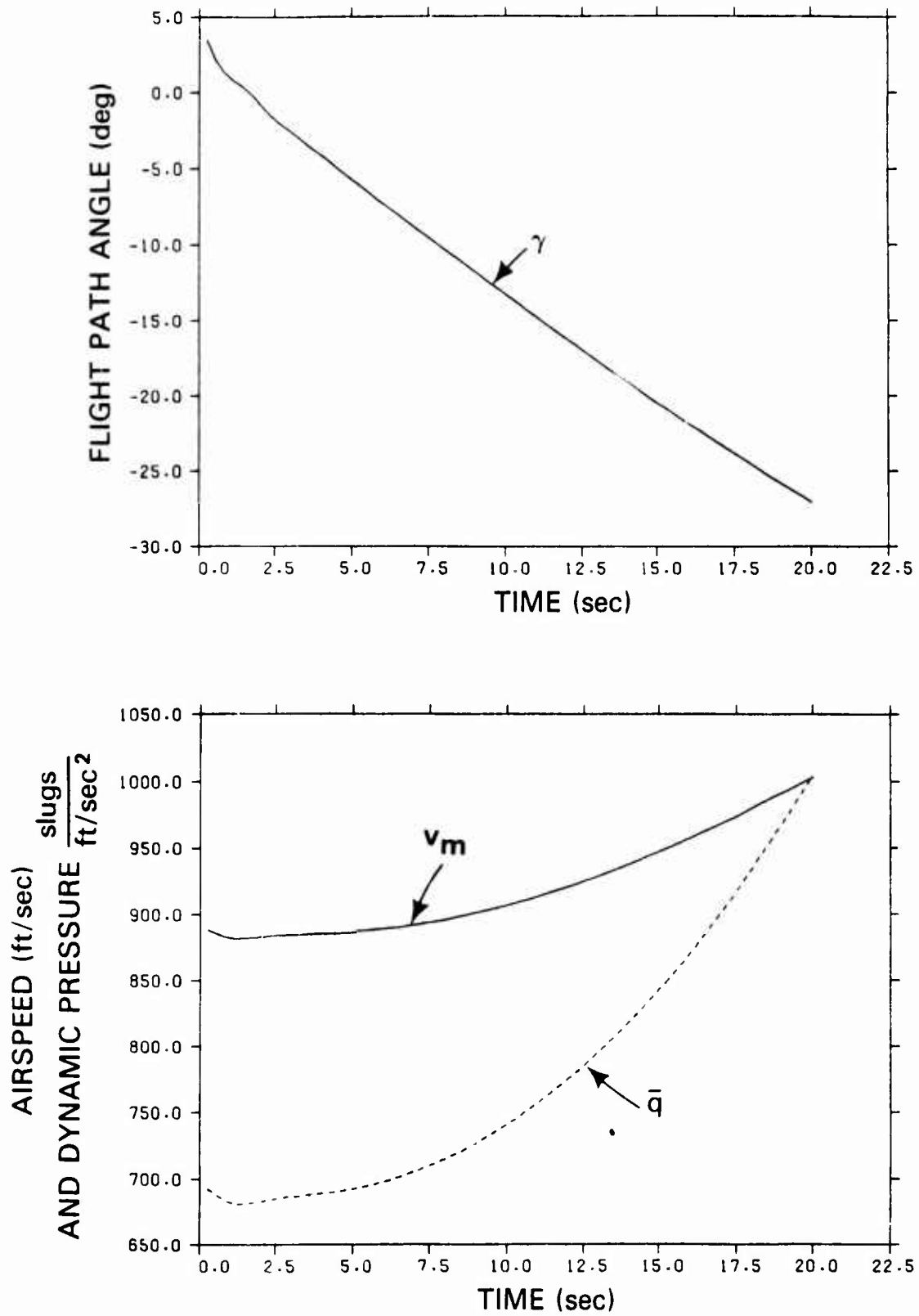


Figure 3.3-1 Maneuver I: Wind-Up Turn
(First 20 seconds) (Continued)

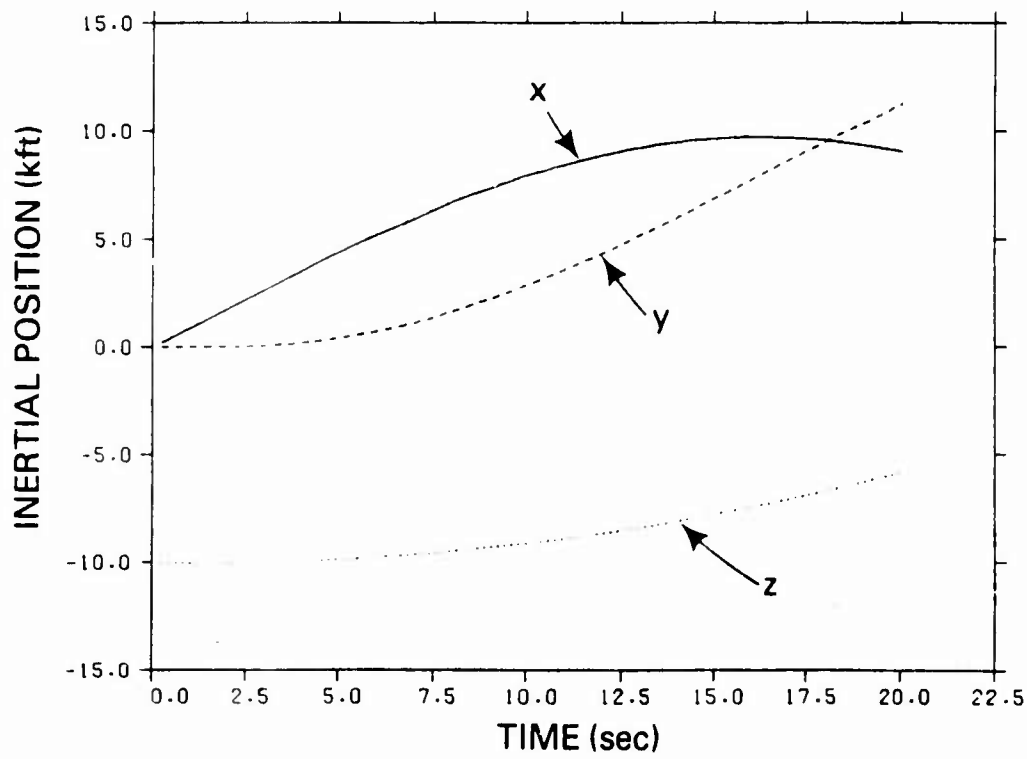
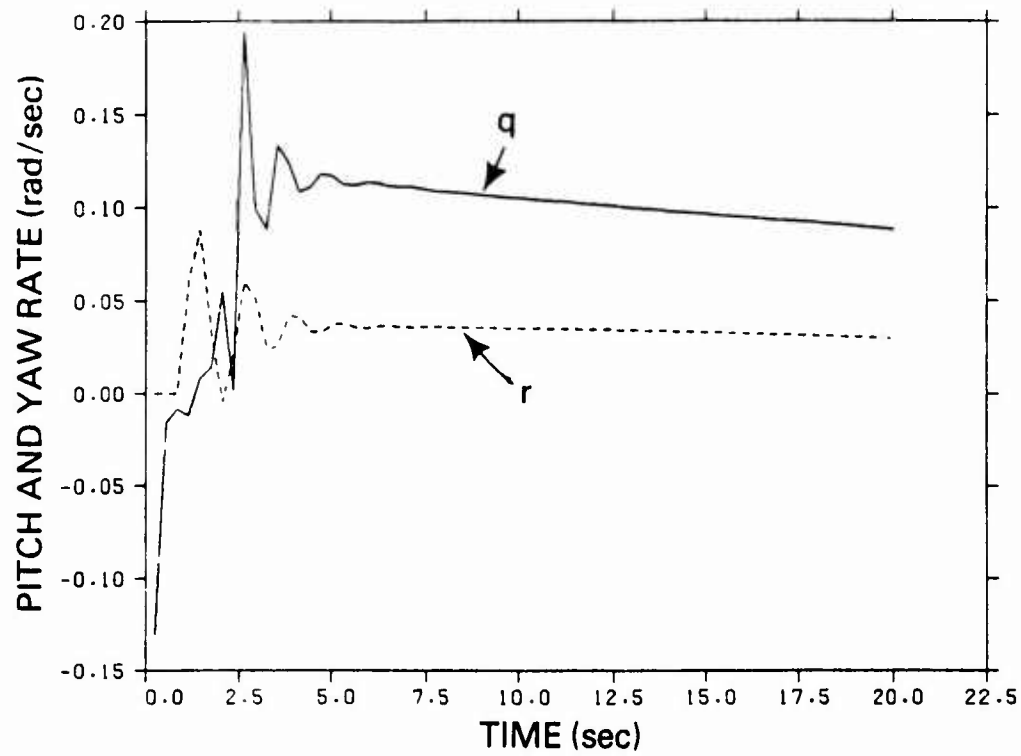


Figure 3.3-1 Maneuver I: Wind-Up Turn
(First 20 seconds) (Concluded)

pull-up followed by a 360 deg roll initiated at $t=1.5$ sec. Figure 3.3-2 contains simulation traces of the rolling reversal. Maneuver II is a more severe nonlinear maneuver for the canonical system analysis because of the high rotational rates involved, the short duration of the roll rate pulse, and the excitation of the Dutch Roll mode (the lateral dynamics were not augmented to improve the Dutch Roll damping, hence the underdamped response in sideslip).^{*}

3.3.2 Maneuver I Canonical System Analysis

The canonical systems analysis of Maneuver I included Classes III and IV. Figures 3.3-3 and 3.3-4 contain graphs of the ratios $||\Delta F||/||F||$ and $||\Delta G||/||G||$ versus time. The relative controllability versus time is also presented.

The upper plots of both Figs. 3.3-3 and 3.3-4 contain curves of the norms of the differences between the true canonical systems for both the F and G matrices. Note the different scales for both $||\Delta F||$ and $||\Delta G||$ and that the curves for $||\Delta G||$ are identical in both figures.[†] The curves of $||\Delta F||$ and $||\Delta G||$ are normalized by the norms of F and G to yield a curve which is indicative of the suitability of the match. The bounds on $||\Delta x(t)||$ derived in Chapter 2 suggest that $||\Delta F||$ be as small as possible while the ratio $||\Delta F||/||F||$ should be less than one. The Class III canonical system match (Fig. 3.3-3) exhibits this property for all of trajectories except between approximately 12 and 20 seconds. The Class IV canonical match maintains a ratio just less than one throughout the maneuver. Although

^{*}However, both maneuvers were executed with a unity feedback of roll attitude in the roll channel and a three gain one-state acceleration autopilot in the pitch channel.

[†]Recall that Classes III and IV have the same structure for the canonical control effectiveness matrix.

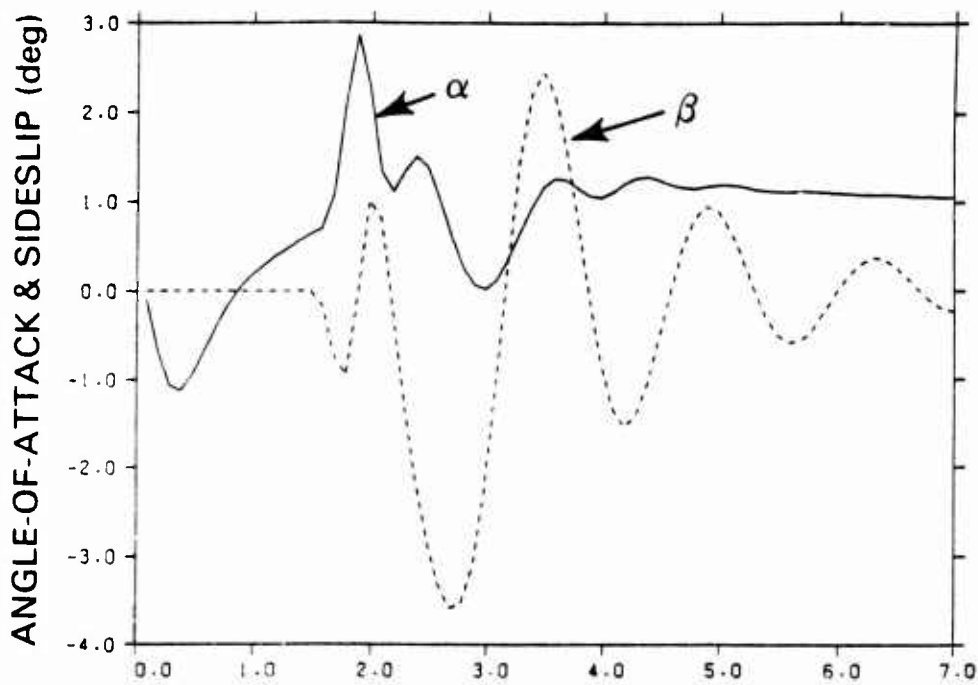
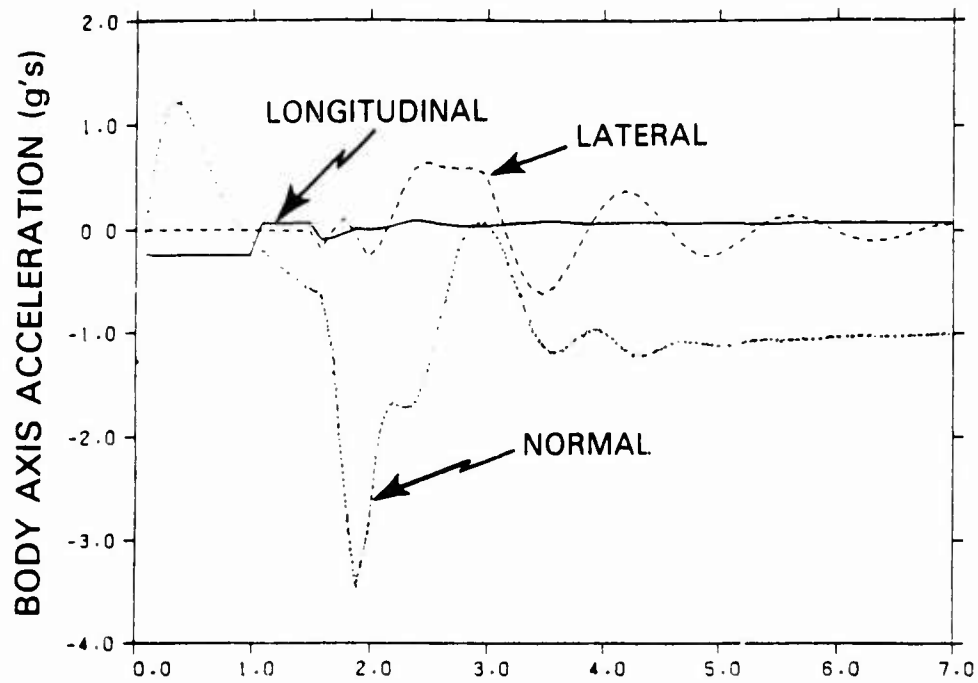


Figure 3.3-2 Maneuver II: Rolling Reversal

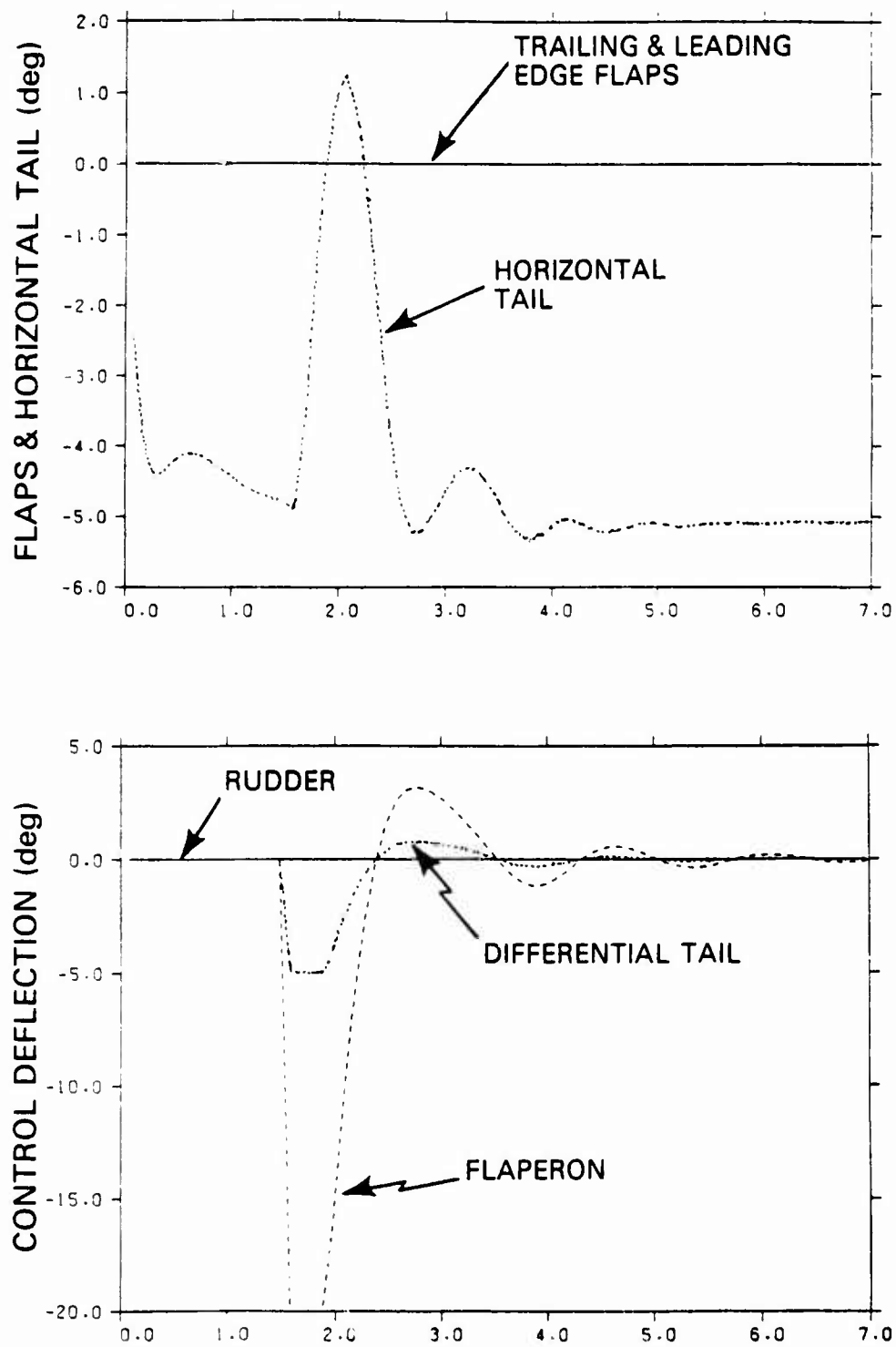


Figure 3.3-2 Maneuver II: Rolling Reversal
(Continued)

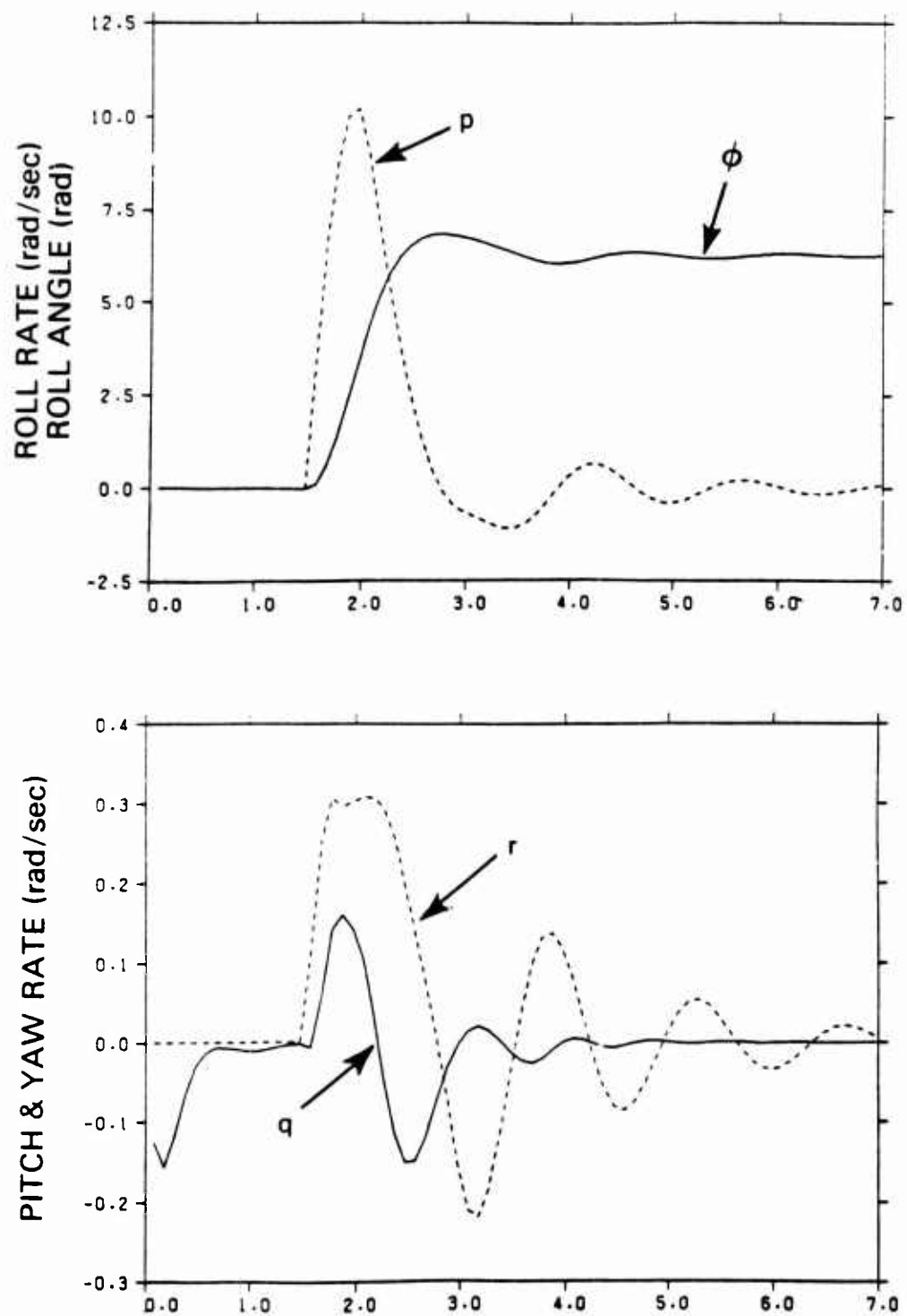


Figure 3.3-2 Maneuver II: Rolling Reversal
(Continued)

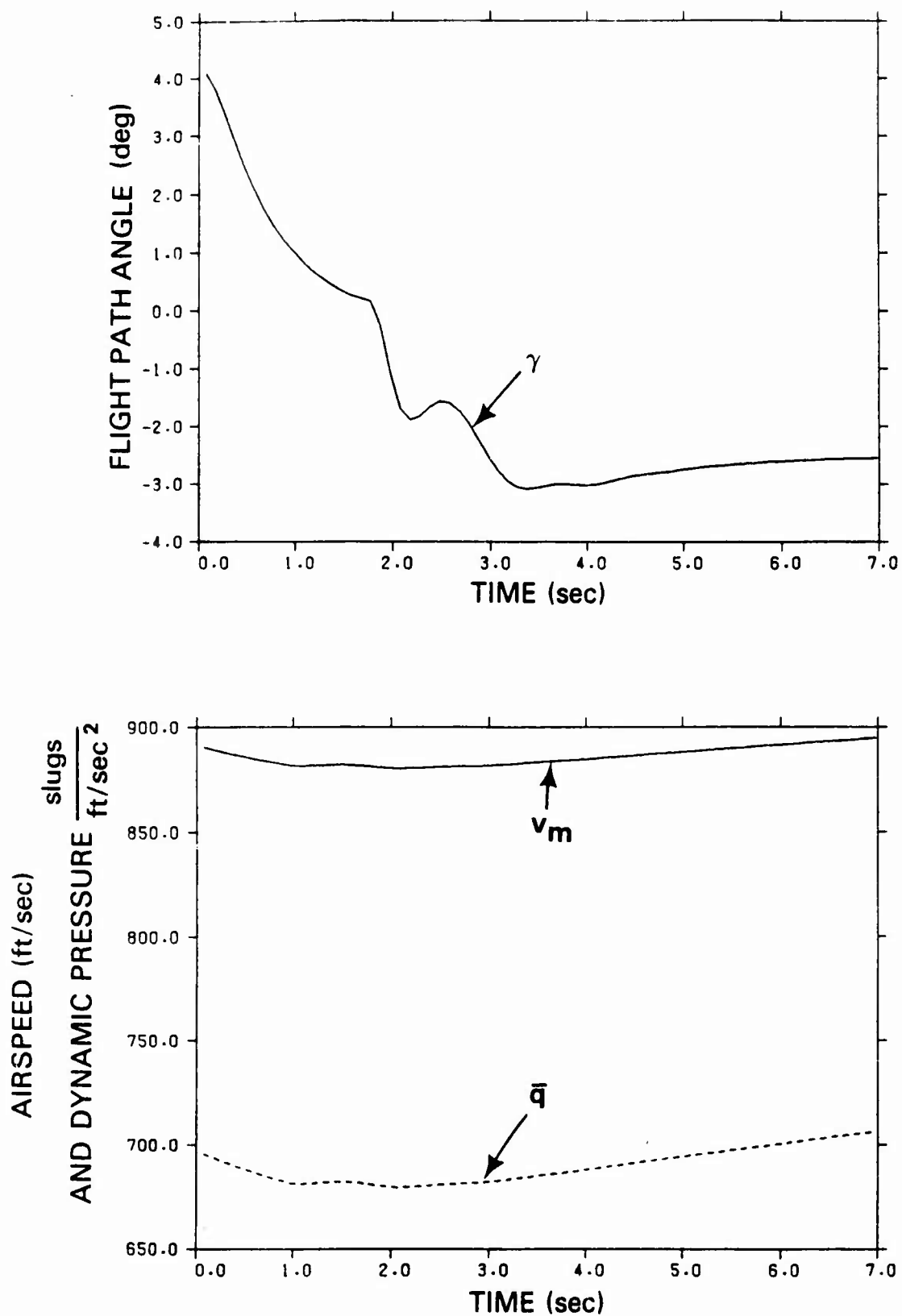


Figure 3.3-2 Maneuver II: Rolling Reversal
(Continued)

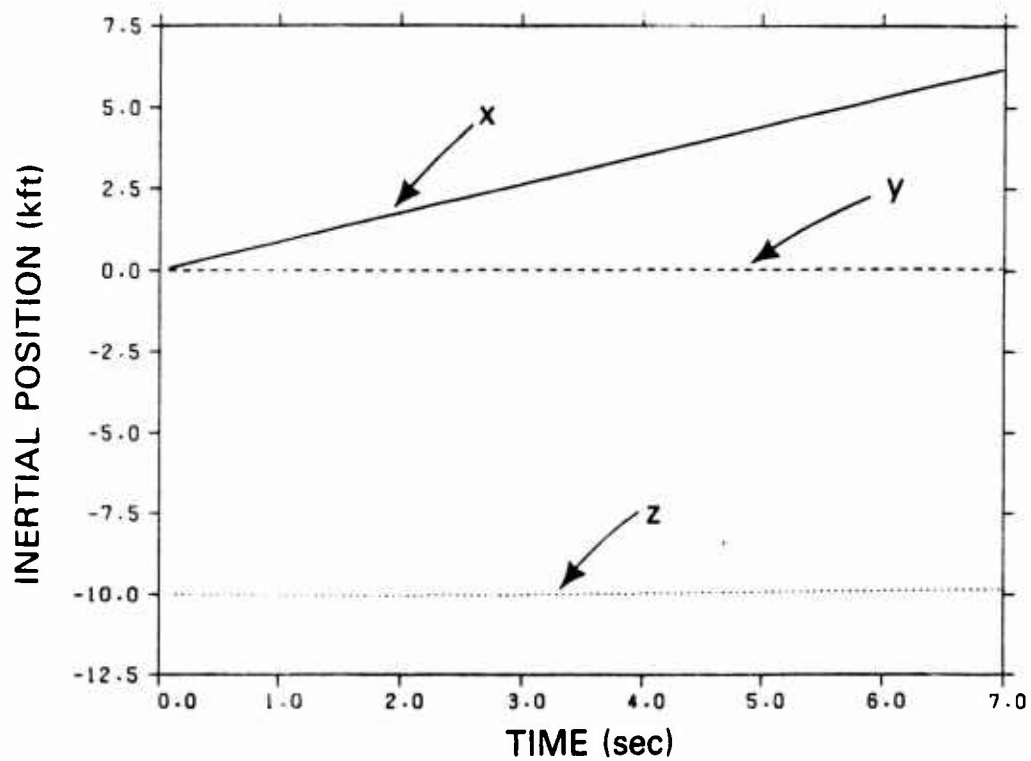
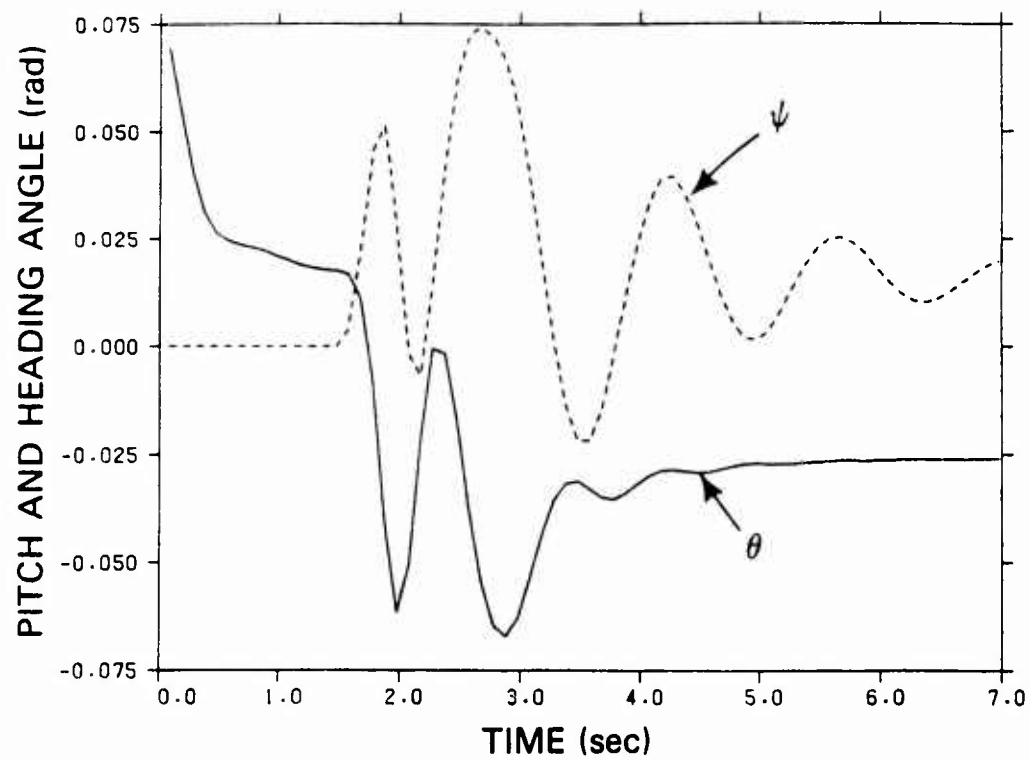


Figure 3.3-2 Maneuver II: Rolling Reversal (Concluded)

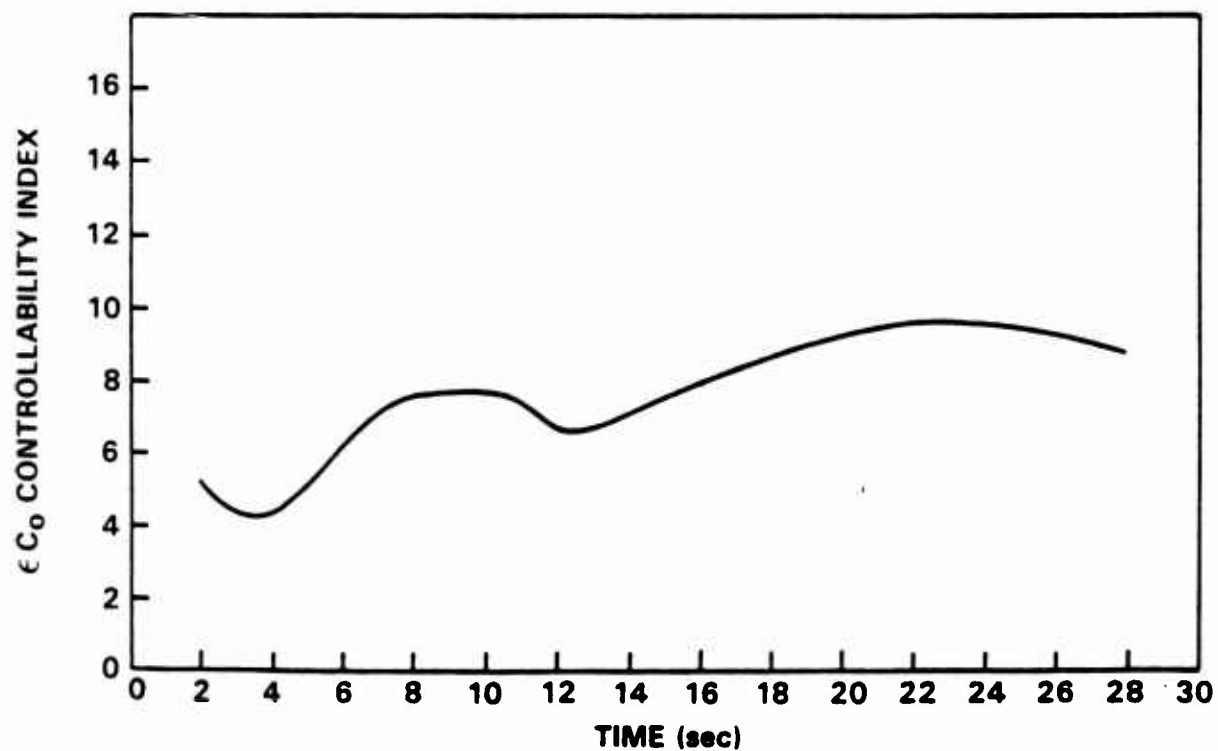
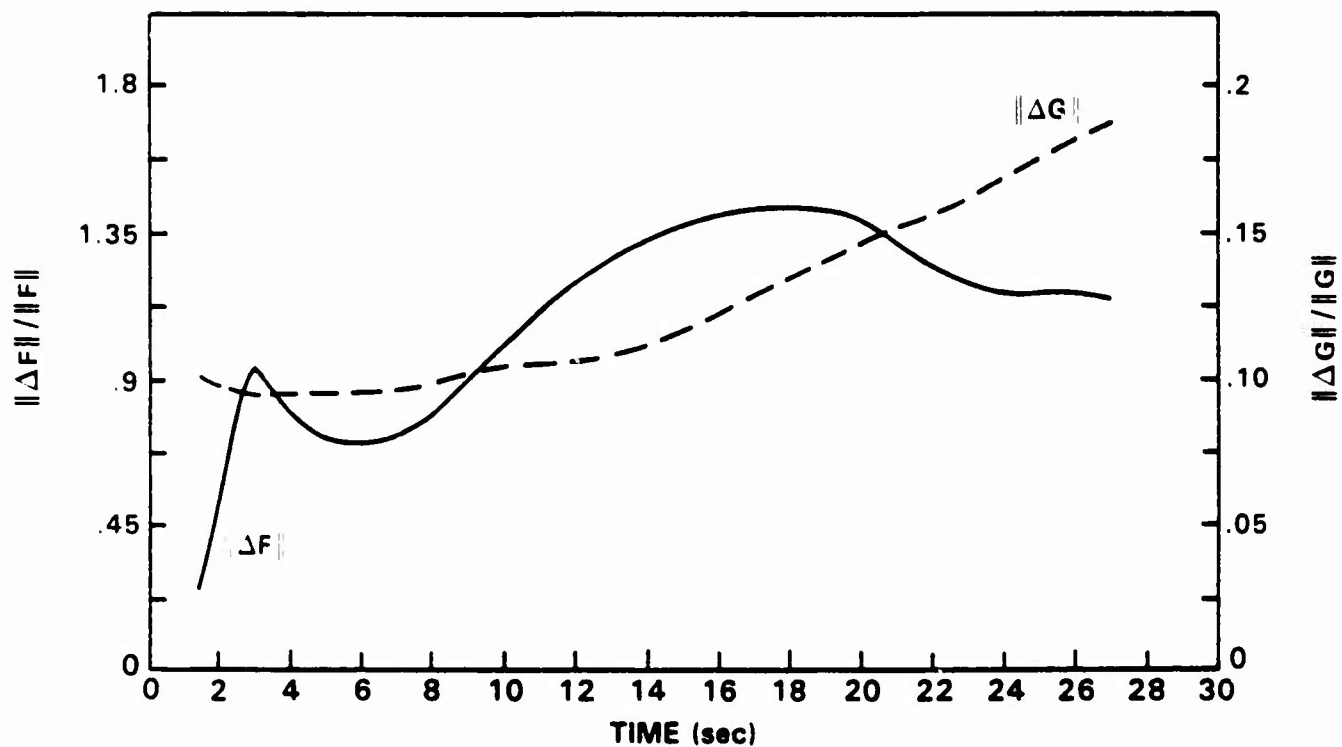


Figure 3.3-3 Maneuver I: Class III Canonical System Analysis

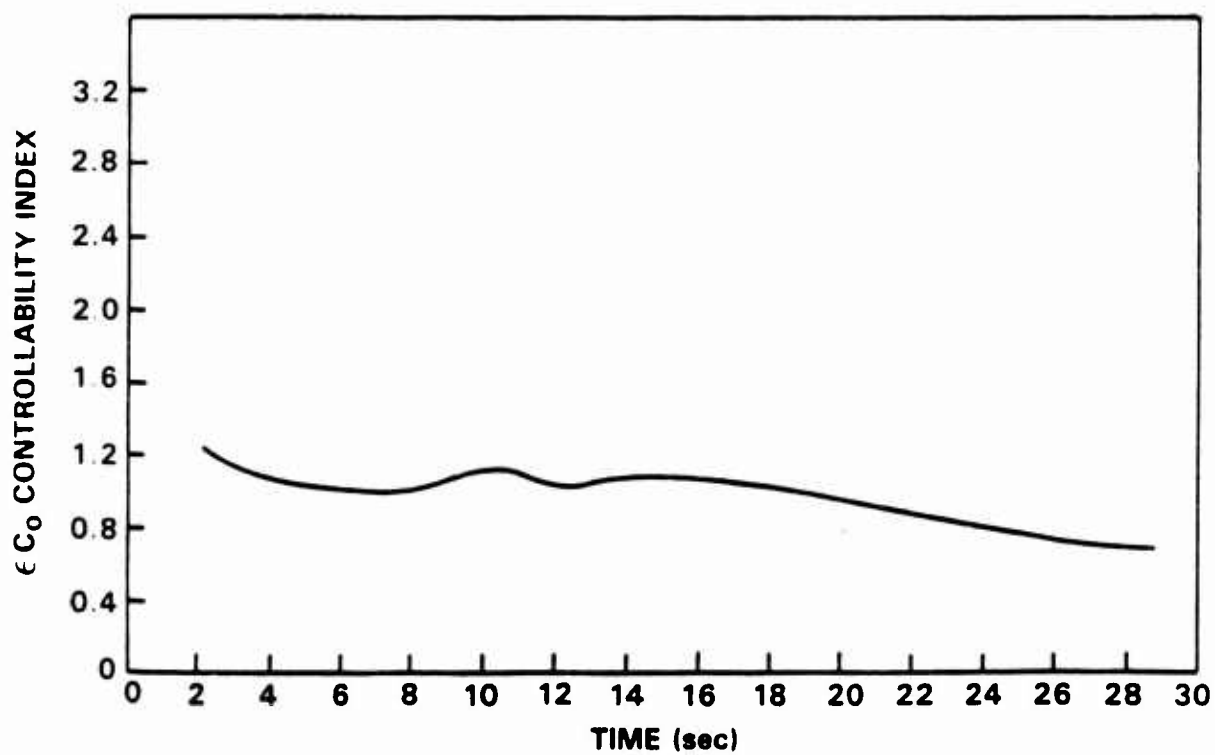
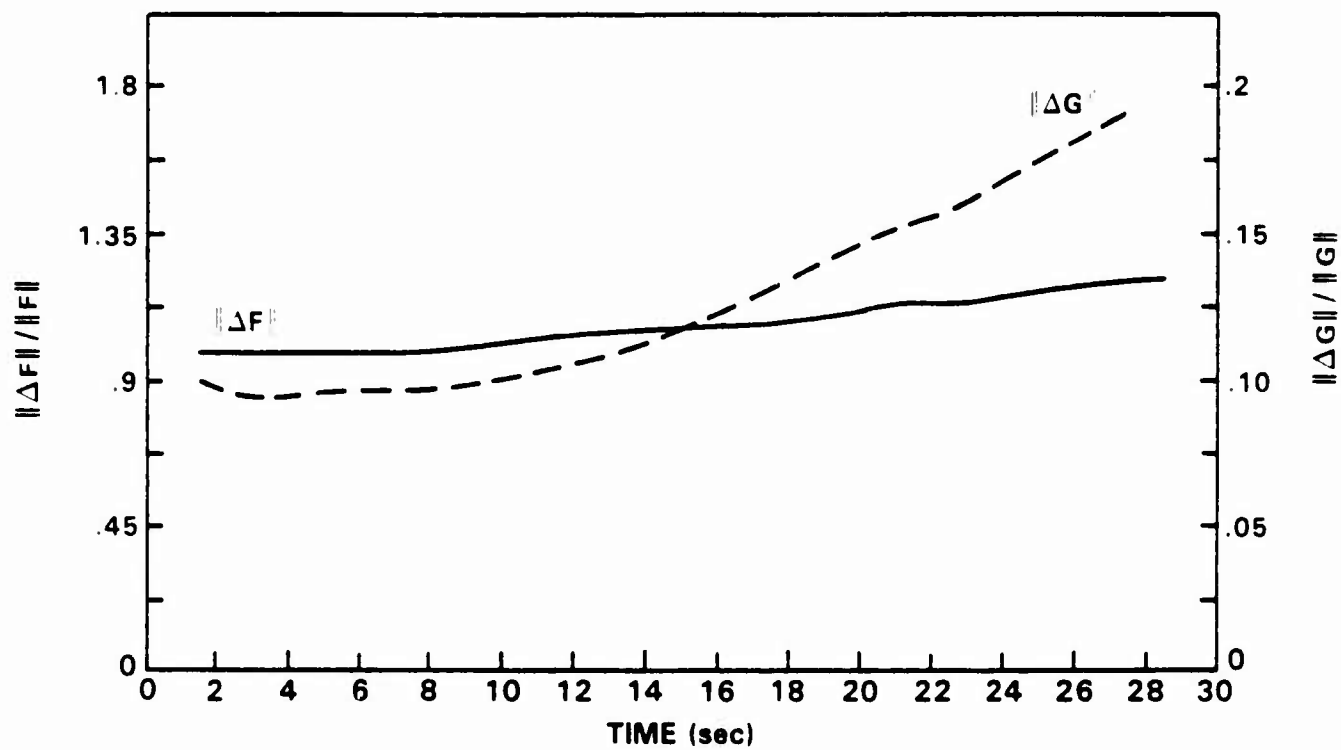


Figure 3.3-4 Maneuver I: Class IV Canonical System Analysis

the two canonical system matches meet the analytical requirements for generating a trajectory near the true perturbed dynamics trajectory, the smaller values of the dynamics matrix ratio and the apparently greater sensitivity (i.e., greater dynamic behavior) of the Class III match suggest that the Class III structure is preferable to the Class IV. The Class IV match exhibits a dynamic matrix ratio which is nearly constant over the trajectory and is close to one. However, a careful investigation revealed that the behavior of the Class III and Class IV matches actually reveals that the Class IV structure is superior.

The changes in the Class III match have been traced to changes in the heading angle during the wind-up turn. As the aircraft changes heading (initial condition is zero degrees), the position state derivative \dot{x} is no longer a function of u . Instead \dot{y} becomes a function of u since the flight path becomes aligned with the inertial y axis as the heading approaches 90 degrees. However, the position state decoupling in the Class III structure, i.e., x and z are in the longitudinal block and y is in the lateral block of Eq. 3.2-6, prevents the y inertial position derivative from ever being a function of u . Hence, the Class III structure is only valid for small heading angles about 0 or ± 180 degrees. A similar problem occurs when there are significantly nonzero roll angles; in that case \dot{y} should become a function of the normal body axis velocity w as well as the sideslip velocity v , however, Eq. 3.2-6 precludes this. This effect is much smaller than the heading angle dependence because w and v are small compared to u for the angle-of-attack magnitudes present in Maneuver I.

The Class IV canonical system structure also mandates longitudinal-lateral decoupling. However, the Class IV structures also decouples the position states completely, i.e., the diagonal submatrices in Eqs. 3.2-13 and 3.2-15. Hence, the

parameters f_{10} , f_{11} , and f_{24} in Eqs. 3.2-13 and 3.2-15 represent the uncoupled modal values of the position states directly without dependence on u , v , or w . Thus, when the heading angle approaches 90 degrees, the x position mode (f_{10}) approaches zero; the velocity of the aircraft is normal to the x inertial axis and no growth in that state should occur. Similarly, when the heading angle is near 0 degrees or 180 degrees the modal value of x (f_{10}) is similar but opposite in sign; when $\psi = 0$ degrees x should be increasing but when $\psi = 180$ degrees, x should be decreasing. Consequently, the increased dynamic behavior of the Class III canonical system match versus the Class IV match and the fact that the Class III ratio exceeds one during part of the maneuver indicate that the Class III is less suited than the Class IV structure for matching the dynamics of a wind-up turn.

Finally, note that $||\Delta G||$ appears to be monotonically increasing. This can be traced to a dependence on u_0^2 . Because the airspeed is approaching Mach 1, the tendency of both $||\Delta F||$ and $||\Delta G||$ to increase for Class IV case may be due to the onset of transonic aerodynamics. In general, the small value of the control effectiveness matrix ratio indicates an excellent match. However, it must be noted that since the AFTI/F-16 model has minimal control cross-coupling (see Eqs. A.2-11 to A.2-16) the canonical control matrix in Eq. 3.2-8 has a structure almost identical to the true G matrix. The most significant cross-coupling in AFTI/F-16 model is in the leading and trailing edge flap deflections; however, Fig. 3.3-1 reveals that during Maneuver I the flaps are almost always zero.

3.3.3 Maneuver II Canonical System Analysis

Figures 3.3-5 and 3.3-6 contain the results of the Maneuver II canonical systems analysis. Once again, plots of

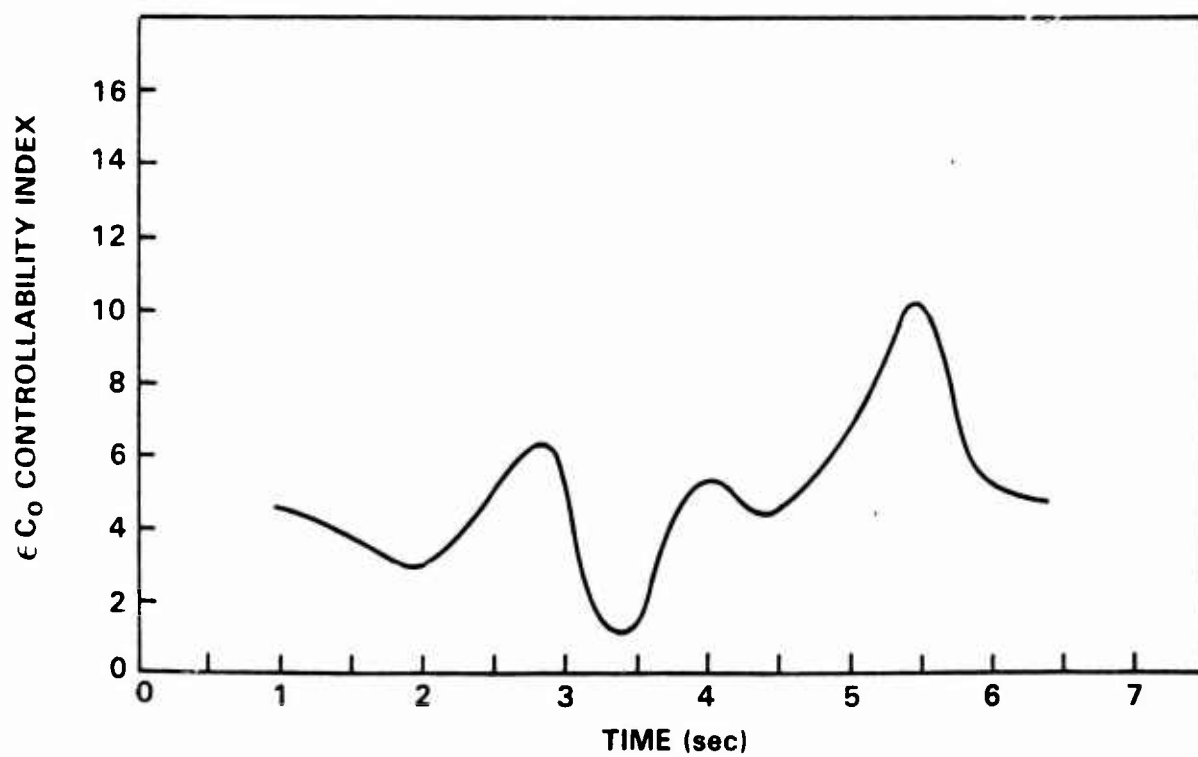
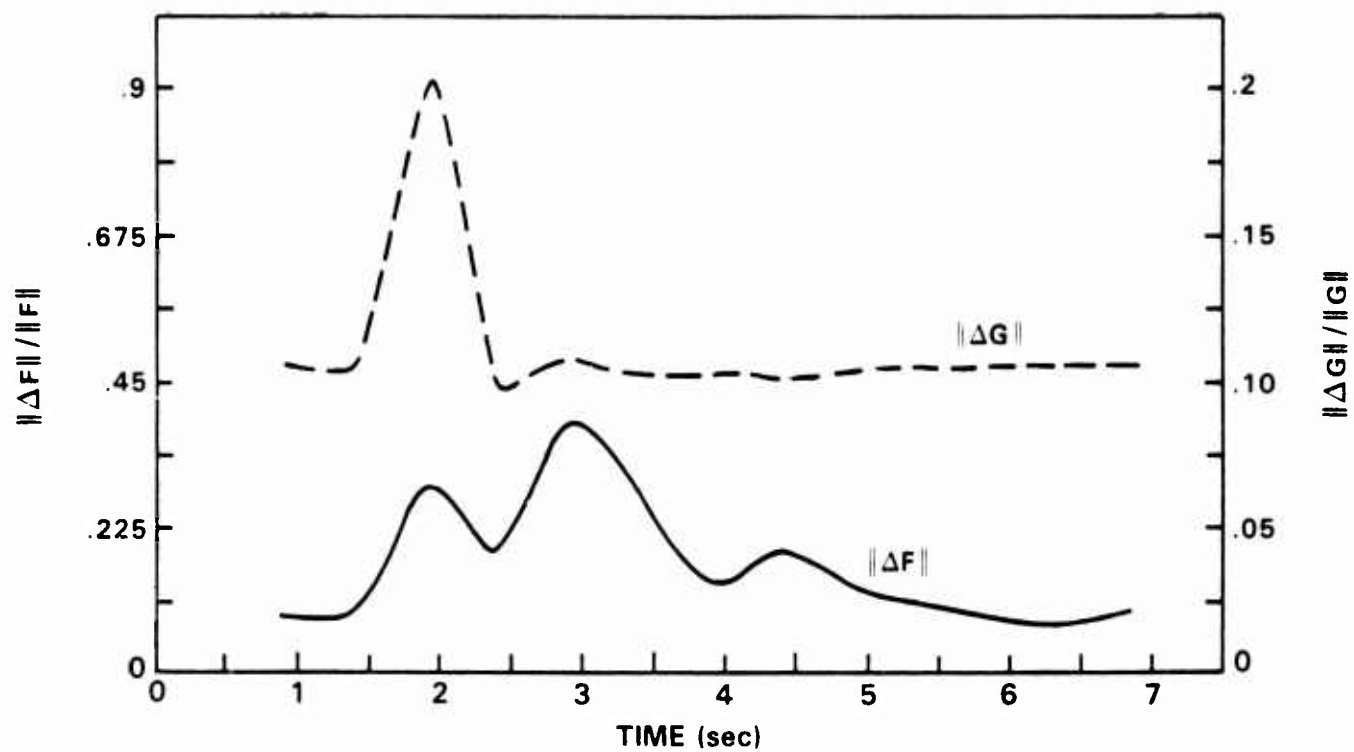


Figure 3.3-5 Maneuver II: Class III Canonical System Analysis

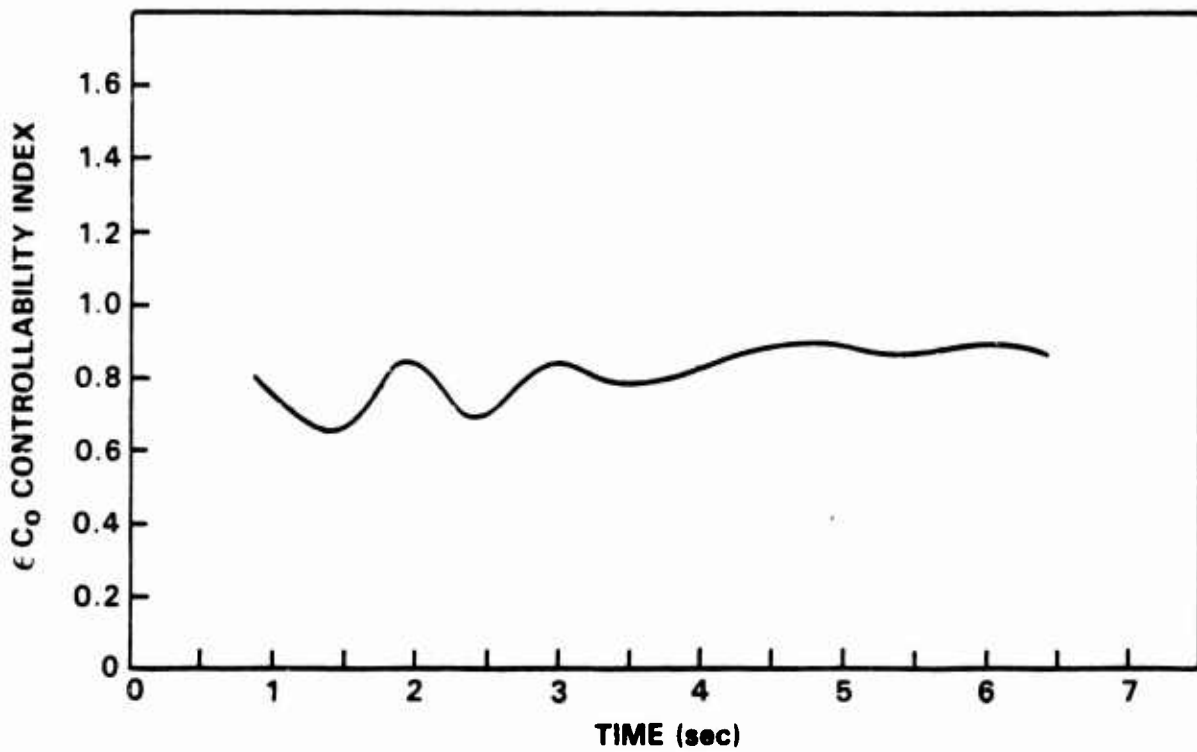
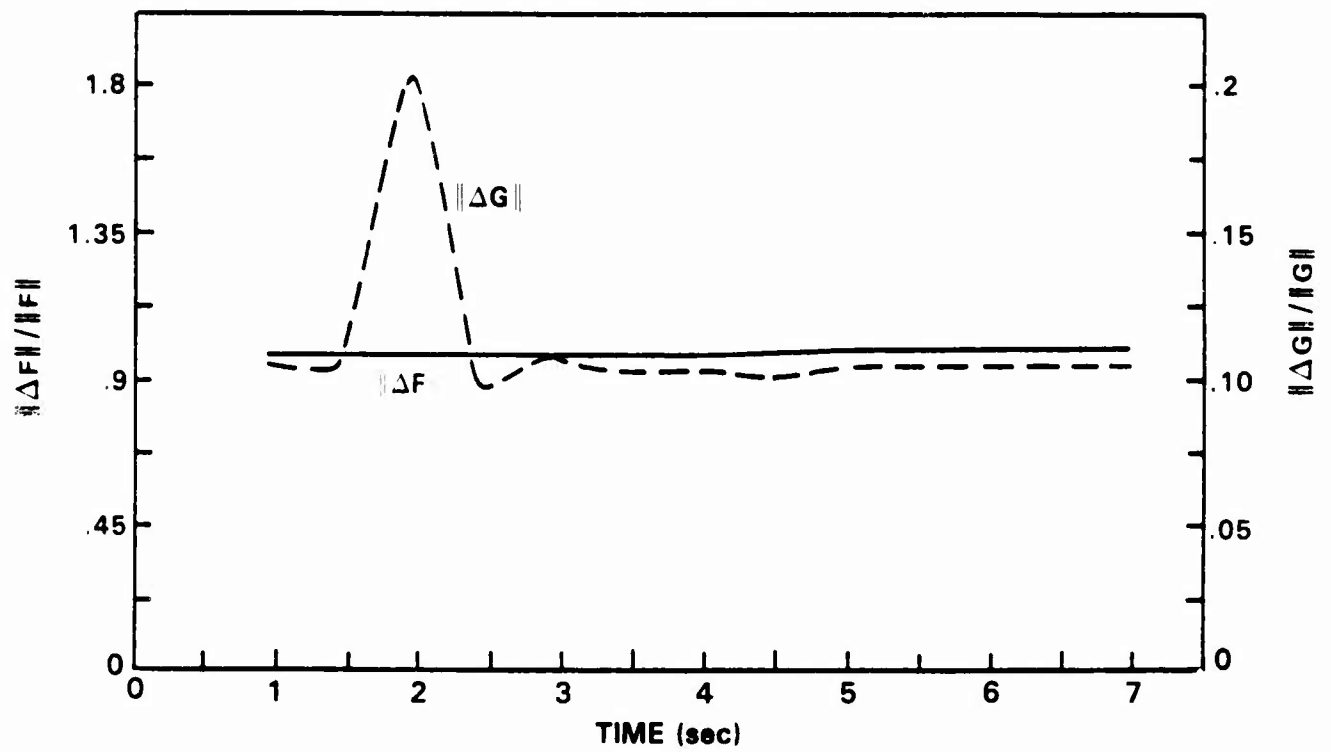


Figure 3.3-6 Maneuver II: Class IV Canonical System Analysis

the norms of the closest canonical system and the relative controllability index are included. The rolling-reversal analysis provides some distinctively different results. First, $||\Delta G||$ has a large excursion during the most coupled portion of the maneuver, (when p , q , and r are at a maximum). Thus indicating the inadequacy of the longitudinal-lateral control decoupling of the canonical control matrix to model the true-linearized control matrix.

The dynamics matrix norms $||\Delta F||$ for both canonical system classes are remarkably different. Not only are the magnitudes different (unlike the maneuver I analysis) but the Class III canonical system changes more during the trajectory. However, the trajectory for the rolling reversal maintains a near zero heading angle throughout the maneuver, thus the Class III does not suffer from the inadequacy just described in the Maneuver I analysis. Hence, the greater dynamic behavior and smaller dynamics matrix ratios for the Class III match versus the Class IV match are welcomed. The changes in $||\Delta F||$ in Fig. 3.3-5 appear to track the underdamped Dutch-roll oscillation excited in this maneuver (see Fig. 3.3-2). Although the Class IV canonical system structure contains elements that can model the Dutch-roll mode (i.e., Eq. 3.2-14) apparently $||\Delta F||$ is insensitive to these changes. Hence, one finds that the more abstract canonical system structure (Class III) is more sensitive to the time-varying dynamics than the structure (Class IV) that more closely approximates the linearized-dynamic equation structure.

The relative controllability index profiles exhibited in Figs. 3.3-5 and 3.3-6 reflect the $||\Delta F||$ and $||\Delta G||$ activity as expected. Recall that the relative controllability index is a function of both $||\Delta F||$ and $||\Delta G||$ hence, although the Class III and Class IV system matches have distinctly different

dynamic matrices, the fact the canonical control matrices are the same softens the differences in εC_0 . The Class IV analysis does exhibit a smoother curve than the Class III analysis, the important difference is the average magnitude of εC_0 . The larger εC_0 for the Class III canonical system indicates less sensitivity (or vice/versa more controllability) with respect to the Class IV system. Thus, the Class III canonical system better preserves the controllability properties of the linearized system, and thus, measures the controllability of the non-linear aircraft dynamics.

3.4 CONCLUDING REMARKS

This chapter has presented a brief suite of numerical results obtained through the application of the NFQ formulation described in Section 2.3. Although the number of experiments was restricted, there is sufficient data to conclude that the canonical systems technique provides a multivariable, time-domain equivalent systems methodology. The same questions that arise in the application of equivalent systems applies to the canonical systems based, NFQ analysis. The most persistent issues are:

- Upon what basis is a canonical (equivalent) system structure derived and which parameters are to be free in the matching process
- What values of the matching process norms, e.g., $||\Delta F||$ and $||\Delta G||$ for canonical systems, imply a satisfactory match.

The first issue was directly addressed in the statement of objectives for the NFQ formulation outlined in Section 2.4.1.

The results obtained to date have indicated that the Class III and Class IV canonical systems meet the objectives of Section 2.4.1.

The second issue, the relevance of the magnitudes of $||\Delta F||$ and $||\Delta G||$, can only be resolved through the empirical investigation of the ratios $||\Delta F||/||F||$ and $||\Delta G||/||G||$, the magnitude of the trajectory deviation $||\Delta \underline{x}(t)||$ for each maneuver, and the sensitivity of pilot opinion to these deviations. Although an analytical approach to this problem is discussed in Sections 2.1 and 2.2 where upper bounds for $||\Delta \underline{x}(t)||$ as a function of $||\Delta F||$, $||\Delta G||$, $||F||$, and $||G||$ are derived, the magnitudes of $||\Delta \underline{x}(t)||$ observed were much smaller than the bounds. The empirical results suggest that a high quality match is obtained, i.e., $||\Delta \underline{x}(t)||/||\underline{x}(t)||$ is less than 10%, when $||\Delta F||/||F||$ and $||\Delta G||/||G||$ are 25% or less. Furthermore, this matching performance is obtained when all the eigenvalues of both F and F_c have negative real parts (at each interval). The results of the Class III and IV canonical system analyses reveal that the closest F_c is not always completely stable. However, since F_c contains completely decoupled submatrices, one need only apply the rule to the stable subspaces of the canonical system. Hence, a subset of $\underline{x}(t)$ which includes only the stable modes is evaluated for determining the quality of the canonical system match. Note that is consistent with the order-reduction characteristics that one may want to enforce, e.g., when augmentation states are modeled as decoupled modes in the canonical system.

A further issue which requires additional investigation, is the reason for the poor quality of the canonical system match for the Class IV structure. At this time it is unclear whether the relatively large magnitudes of $||\Delta F||$ and $||\Delta G||$ are the result of poor convergence in the optimization

procedure of if the values are the true minimums. If the relatively large magnitudes of $||\Delta F||$ and $||\Delta G||$ are the true minimums then what is the cause and is it indicative of poor flying qualities in the modeled aircraft (a conclusion often drawn when equivalent systems exhibit a poor match)? It is wise to recall from the Chapter 2 discussion that a zero value of $||\Delta F||$ need not exist because the choice of free parameters may preclude the possibility that $F - F_c = 0$. However, the quality of the canonical system match for the Class IV systems did change with the maneuver, in fact it exceeded the Class III system performance in some portions of the wind-up turn. This limited result suggests that the choice of a canonical system structure can be maneuver dependent, hence that it is possible to specify a canonical system structure that is the most sensitive to the aircraft dynamics in a specific maneuver.

The strongest conclusion to be drawn from the results presented in this chapter is that the computability of the canonical system methodology has been demonstrated. Thus, Step 3 of the NFQ formulation outlined in Section 2.3.3 has been satisfied. The resulting computer software tool that solves the canonical system matching problem and computes the relative controllability index is a finished product, ready to be used in additional NFQ experiments.

The numerical results in this chapter have made a strong case for two concepts developed in the NFQ research; the use of canonical system theory to provide what is in effect an extended equivalent system methodology and the use of a relative controllability measure as a flying qualities criterion. However, the two concepts rely on local (linearized) results of nonlinear analysis and system theory. Hence, the applicability of more advanced, i.e., global, nonlinear analysis and its ability to overcome the limitations encountered

with the NFQ formulation issues remain to be resolved. The next chapter addresses these issues through an examination of leading techniques in nonlinear analysis. In addition, Section 4.3 contains a complete description, i.e., definition, proof, and numerical procedure, for the relative controllability theorem used to supply the results presented in Section 3.3.

4.

REVIEW OF RELEVANT TECHNIQUES IN NONLINEAR SYSTEM THEORY

Nonlinear system theory, in this report, denotes the body of mathematical research applicable to systems governed by nonlinear ordinary differential equations. Although results in nonlinear system theory have been limited, the theory has drawn heavily from all areas of pure mathematics, e.g., functional analysis and differential geometry. The present chapter will document the research results uncovered in a comprehensive literature search for techniques applicable to flying qualities analysis. An overview of the literature search and a categorization of nonlinear systems is provided in Section 4.1. Section 4.2 describes the system-theoretic concepts, e.g., reachability, for which significant progress has been made in deriving a computable test. Section 4.3 then discusses the relative controllability theorem of Sastry and Desoer that was used to generate εC_0 in the previous chapter. (Since the following discussion is laden with numerous symbols, a glossary has been provided at the end of this report.)

4.1 OVERVIEW OF NONLINEAR SYSTEMS THEORY

This section describes the significant nonlinear system techniques revealed by the literature search. The presentation of this diverse material requires the categorization of nonlinear system theory research and the description of the subsets (i.e., classes) of nonlinear systems prevalent in current research.

4.1.1 Categorization of Nonlinear System Theory

Nonlinear system theory properly encompasses an area of applied mathematical research which emphasizes the search for nonlinear analogues to linear system-theoretic concepts. Note that this description by no means includes all techniques associated with nonlinear analysis, nor does this definition include the specialities of optimal control, stability theory or frequency-domain nonlinear, feedback system analysis. However, the literature search for the NFQ program took a broad perspective, hence it included an examination of relevant techniques from nonlinear dynamics analysis, nonlinear system theory and modern control theory. Consequently, a major categorization of nonlinear system theory is by system-theoretic concept and related fields of study (e.g., optimal control).

A further subtlety of nonlinear system theory is the dependence of specific approaches on a core set of tools and concepts from pure mathematics. Specifically one finds that functional analysis, differential geometry and Lie algebra are especially popular in nonlinear system theory characteristically they produce different tests for the given system-theoretic concept. Thus, an additional categorization of nonlinear system theory is based on the primary mathematical tools employed.

Finally, note that nonlinear systems is an extremely broad class of dynamic systems. Many researchers have responded to this unwieldy class of systems by concentrating on specific subsets of nonlinear systems, e.g., polynomial, which are both more manageable and more common in applications. Thus, the third categorization of nonlinear system theory is with respect to the specific classes of nonlinear systems for which a particular piece of research was derived.

In summary, there are three categorizations of nonlinear system theory, in descending order of priority. They are:

- The system-theoretic concept under investigation, e.g., controllability, feedback control
- The mathematical tools which the researcher draws upon, e.g., Volterra Series
- The the class of nonlinear systems for which the result was derived, e.g., bilinear systems.

Figure 4.1-1 summarizes the results of the nonlinear system theory literature search into the aforementioned categories.* Because of the extensive amount of research concerning stability, feedback control and optimal control, key references for these areas are an extremely small sample of the available work. Descriptions of the system-theoretic concepts can be found in subsequent sections of this chapter. A discussion of the classes of nonlinear system identified in Fig. 4.1-1 closes this section.

4.1.2 Classes of Nonlinear Systems

The classes of nonlinear systems tabulated in Fig. 4.1-1 are the principal ones to which significant research has been devoted. The classes are not necessarily mutually exclusive,

*Although reachability and observability are dual properties in linear system theory, i.e., proving one property provides a proof for the other, this duality does not extend to nonlinear systems. For example a nonlinear system may be linear in control but have a nonlinear measurement equation. Hence, results in reachability and observability are considered separately in Fig. 4.1-1.

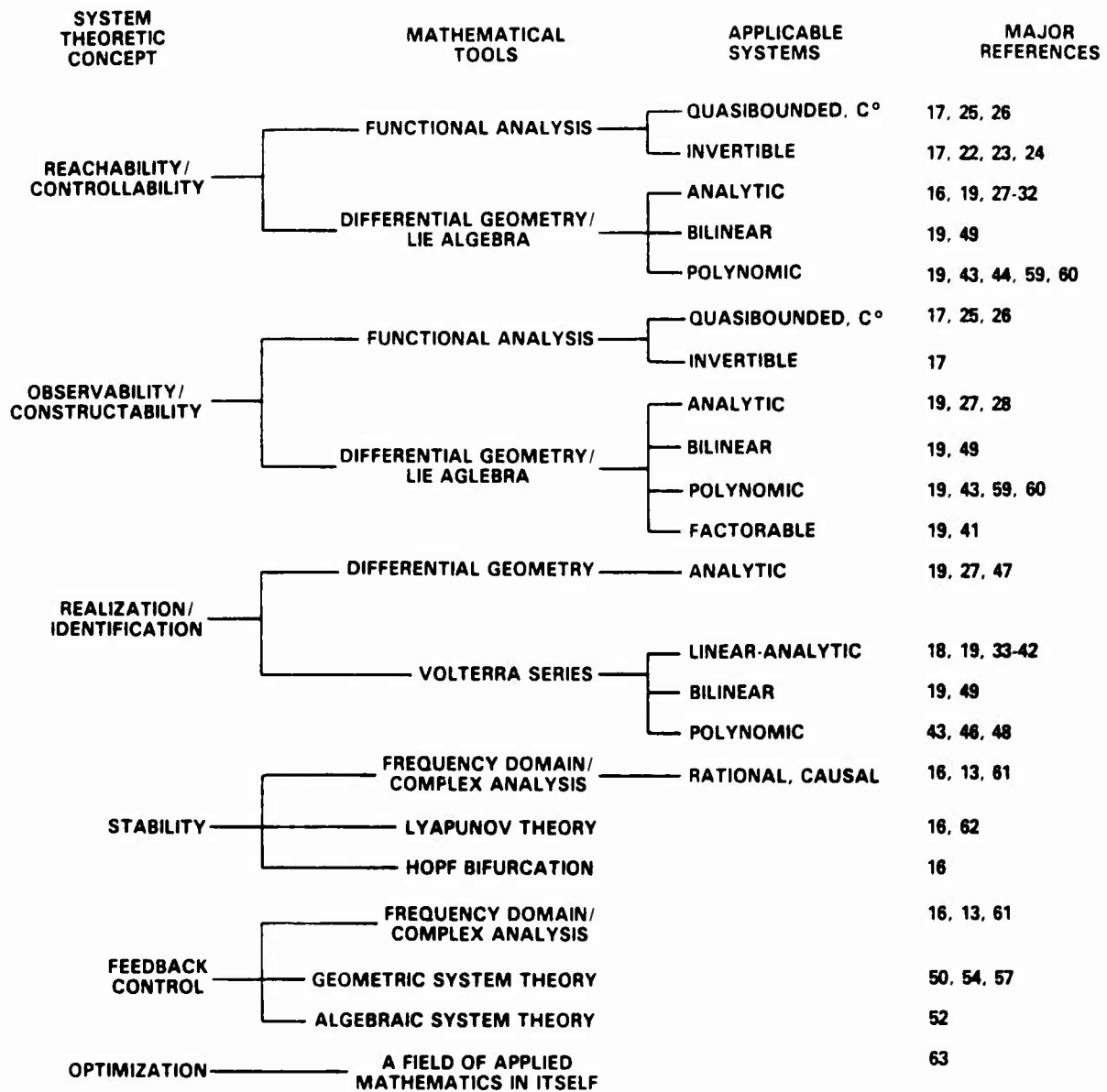


Figure 4.1-1 Nonlinear System Theory Overview

nor are most of them subsets of one another. In order of decreasing generality, the classes of nonlinear systems encountered in the literature search are:

- Smooth Systems
- Analytic Systems
- Linear-Analytic Systems
- Polynomic Systems
- Bilinear Systems
- Factorable Systems.

Prior to definitions of these system classes, note that the applicable definition depends on whether one is determining reachability or observability properties. The classification may be different because the state equation and measurement (output) equation may belong to different classes. For example a given nonlinear system may be described by a differential equation of analytic functions and yet have a bilinear form for the output equation. Hence, for controllability determination the system would be treated as an analytic system but for observability analysis, theorems relevant for bilinear systems would be used. The reader is advised to bear this in mind when attempting to classify a nonlinear system.

Smooth Systems - This is the broadest class of the aforementioned nonlinear systems. The general form for smooth systems is:

$$\dot{\underline{x}}(t) = \underline{f}(\underline{x}, \underline{u}) \quad (4.1-1)$$

$$\underline{x}(0) = \underline{x}_0 \quad (4.1-2)$$

and

$$\underline{y}(t) = \underline{h}(\underline{x}) \quad (4.1-3)$$

where $\underline{u} \in \mathcal{U} \subset \mathbb{R}^m$, $\underline{x} \in M$ a C^∞ connected manifold of dimension n and \underline{f} and \underline{h} are C^∞ function of their arguments. C^∞ means that partial derivatives (of \underline{f} and \underline{h}) of all orders exist and are continuous. A C^∞ manifold is a smooth manifold hence the system's name smooth for the system described by Eqs. 4.1-1 to 4.1-3. A manifold is a special entity of differential geometry which is beyond the scope of this report to define. The reader is referred to Ref. 56, Chapter 5 for a concise definition of a manifold. Note, however, that manifolds and differential geometry are important tools for establishing reachability, observability, and realization results for smooth systems, as well as analytic, and linear-analytic systems.

Analytic Systems - Analytic systems have the same form as presented in Eqs. 4.1-1 to 4.1-3 but have $\underline{u} \in \mathcal{U} \subset \mathbb{R}^n$, $\underline{x} \in M$ a C^ω -connected manifold of dimension n and \underline{f} and \underline{h} are C^ω functions of their arguments. C^ω , where ω is finite, means that all partial derivatives of order less than or equal to ω exist and are continuous. Furthermore \underline{f} and \underline{h} are analytic functions, signifying that for a value of $\underline{x}_0, \underline{y}_0 \in \mathbb{R}^n, \mathbb{R}^m$, \underline{f} and \underline{h} are analytic at a point $\underline{x}_0, \underline{u}_0$ if the partial derivatives of \underline{f} and \underline{h} exists not only at $\underline{x}_0, \underline{u}_0$ but at each point $\underline{x}, \underline{u}$ in some neighborhood. \underline{f} and \underline{h} are analytic in a region Ω if they are analytic at every point in $\mathbb{R}^n, \mathbb{R}^m$ (Ref. 55). The advantage of real analytic functions is that they may be expressed as a convergent Taylor series in a neighborhood of each point.

Linear-Analytic Systems - The next class of nonlinear systems are linear-analytic systems, which are expressed as

*This definition enforces the fact that the admissible controls do not span the entire space \mathbb{R}^m , but typically only form a subset of \mathbb{R}^m denoted \mathcal{U} .

$$\dot{\underline{x}} = \underline{f}(\underline{x}) + \sum_{i=1}^r u_i(t) g^i(\underline{x}) \quad (4.1-4)$$

$$\underline{x}(0) = \underline{x}_0 \quad (4.1-5)$$

where $\underline{f}(\underline{x})$ and $\underline{g}(\underline{x})$ are analytic functions of their arguments \underline{x} and the output equation is described by Eq. 4.1-3. Equation 4.1-4 is linear in the control \underline{u} , hence the term linear-analytic. The importance of linear-analytic systems stems from attempting to construct reachability results for analytic systems. In particular Ref. 31 demonstrates that if an analytic system is linear in the control, hence linear-analytic, a computable reachability test can be derived. Linear-analytic systems can also be used to model the application of linear feedback control to a nonlinear plant.

Polynomial Systems - Another important class of nonlinear systems in recent research is polynomial systems. Their importance stems from their occurrence in the modeling of physical systems and in approximation techniques based on series of orthogonal polynomials. Furthermore, they are very amenable to Volterra series representations, hence much of the work with polynomial systems is through the use of Volterra series. The relationship with functional expansions is significant because of the powerful tools from functional analysis regarding the representation of functions with a polynomial expansion, i.e., the Weierstrass Approximation Theorem (see Ref. 58, Ch. 6). This theorem allows one to determine if a certain polynomial, e.g., the trigonometric functions (1, sin t, cos t, ..., sin nt, cos nt), can be used to approximate an arbitrary function.

The general form for polynomial systems is

$$\dot{\underline{x}}(t) = \underline{P}(\underline{x}, \underline{u}) \quad (4.1-6)$$

$$\underline{y}(t) = \underline{h}(\underline{x}) \quad (4.1-7)$$

where $\underline{u} \in R^m$, $\underline{x} \in R^n$, $\underline{y} \in R^p$, and $\underline{p}(\cdot, \cdot)$ and $\underline{h}(\cdot)$ are polynomial functions of their arguments. Note that Eqs. 4.1-6 and 4.1-7 are sufficiently general to include linear systems and bilinear systems. The generality of including linear systems and being applicable to almost any problem through approximation has led researchers to develop a special field of systems theory called polynomial systems (e.g., Refs. 43 and 46). In the present report, however, linear and bilinear systems are discussed separately from any general polynomial system theory.

Bilinear Systems - The next class of nonlinear systems, bilinear, represents a subset of polynomial systems. This is the most widely studied class of nonlinear systems. The attractiveness of bilinear systems originates in their nearly linear characteristics and in the applicability of bilinear models to physical phenomena in engineering, chemistry, biology, and economics (Ref. 49). Bilinear systems are represented by the differential equation

$$\dot{\underline{x}}(t) = F(t) \underline{x} + G(t) \underline{u} + \sum_{i=1}^n N_i(t) \underline{x} u_i \quad (4.1-8)$$

where $F \in R^{n \times n}$ $G \in R^{n \times m}$ and

$$\sum_{i=1}^m N_i(t) \underline{x} u_i = (N(t)\underline{x}) \underline{u} \quad (4.1-9)$$

a bilinear function in \underline{x} and \underline{u} where $N(t)$ is a $n \times m$ matrix. In addition, bilinear systems are typically assumed to possess linear output equations, i.e.,

$$\underline{y}(t) = H(t) \underline{x}(t) \quad (4.1-10)$$

Consequently, bilinear systems are linear systems with the addition of the bilinear form $(N(t)\underline{x})\underline{u}$. Figure 4.1-2 contains a block diagram of a generic bilinear system. A specific type of bilinear systems in which F and G are skew-symmetric and time-invariant occurs in the modeling of conservative (i.e., conservation of energy) systems. Aircraft equations of motion, perturbed about a reference flight condition, represent a physical system that becomes a bilinear form with a skew symmetric matrix N . These conservative systems are said to evolve on spheres for any control, i.e., $||\underline{x}(t)|| = ||\underline{x}(0)||$. In Ref. 57 significant theorems regarding controllability and optimization of conservative bilinear systems have been derived. Further discussion of system-theoretic results for bilinear systems can be found in Section 4.2.

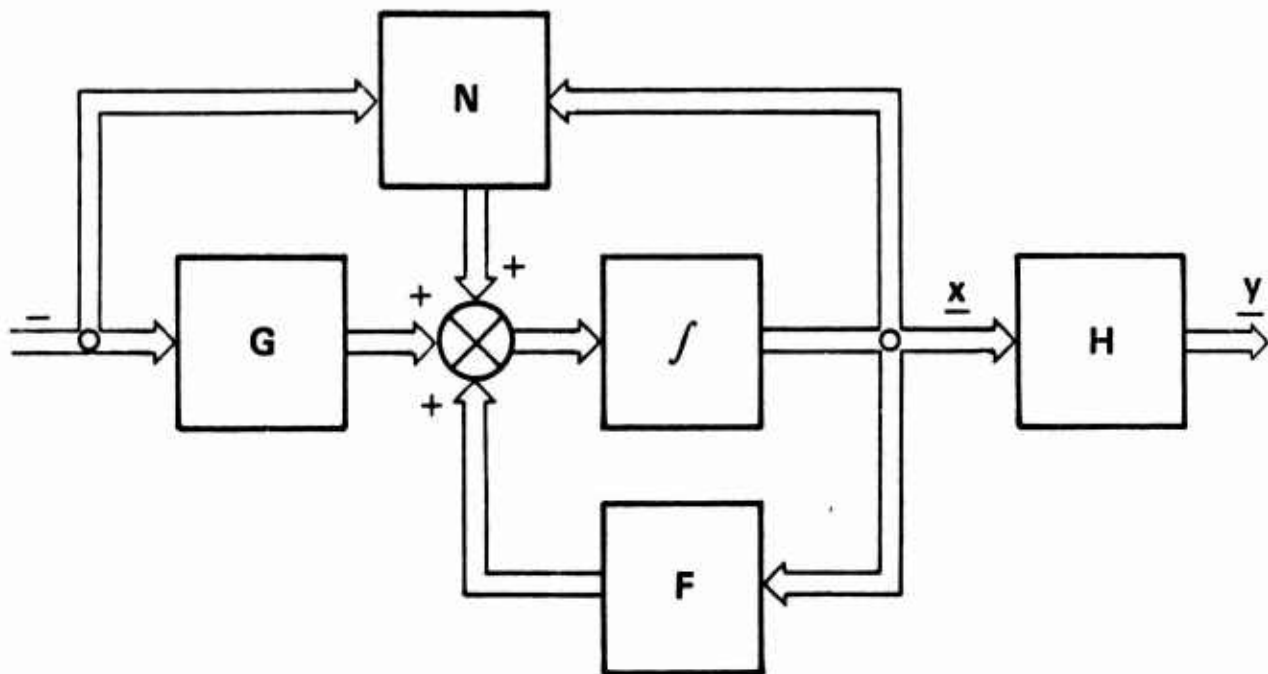


Figure 4.1-2 Bilinear System Block Diagram

Factorable Systems - The final class of nonlinear systems to be considered is factorable systems. Factorable systems are composed of linear systems connected in parallel with their outputs multiplied. The usefulness of factorable systems arises in the application of Volterra series, where it is known that systems with separable Volterra kernels may be expressed as finite sums of factorable systems (Ref. 41). Furthermore, as in the case of polynomial systems, factorable systems are extremely useful approximations to common nonlinearities. In Ref. 27 the authors state "over a finite time interval, any continuous-time system can be arbitrarily approximated by a factorable system."

The general form for factorable systems is

$$\dot{\underline{x}}(t) = F \underline{x}(t) + G \underline{u}(t) \quad (4.1-11)$$

and

$$\underline{y}(t) = \prod_{i=1}^K h_i \underline{x}_i(t) \quad (4.1-12)$$

where each \underline{x}_i is of dimension n_i ; i.e., the state vector of each of the parallel subsystems. However, Eq. 4.1-11 is simply a linear time-invariant differential equation; hence linear system theory can be applied for determining reachability/controllability. The output equation, Eq. 4.1-12, requires nonlinear theory to deduce observability/reconstructability and realization properties. Furthermore, if a control design is desired, nonlinear theory is once again required for both open and closed-loop analysis. Thus, even the apparently innocuous system of Eqs. 4.1-11 and 4.1-12 far exceeds the capabilities of linear system theory. Finally, factorable systems are specific examples that reinforce the fact that reachability and observability are not duals of one another for certain classes of nonlinear systems.

The nonlinear system classes that are described in this subsection: smooth, analytic, linear-analytic, polynomic, bilinear, and factorable are by no means an exhaustive list of either possible classes of nonlinear systems or of the special nonlinear systems that arise in applications. One obvious omission has been nonlinear differential equations of mathematical physics which have been the subject of intense investigation, e.g., the Van der Pol and Rayleigh equations. The existence of so many classes of nonlinear systems and so much specialized investigation may lead one to conclude that the pursuit of global nonlinear system theory is futile. Nevertheless specific works, e.g., Ref. 16 stressing a qualitative approach to nonlinear systems and Ref. 18 emphasizing the Volterra/Wiener (frequency-domain) approach, provide sufficiently general results that can be applied to diverse systems. The specialization occurs when one uses the physics, chemistry or empirical data in a problem to simplify the differential equations or to generate special theorems. A classic example is the linearization about steady-trimmed flight of the nonlinear equations of motion of an air vehicle.

In the NFQ research, the crucial issues regarding the usefulness of a particular technique from nonlinear system theory are:

- The applicability of the nonlinear system-theoretic concept, e.g., realization, to the aircraft equations of motion with the flexibility to provide flying qualities criteria
- The capability to approximate the aircraft equations of motions by recasting into a particular class of nonlinear systems.

The following sections (4.2 and 4.3) address the first topic by describing what are considered to be the most promising

techniques in reachability, observability, realization, stability theory, nonlinear feedback, and optimal control; the system-theoretic concepts outlined in Fig. 4.1-1.

4.2 NONLINEAR REACHABILITY, OBSERVABILITY, AND REALIZATION

The system-theoretic concepts of: reachability/controllability, observability/reconstructability and realization are defined in this section. Significant theorems for determining these properties for a given nonlinear system are documented as well. The material presented in this section is emphasized throughout the remainder of this report because of its applicability to flying qualities analysis. The system-theoretic concepts take on the following meanings when applied to aircraft:

- Reachability/controllability of the aircraft system from pilot inputs quantifies the map of pilot inputs to possible states of the aircraft
- Observability/reconstructability permits the evaluation of which modes can be perceived by the pilot or can be sensed by the flight instruments
- Realization theory is essential for reconstructing flying qualities, e.g., canonical systems, models of the aircraft from flight test data.

In discussing these concepts, theorems will be presented without proof,^{*} with an emphasis on theorems that provide tests and are apparently computable; i.e., are amenable to conventional numerical algorithms. However, the determination of

^{*}The reader is reminded to consult subsection 4.1.2 when theorems are restricted to a specific class of nonlinear systems.

the applicability of these concepts to nonlinear flying qualities analysis has led to the selection of a particular controllability theorem which is described in detail in Section 4.3.

4.2.1 Nonlinear Reachability/Controllability

The majority of contributions to nonlinear reachability/controllability have been derived with the aid of functional analysis or differential geometry. Although the methods differ, the aim of all approaches is to state a theorem with which a system can be determined to be reachable or controllable. Prior to examining these theorems it is useful to review reachability/controllability for linear systems:

- Definition -- REACHABILITY -- Given the linear system

$$\dot{\underline{x}} = F \underline{x} + G \underline{u} \quad \text{and} \quad (4.2-1)$$

$$\underline{y} = H \underline{x} \quad (4.2-2)$$

for $\underline{x}_0 \in R^n$, $\Omega(\underline{x}_0)$ equals the set of reachable states: $\underline{x} \in \Omega(\underline{x}_0)$ if there is an input $u(t)$, $t_0 \leq t \leq t$, such that

$$(\underline{x}_0, t_0) \xrightarrow{u(t)} (\underline{x}_1, t_1)$$

i.e., $u(t)$ forces the system from the initial state (\underline{x}_0, t_0) to the final state $(\underline{x}_1, t_1) \in \Omega(\underline{x}_0)$.

However, the statement that a system is simply reachable is of little practical value; something must be stated concerning the reachable set $\Omega(\underline{x}_0)$. Hence, the concept of complete reachability.

- Definition -- A system is completely reachable if the set of reachable states $\Omega(\underline{x}_0) = \mathbb{R}^n \forall \underline{x}_0$, i.e., the set of solutions to Eq. 4.2-2 includes all possible values of \underline{x} for any value of \underline{x}_0 .

The concept of controllability is a corollary of reachability.

- Definition -- A system is completely controllable if $\underline{x}^* = \underline{0} \in \Omega(\underline{x}_0) \forall \underline{x}_0$, i.e., the set of reachable states includes the zero vector.

For continuous-time systems completely reachable \Leftrightarrow completely controllable. Hence, the separation of controllability and reachability is only of importance for systems described by finite difference equations, i.e., discrete-time systems. (The critical issue is the invertibility of the discrete-time dynamics matrix. In the NFQ program the only use of discrete-time systems is in forming discrete equivalents of continuous representations of the aircraft dynamics (see Subsection 4.3.3) hence the discrete equivalent dynamics matrix is always invertible because it is the transition matrix of the continuous system.)

In the present discussion of nonlinear systems reachability is the only concept of interest, primarily because the $\underline{x} = \underline{0}$ solution of nonlinear differential equation is not necessarily an equilibrium point as it is for linear systems. However, when linear time-varying systems are discussed, especially in Section 4.3, reachability and controllability will be used interchangeably.

The definition of reachability for linear systems must also be changed if it is to be a useful concept for nonlinear

systems. A particularly troubling aspect of the previous definition of reachability is that it may take an infinite amount of time or an infinite distance (i.e., $||\Delta \underline{x}||$) to reach a particular reachable state.* Consequently, it is more practical to define concepts of locally reachable and weakly reachable.

Consider the general nonlinear system,

$$(\theta) \begin{cases} \dot{\underline{x}}(t) = \underline{F}(\underline{x}, \underline{u}) & (4.2-3) \\ \underline{y}(t) = \underline{h}(\underline{x}) & (4.2-4) \end{cases}$$

where $\underline{u} \in V \subset \mathbb{R}^m$, $\underline{x} \in M$ a C^∞ - connected manifold of dimension n , \underline{f} and \underline{h} are C^∞ functions of their arguments. (Note, the C^∞ requirement signifies that (θ) is a smooth system as discussed in Section 4.1.) The global definition of reachability is equivalent to the linear-system reachability definition presented earlier with the exception that each reachable state is contained on M , $\underline{x}^* \in M$ and the trajectory \underline{x}_0 to \underline{x}^* remains in M : $\underline{x}(t) \in M$, $0 \leq t \leq T$. The definition of local reachability is:

- Definition -- LOCAL REACHABILITY -- The system (θ) is locally reachable at \underline{x}_0 for every neighborhood $O_\varepsilon(\underline{x}_0)$ if $\Omega(\underline{x}_0)$ is also a neighborhood of \underline{x}_0 with the trajectory from \underline{x}_0 to $\Omega(\underline{x}_0) \cap O_\varepsilon(\underline{x}_0)$ lying entirely within $O_\varepsilon(\underline{x}_0)$. The system (θ) is locally reachable if it is locally reachable for every $\underline{x} \in M$.

Global reachability and local reachability are not symmetric, i.e., \underline{x}^* may be reachable from \underline{x}_0 but not vice versa.

*Hence the impetus for the relative controllability theorems discussed in Section 4.3.

Hence one can define an alternative concept which will be called weak reachability,

- Definition -- WEAK REACHABILITY -- (Ref. 19)
Two states \underline{x}^* and \underline{x} are weakly reachable from each other if and only if there exist states $\underline{x}^0, \underline{x}^1, \dots, \underline{x}^k$ such that $\underline{x}^0 = \underline{x}^*$, $\underline{x}^k = \underline{x}$ and either \underline{x}^1 is reachable from \underline{x}^{i-1} or \underline{x}^{i-1} is reachable from \underline{x}^1 , $i = 1, 2, \dots, k$. The system (θ) is weakly reachable if every $\underline{x} \in M$ is weakly reachable.

The concept of locally-weakly-reachable can also be defined as a system that meets both conditions of locally and weakly reachable.

The rationale for this variety of reachability concepts is that the most practical nonlinear reachability theorems, i.e., those which admit an algebraic test, have been derived for locally weakly reachable systems. Prior to stating the reachability results one additional concept must be defined:

- Definition -- Let $p(\underline{x}), q(\underline{x})$ be two C^∞ vector fields on M . Then the Jacobi bracket of p and q is

$$[p, q](\underline{x}) = \left(\frac{\partial q}{\partial \underline{x}} \right) p - \left(\frac{\partial p}{\partial \underline{x}} \right) q \Big|_{\underline{x}} \quad (4.2-5)$$

If we then define a set of vector fields f_o , the set of vectors generated by $f(\underline{x}, \cdot)$ i.e., for a constant control, then the elements of F are linear combinations of the form

$$[f^1, f^2, f^3 \dots [f^i, f^{i+1}] \dots] \quad (4.2-6)$$

where $f^i(\underline{x}) = f(\underline{x}, \underline{u}^i)$. The reachability theorem for C^∞ (smooth) systems is: A system (θ) is said to be locally weakly reachable at \underline{x}_0 if it satisfies the reachability rank condition at \underline{x}_0 , i.e., the dimension of $F(\underline{x}_0)$ is n for every $\underline{x} \in M$. A proof of this theorem can be found on p. 730 of Ref. 27. In addition, Ref. 41 provides a reachability theorem for analytic systems, hence a strengthening of the foregoing theorem,

- THEOREM -- REACHABILITY OF ANALYTIC SYSTEMS -- if (θ) is analytic, then (θ) is weakly reachable if and only if it is locally weakly reachable and if and only if the reachability rank condition is satisfied.

The reachability theorem for analytic systems is based on an algebraic test like the reachability theorems for linear systems. However, unlike the linear tests which require a finite matrix, the sequence of Lie brackets in Eq. 4.2-6 can be computed indefinitely until the set of vectors spans the vector space of $f(\underline{x}, \underline{u}^i)$. Further qualification of the nature of the vector fields f^1 , specifically, requiring that they be "involutive" (see Ref. 19, p. 310), permits the restatement of the reachability rank condition such that the Lie brackets in Eq. 4.2-6 terminate in a finite number of terms. Linear-analytic systems especially lend themselves to a tractable algebraic test which is a simplification of the reachability rank condition.

This brief discussion of nonlinear reachability/controllability emphasizes the results obtained with the tools of differential geometry and Lie algebra. Significant theorems have also been derived with the aid of functional analysis, especially fixed-point theorems (Refs. 22-26). Although the theorems are meaningful and practical, the theorem that Section 4.3 describes is a sufficient example. The reader is

referred to the discussion of the relative controllability theorem of Sastry and Desoer in Section 4.3 for an exposition of the application of functional analysis to nonlinear controllability.

One additional area to review is the reachability of polynomial systems. Recall the definition of polynomial systems given in Section 4.1 (Eqs. 4.1-6 and 4.1-7)

$$\dot{\underline{x}}(t) = \underline{f}(\underline{x}) + \underline{g}(\underline{x}) \underline{u}(t) \quad (4.2-7)$$

where \underline{f} and \underline{g} are vector fields having components which are polynomials in the entries of \underline{x} . Because \underline{f} and \underline{g} are polynomial maps, concepts of algebraic geometry are used extensively. Prior to stating the reachability theorem, a few preliminary concepts are reviewed. First on algebraic set in k^n is the zero set for a collection of polynomials in $k[s]$. If $Q \subseteq k[s]$ then the natural algebraic set

$$V(Q) = \{x \in k^n : f(x) = 0 \text{ for all } f \in Q\}$$

Furthermore, if $f \in k[s]$, $x \in k^n$, the differential of f at x is the linear function $d_x f : k^n \rightarrow k$ given by

$$d_x f(v) = \sum_{i=1}^n \frac{\partial f}{\partial s_i}(x) v_i \quad (4.2-8)$$

The Lie derivative of f with respect to F , $L_F(f(s))$ is given by

$$L_F(f(s)) = d_s f(F(s)) = \sum_{i=1}^n \frac{\partial f}{\partial s_i}(s) F_i(s) \quad (4.2-9)$$

Finally, the set $I(Q;P) \triangleq$ the smallest polynomial ideal in $k[s]$ containing Q and closed under Lie differentiation with

respect to elements of P . The foregoing definitions and concepts are key elements of the following theorem:

● THEOREM -- POLYNOMIC SYSTEM REACHABILITY --

Let V be an algebraic set in k^n . If $\Omega(\underline{x}_0) \subseteq V$ for each $\underline{x}_0 \in V$ then $I(v(v); \{f, g\}) = v(v)$. If for any ideal v defining V we have $I(v; \{f, g\}) = v$ then $\Omega(\underline{x}_0) \subseteq V$ for each $\underline{x}_0 \in V$.

This theorem, although extremely abstract does provide a basis for testing whether or not a given algebraic set contains points reachable from \underline{x}_0 and also provides a means for constructing points reachable from \underline{x}_0 . Specific examples of such a procedure can be found in Refs. 59 and 60.

In this subsection, a brief outline of reachability theorems for smooth, analytic, linear-analytic, and polynomic systems has been presented. Although not comprehensive, the discussion should impress upon the reader both the advanced state and difficulty of nonlinear system theory. What is apparent from this overview is that the computation of these tests can be an enormous task. The reachability theorem for analytic systems presents the difficulties of computing the partial derivatives necessary for the Lie brackets. On the other hand the reachability theorem for polynomic systems requires finding the zeros of the dynamical and control polynomial and then computing the ideal of that set. A general numerical procedure for either of these procedures is far off indeed, hence, it may be best to pursue a version of these theorems for a specific system, e.g., the equations of motion for an aircraft. In other words it may be best to derive controllability tests for the nonlinear aircraft equations of motion rather than try to apply a specialization of the theorems just described.

4.2.2 Nonlinear Observability/Reconstructability

Nonlinear observability/reconstructability shares many of the problems associated with reachability/controllability. As in the case of nonlinear reachability, concepts of weak observability, local observability and locally weak reachability are necessary to avoid the shortcomings of global observability theorems.

4.3 RELATIVE (ROBUSTNESS OF) CONTROLLABILITY FOR NONLINEAR SYSTEMS

The survey of research in nonlinear controllability/observability presented in Section 4.2 emphasized existence and sufficient conditions for controllability in various types of nonlinear systems. Characteristically these theorems do not lend themselves to constructive proofs, hence explicit numerical techniques for testing the controllability of a nonlinear system are not obvious. One notable piece of research, however, has succeeded in generating a constructive proof which can be solved numerically. The nonlinear controllability/observability results of Sastry and Desoer (Refs. 25 and 26), have led to a constructive proof which also provides bounds on the controllability of a perturbed nonlinear system, hence providing a measure of the relative (or robustness of) controllability for the linear time-varying component of the nonlinear differential equation. The computability of the controllability measure is beneficial to the development of nonlinear flying qualities criteria based on the system-theoretic concept of controllability. This section concerns itself with the relative controllability theorem^{*} and overview of its proof.

^{*}The relative observability theorem will not be discussed, however, it is an equally significant result which can be of great value in flight control design problems.

An exposition on the use of relative controllability in flying qualities analysis is contained in Chapter 2.

4.3.1 Theorem Statement

In the review of controllability for linear systems presented in Appendix C, it is clear that the binary test, i.e., invertibility of the Grammian, can be expanded to provide a measure of the system controllability. Recall the definition of the Grammian

$$W(t_0, t_0+T) = \int_{t_0}^{t_0+T} \Phi^T(t_0, \tau) G^T(\tau) G(\tau) \Phi(t_0, \tau) d\tau \quad (4.3-1)$$

The Grammian is a $n \times n$ matrix with n eigenvalues λ_i , hence we can define a reachability condition number (reminiscent of the condition number of a matrix in numerical analysis) as (Refs. 25 and 26)

$$\chi_R = \frac{\lambda_L}{\lambda_S} \quad (4.3-2)$$

where

$$\lambda_L = \sup_{t_0 \in R_+} \sup_{t \in [0, T]} \sqrt{\lambda_{\max}(W[t_0, t_0+t])} \quad (4.3-3)$$

and

$$\lambda_S = \inf_{t_0 \in R_+} \sqrt{\lambda_{\min}(W[t_0, t_0+T])} \quad (4.3-4)$$

The maximum and minimum eigenvalues of the grammian qualitatively are a natural basis for a controllability measure because they gauge the rank of the matrix. Hence, if the system is

uncontrollable λ_{\min} (and thus λ_S) will be 0, causing the reachability condition to be undefined. If the system is controllable but may take nearly an infinite time to reach the desired state (especially a problem of global controllability theorems) the reachability condition number will be very large ($\lambda_S \ll 1$). Furthermore, note that the supremum of the square root of λ_{\max} on an interval and infimum of the square root of λ_{\min} are valid L_2 norms of the controllability grammian, hence, all the properties of a norm apply to λ_{\max} and λ_{\min} .

When confronted with a nonlinear system of the form

$$\dot{\underline{x}} = \underline{f}(\underline{x}, \underline{u}, t) \quad (4.3-5)$$

which can be decomposed into

$$\dot{\underline{x}} = A(t) \underline{x}(t) + B(t) \underline{u}(t) + \underline{h}(\underline{x}, \underline{u}, t) \quad (4.3-6)$$

where $A(t)$, $B(t)$ are a completely controllable pair and $\underline{h}(\underline{x}, \underline{u}, t)^*$ is globally Lipschitz continuous[†] with

$$\sup_{\substack{\underline{x} \in R^n, \underline{u} \in R^m, t \in R_+}} |\underline{h}(\underline{x}, \underline{u}, t)| = k_0 < \infty \quad (4.3-7)$$

the theorem of Sastry and Desoer permits the direct evaluation of the permissible function $\underline{h}(\underline{x}, \underline{u}, t)$ such that the overall differential Eq. 4.3-5 or Eq. 4.3-6 remains controllable. Differential equations such as Eq. 4.3-6 may arise in two situations: problems where a linear time-varying system is perturbed by nonlinear dynamics; or in the case where the

* $\underline{h}(\underline{x}, \underline{u}, t)$ can also be viewed as the higher order terms of a Taylor series expansion on $\underline{f}(\underline{x}, \underline{u}, t)$.

†See Ref. 58 for definition of Lipschitz condition and Lipschitz continuity.

original nonlinear differential equation, e.g., Eq. 4.3-5, may be naturally decomposed into a linear plus nonlinear part like Eq. 4.3-6. Bilinear systems (see Subsection 4.1.2) are a specific example of a nonlinear system which is composed of linear and nonlinear parts.

The robustness of controllability results of Sastry and Desoer exist as a collection of theorems for various cases. This discussion will describe the two most useful theorems for NFQ analysis. The first theorem states that if the linear time-varying portion of Eq. 4.3-6 is bounded, i.e., $||A(\cdot)||$, $||B(\cdot)||$, and $||C(\cdot)||$ bounded on R_+ and is strongly completely controllable, i.e., it is completely controllable in the sense of the definition in Appendix C where strongly also implies,

$$W[t_0, t_0+T] \geq \lambda_S^2 I \quad (4.3-8)$$

where I is an identity matrix of the same dimension as W , then the perturbed system represented by Eqs. 4.3-6 and 4.3-7 is completely controllable on the same interval, $[t_0, t_0+T]$ (Theorem V.1, p. 15, Ref. 26).

The next theorem of interest states an explicit formula for computing the interval on which the perturbed system remains controllable when the nonlinear perturbation does not satisfy Eq. 4.3-7, i.e., is unbounded. The case of unbounded nonlinear perturbation arises more often; Eq. 4.3-7 is extremely restrictive. For example, the nonlinear one-dimensional system,

$$\dot{x} = ax + bu + x^2$$

contains a nonlinear perturbation $h(x) = x^2$ which does not satisfy Eq. 4.3-7. In general, Eq. 4.3-7 describes functions like sinusoids, exponentials, and inverses of polynomials.

Consequently, the second theorem begins with the system defined by

$$\dot{\underline{x}} = A(t) \underline{x} + B(t) \underline{u} + \varepsilon \underline{h}(\underline{x}, \underline{u}, t) \quad (4.3-9)$$

where \underline{h} is a Lipschitz continuous vector function satisfying

$$\underline{h}(\underline{0}_n, \underline{0}_m, t) = \underline{0}_n \quad \forall t \in R_+ \quad (4.3-10)$$

(i.e., it has a fixed point) and

$$|\underline{h}(\underline{x}, \underline{u}, t) - \underline{h}(\underline{y}, \underline{v}, t)| \leq C_0 |\underline{u} - \underline{v}| + C_0 |\underline{x} - \underline{y}| \quad (4.3-11)$$

for some $C_0 \in R_+$. Furthermore the linear portion of Eq. 4.3-9 is required to be bounded and strongly completely controllable, as in the case of the previous theorem. Given the aforementioned conditions, Eq. 4.3-9 is completely controllable on $[t_0, t_0 + T]$ for an interval of width ε , i.e., $\varepsilon \in [-\varepsilon_0, \varepsilon_0]$

where

$$\frac{1}{\varepsilon_0} = \chi_R \cdot 2 C_0 \mu T^{\frac{1}{2}} \left\{ 1 + \gamma(G) \cdot \lambda_S^{-1} \lambda_L^{-1} \sup_{t_0 \in R_+} \sup_{\tau \in [0, T]} |\phi(t_0 + T, t_0 + \tau)|_i \right\} \quad (4.3-12)^*$$

where χ_R , λ_L , λ_S , and C_0 have been defined in Eqs. 4.3-2, 4.3-3, 4.3-4 and 4.3-11, μ is the intrinsic drift factor,

$$\mu \triangleq \sup_{t_0 \in R_+} \sup_{T \in [0, T]} \sqrt{\lambda_{\max}(W_I[t_0, t_0 + T])} \quad (4.3-13)$$

*Equation 4.3-12 differs from the theorem as stated in Refs. 25 and 26 due to typographical errors in those references. The correct form is in Eq. 4.3-12 which has been confirmed with S.S. Sastry.

where W_I is the intrinsic Grammian, the Grammian of Eq. 4.3-1 when $G(t) = I$. Finally, the term $\gamma(G)$ is,

$$\gamma(G) \triangleq \sup_{t \in R_+} \|G(t)\|_i < \infty \quad (4.3-14)$$

Note in the previous equations three types of norms have been used:

- $\|\cdot\|$ symbolizes the Euclidean norm in R^n
- $\|\cdot\|$ symbolizes the L_2 norm on $[t_0, t_0+T]$
- $\|\cdot\|_i$ symbolizes the operator norm induced on a linear map from $L_2^n([t_0, t_0+T])$ to R^n by the previous two norms.

Also note n can be the dimension of the state or control space, n or m .

Equation 4.3-12 is a strong result that permits explicit computation of the controllability of a nonlinear system, hence it is a constructive theorem quite unlike the controllability theorems presented in Section 4.2. However, bear in mind that the properties of $\underline{h}(\underline{x}, \underline{u}, t)$ summarized in Eqs. 4.3-10 and 4.3-11 are fairly restrictive and furthermore the original nonlinear differential equation (Eq. 4.3-5) must be decomposable into Eq. 4.3-9 where the linear part is strongly completely controllable. If the $\underline{h}(\underline{x}, \underline{u}, t)$ part of a system does not meet the conditions of this theorem then the test in Eq. 4.3-12 cannot be used and one must resort to the global nonlinear reachability theorems discussed in Section 4.2.

Equation 4.3-9, however, can be viewed as the original problem statement, rather than decomposition of an original nonlinear equation. When viewed in this way, Eq. 4.3-12 permits

the computation of the maximum perturbation such that the perturbed system maintains complete controllability. When this concept is extended to classical flying qualities analysis (i.e., equivalent systems), Eq. 4.3-12 creates the basis of a canonical system theory based on matching the controllability properties of the true and ideal (canonical, equivalent) system. This concept of controllability as an essential property of flying qualities analysis is more fully expounded in Chapter 2.

In summary, the results of Sastry and Desoer produce two main theorems. The first states conditions for which a nonlinear system decomposable into bounded linear and nonlinear parts is controllable. The second theorem yields a formula, Eq. 4.3-12, for computing the magnitude of a nonlinear perturbation applied to a linear time-varying system, such that the composite nonlinear differential Eq. 4.3-9 remains completely controllable. Hence, the parameter ϵ in Eq. 4.3-9 can be viewed as a controllability measure, or equivalently Eq. 4.3-12 is a relative controllability statement.

4.3.2 Outline of Proof

Proof of the two theorems stated in Subsection 4.3.1 requires the use of fixed-point theorems from nonlinear analysis.* Specifically Sastry employs a solvability theorem for operator equations with a quasibounded nonlinearity developed by Granas in Ref. 65. The mathematical details are much too extensive to be presented in this report. References 64 and 65 should be consulted; also Section IV of Ref. 26 gives a detailed account of how Granas' theorem is used. Nevertheless, it is prudent to define the term quasinorm.

*Reference 64 is an excellent survey and tutorial on fixed point theorems.

Given Banach spaces, \mathcal{X} and \mathcal{Y} with norms $|\cdot|_{\mathcal{X}}$ and $|\cdot|_{\mathcal{Y}}$ and a mapping, F , from \mathcal{X} to \mathcal{Y} , F is said to be quasibounded if the number

$$\rho(F) \triangleq \inf_{0 \leq \rho < \infty} \sup_{|x|_{\mathcal{X}} \geq \rho} \frac{|F(x)|_{\mathcal{Y}}}{|x|_{\mathcal{X}}} \quad (4.3-15)$$

is finite. ρ is the quasinorm of F . Note that Eq. 4.3-15 is the definition of an induced norm of a mapping, furthermore if F is a linear map it is quasibounded and its quasinorm is the usual induced norm (for the finite-dimensional problems being considered this is the L_2 norm). Granas' theorem is then: given $F: \mathcal{X} \rightarrow \mathcal{X}$ a continuous, quasibounded, compact map on the Banach space \mathcal{X} and if

$$\rho(F) < 1 \quad (4.3-16)$$

then the equation

$$x + F(x) = y \quad (4.3-17)$$

has at least one solution for every $y \in \mathcal{X}$. The proof of this theorem can be found in Ref. 11 Section IV.

The outline of the proof of Theorem 4.3.1 follows from the use of Granas' solvability theorem. Sastry demonstrates that given two systems

$$\dot{x}_1(t) = A(t) x_1(t) + B(t) u(t) \quad (4.3-18)$$

$$x_1(t_0) = x_0 \quad (4.3-19)$$

the completely controllable linear equation and

$$\dot{x}_2(t) = A(t) x_2(t) + B(t) u(t) + h(x_2(t), u(t), t) \quad (4.3-20)$$

$$x_2(t_0) = x_0 \quad (4.3-21)$$

the perturbed nonlinear differential equation, then the solutions of Eq. 4.3-18 and 4.3-20 are:

$$x_1(t_0+T) = \mathcal{L}_R(u) + \phi(t_0+T, t_0)x_0 \quad (4.3-22)$$

and

$$x_2(t_0+T) = \mathcal{L}_R(u) + \phi(t_0+T, t_0)x_0 + N_{x_0}(u) \quad (4.3-23)$$

where $\mathcal{L}_R(u)$ is the reachability map of the linear system, viz,

$$\mathcal{L}_R(u) = \int_{t_0}^{t_0+T} \phi(t_0+T, \tau) B(\tau) u(\tau) d\tau \quad (4.3-24)$$

and N_{x_0} is the contribution of the nonlinear perturbation, viz,

$$N_{x_0}(u) = \int_{t_0}^{t_0+T} \phi(x_0+T, \tau) h(x(\tau), u(\tau), \tau) d\tau \quad (4.3-25)$$

Both follow from the variation of constants formula for the solution of a system of first-order linear differential equations (See Ref. 15, Chapter 1).

The remaining part of the proof demonstrates that the function $(\mathcal{L}_R + N_{x_0})$ is onto for each $x_0 \in P^n$, using Granas' solvability theorem. Thus it is proved that the perturbed differential equation is completely controllable when the linear system is completely controllable. Another perspective on the proof is that Granas' theorem tells us that Eq. 4.3-23 can be solved for the u necessary to drive Eq. 4.3-20 from $x_2(t_0)$ to $x_2(T)$; therefore Eq. 4.3-20 is completely controllable.

The proof of Theorem 4.3.2 (Eq. 4.3-12) requires use of separate theorems for independent perturbations of the state and control variables. The starting point of this proof is once again the statement of the linear and perturbed nonlinear equations, i.e., Eq. 4.3-18 and 4.3-20 modified to yield

$$\Delta \dot{x} = A(t) \Delta x + \varepsilon h(x_2, u, t) \quad (4.3-26)$$

$$\Delta x(t_0) = 0_n \quad (4.3-27)$$

Subsequently Sastry proves that N_{x_0} , as stated in the previous proof, can be found to have a quasinorm

$$\rho(N_{x_0}) \leq 2 \varepsilon C_0 \mu T^{\frac{1}{2}} \{ \lambda_L + \gamma(B) \lambda_S^{-1} \cdot \sup_{t_0 \in R_+} \sup_{\tau \in [0, T]} |\phi(t_0 + T, t_0 + \tau)|_i \} \quad (4.3-28)$$

Thus, rewriting Eq. 4.3-28 in terms of ε provides the main formula of Theorem 4.3.2, Eq. 4.3-12. Once again the reader is referred to Ref. 26 for the complete proof. Note, however, that Refs. 25 and 26 contain typographical errors in the statement of Eq. 4.3-12 and in the exposition of the proof.

4.3.3 Computation of the Relative Controllability Index

The application of the relative controllability theorem requires the computation of the controllability index defined in Eq. 4.3-12 for the system under consideration. Specifically this requires computation of the Grammian (Eq. 4.3-1), the reachability condition number (Eqs. 4.3-3 and 4.3-4), the transition matrix $\phi(t_0, t_0 + T)$ (Eq. 4.3-12), and the induced norms of $G(t)$ and $\phi(t_0, t_0 + T)$.

For a general linear time-varying system computation of the transition matrix requires the use of the Peano-Baker series,^{*} i.e.,

$$\begin{aligned} \phi(t, t_0) = I + \int_{t_0}^t d\sigma_1 A(\sigma_1) + \int_{t_0}^{t_1} d\sigma_1 A(\sigma_1) \\ \cdot \int_{t_0}^{\sigma_1} d\sigma_2 A(\sigma_2) + \dots \end{aligned} \quad (4.3-29)$$

which is difficult to solve numerically. However, if one assumes that the time-varying nature of $F(t)$ can be represented by a matrix of piecewise constant functions, then at any specific time the F matrix is constant, i.e.,

$$F(t) = \begin{cases} F_{t_0} & t_0 \leq t < t_1 \\ F_{t_1} & t_1 \leq t < t_2 \\ \vdots & \\ F_{t_n} & t_{n-1} \leq t < t_n \end{cases} \quad (4.3-30)$$

across any interval the solution to the linear time-varying equation is

$$\underline{x}(t) = \phi(t, t_i) \underline{x}(t_i) \quad t_i \leq t < t_{i+1} \quad (4.3-31)$$

^{*}See Ref. 15 for a discussion of the Peano-Baker series and its use for solving a n -th order system of linear differential equations with time-varying coefficients.

where

$$\phi(t, t_i) = \sum_{k=0}^{\infty} \frac{F_{t_i}^k (t-t_i)^k}{k!} \quad (4.3-32)$$

The advantage of this piecewise time-invariant representation is that highly accurate and reliable algorithms are available for computing the matrix series in Eq. 4.3-32. Furthermore, the semi-group property of the transition matrix can be exploited to yield the transition matrix for an entire interval, namely,

$$\phi(t_n, t_0) = \prod_{i=0}^{n-1} \phi(t_{i+1}, t_i) \quad (4.3-33)$$

Consequently, the numerical computation of the transition matrix in the relative controllability formula is easily accomplished if the dynamics are assumed to be linear, piecewise time-invariant. Furthermore, the linear, piecewise time-invariant matrices can be readily obtained from the nonlinear 6-DOF dynamics through linearization at regular intervals. In other words matrices are obtained at regular intervals from a simulation trajectory of

$$\dot{\underline{x}} = \underline{f}(\underline{x}, \underline{u}, t) \quad (4.3-34)$$

The linear, piecewise time-invariant matrices are

$$F_{t_i} = \left. \frac{\partial \underline{f}(\underline{x}, \underline{u}, t)}{\partial \underline{x}} \right|_{t_i} \quad (4.3-35)$$

and

$$G_{t_i} = \frac{\partial \underline{f}(\underline{x}, \underline{u}, t)}{\partial \underline{u}} \bigg|_{t_i} \quad (4.3-36)$$

The 6-DOF simulation described in Appendix A implements this feature.

Once the computational challenge of computing $\phi(t, t_0)$ is overcome, the remaining elements of Eq. 4.3-12 are easy to solve. The key assumption at this point is to assume that the collection of linear, piecewise time-invariant transition matrices represents the dynamics of a discrete equivalent to the original continuous system. Hence we can define a

$$x(k_{t_{i+1}}) = \phi(k_{t_i}, k_{t_{i+1}})x(k_{t_i}) + \Gamma(k_{t_i}, k_{t_{i+1}})u(k_{t_i}) \quad (4.3-37)$$

where $\Gamma(\cdot)$, the discrete equivalent control matrix, is defined as

$$\Gamma(k_{t_i}, k_{t_{i+1}}) = \int_{t_i}^{t_{i+1}} \phi(t_i, t_i + \tau) G(\tau) d\tau \quad (4.3-38)$$

Note the indices of the discrete system in Eq. 4.3-37 are defined to correspond with the regular intervals of time at which the linear, piecewise time-invariant system is computed.

The impact of the discrete representation in Eqs. 4.3-37 and 4.3-38, is that one can now use the definition of the discrete Grammian, in place of the continuous Crammian defined in Eq. 4.3-1. The discrete Grammian is defined as

$$W(k_{t_f}, k_{t_o}) = \sum_{\ell=k_{t_o}}^{k_{t_f}-1} \Phi(k_{t_f}, \ell+1) \Gamma(\ell) \Gamma^T(\ell) \Phi^T(k_{t_f}, \ell+1) \quad (4.3-39)$$

This equation is easily computed from the collection of transition matrices, which is a more tractable numerical problem than the integral of Eq. 4.3-1.

Standard eigenanalysis algorithms are then used to compute the eigenvalues of $W(t, t_o)$ which provide λ_L (Eq. 4.3-3), λ_S (Eq. 4.3-4), χ_R (Eq. 4.3-2) and μ (Eq. 4.3-13). The remaining elements, $\gamma(G)$ (Eq. 4.3-14) and the induced norm of $\Phi(t_o, t_o+T)$ are computed in accordance with the definition of the L_2 norm, hence

$$|\Phi(t_{i+1}, t_i)|_i = \max_k \sqrt{\lambda_k(\Phi(t_{i+1}, t_i)^* \Phi(t_{i+1}, t_i))} \quad (4.3-40)$$

and

$$|G(t_i)|_i = \max_k \sqrt{\lambda_k(G(t_i)^* G(t_i))} \quad (4.3-41)$$

where $*$ indicates the conjugate transpose. The right-hand sides of Eqs. 4.3-40 and 4.3-41 are equivalent to the maximum singular value of the matrix under consideration. Fortunately, reliable algorithms for numerically computing the singular values of a matrix are readily available.

Finally the supremum, or least upper bound, for the sequence of Eqs. 4.3-40 and 4.3-41 over the interval $[0, T]$ is numerically computed as

$$\sup_{\tau \in [0, T]} \|\phi(t_0 + T, t_0 + \tau)\|_i = \max_i \|\phi(t_{i+1}, t_i)\|_{L_2} + \Delta \quad (4.3-42)$$

and

$$\sup_{\tau \in [0, T]} \|G(\tau)\|_i = \max_i \|G(t_i)\|_{L_2} + \Delta \quad (4.3-43)$$

where Δ is the smallest number within the floating-point representation of the computer in use.

The numerical computations outlined in this section are feasible when the assumption of linear, piecewise time-invariant dynamics is made. This assumption is compatible with the computation of time-varying state variable descriptions of nonlinear 6-DOF dynamics through numerical linearization within a numerical integration of the nonlinear differential equations. Consequently although the numerical computation of the relative controllability for a continuously time-varying system with matrices $F(t)$ and $G(t)$ may be achievable, the formidable task of analytically obtaining $F(t)$ and $G(t)$ from the nonlinear dynamics would remain to be solved.

The numerical procedures presented in this section have been implemented in the Canonical System Evaluator (CASE) software package. A thorough description of the software can be found in Appendix B of this report.

5.

CONCLUSIONS AND RECOMMENDATIONS

5.1 SUMMARY

This report of the Nonlinear Flying Qualities for Large Amplitude Maneuvers Program documents a research and development effort to extend conventional flying qualities procedures and specifications to combat maneuvers. An applied analysis methodology was developed, entitled canonical systems theory, which was found to sufficiently include the additional mathematical structure required to handle large amplitude combat maneuvers. The canonical systems methodology surpasses the conventional flying qualities, equivalent systems methodology, through the use of time-varying, multivariable state-space mathematical forms. The canonical systems theory met the research goals of the program because: it is of sufficient generality to handle nonlinear maneuvers yet remain compatible with the current equivalent systems methodology, admits a tractable numerical solution procedure, and can be applied in a 6-DOF simulation environment of the aircraft under investigation.

In keeping with the goal of developing a useable analysis tool, a complete numerical solution of the canonical system methodology and computation of the intrinsic flying qualities criteria was developed. The tool was then applied to a 6-DOF aeropropulsive model of the AFTI/F-16 aircraft. The objective of the AFTI/F-16 canonical systems analysis was not to evaluate the specific AFTI/F-16 performance, but to evaluate the performance of the canonical systems based methodology as a flying qualities analysis procedure, especially for combat maneuvers.

Two maneuvers were extensively investigated: a rolling reversal and a wind-up turn. The data computed in the sample results and presented in this report include, the norm of the canonical system match, the relative controllability index, both over the trajectory, and a perturbation simulation of the canonical system.

Although the analysis methodology applied in the NFQ derives from local nonlinear system theory (i.e., almost linear) a literature search of nonlinear analysis and system theory was performed. One result of which was the relative controllability theorem subsequently applied in the canonical-system-based analysis. However, the general observations of the literature search have been reported to allow the reader to appreciate the breadth and depth of nonlinear system theory and the multitude of directions that can be pursued by future nonlinear flying qualities research.

5.2 CONCLUSIONS

The principal conclusions that can be drawn from the NFQ research concern the usefulness of canonical systems theory in evaluating intrinsic flying qualities criteria. Extrinsic flying qualities criteria and their correlation with the intrinsic criteria explored in the NFQ research remains to be investigated. Experiments with the intrinsic flying qualities criteria did provide sufficient data to evaluate the sensitivity of the criteria to maneuver differences, dynamic coupling (e.g., dihedral) during a maneuver, and control cross-coupling. In addition to the canonical system experiments, a significant product of the NFQ research is the development of a set of canonical system analysis tools which can be used to analyze other aircraft models and ultimately, provide a fundamental tool for the correlation with extrinsic flying qualities.

Bearing in mind the distinction between intrinsic and extrinsic flying qualities and the proper goals of the current program, the major conclusions are:

- A literature search revealed that global nonlinear system theory is immature for present application to aircraft flying qualities analysis and fails to meet two goals of the current program: compatibility with the current equivalent systems methodology, and computable and constructive theorems that yield numerical results
- Numerical results from applying canonical systems theory to a nonlinear six-degree-of-freedom aircraft model suggest that canonical system matching can measure the tendency of the aircraft dynamics to behave like the pilot-preferred dynamics, e.g., longitudinal-lateral decoupling
- The measure of the closest canonical system match, i.e., $||\Delta F||$ and $||\Delta G||$ both reflected the onset of roll-induced sideslip, kinematic coupling, and control cross-coupling especially during a roll-reversal
- The subsequent application of the relative controllability theorem yielded criteria, indicative of the controllability properties of the canonical and true linearized systems and of the controllability properties of specific subsystems of the 6-DOF dynamics; the criteria tracked the expected controllability variations, e.g., (onset of coupling and loss of control authority) expected during a large amplitude maneuver.

Thus, the analysis methodology and flying qualities criteria developed in this program have been shown to yield representative intrinsic flying qualities criteria; where intrinsic implies that the criteria are functions of the aircraft dynamics alone and are not indicative of pilot reaction to those dynamics.

5.3 RECOMMENDATIONS

The recommendations after this phase of the NFQ research obviously is to suggest the investigation of extrinsic flying qualities with the canonical systems methodology. Another area of research, however, is further development of the canonical system structures. Although the candidates described were not ad hoc choices, being based on the mathematical structure of linearized aircraft dynamics, further development would not be wasted. Finally, improvements in the numerical procedure would be welcomed as well.

The primary recommendations of the NFQ research, in descending priority, are thus:

- An initial approach to calibrating the canonical system-parameters to extrinsic flying qualities should be pursued through the analysis of autonomous flying modes, e.g., automatic landing, terrain-following, in which the vehicle performance can be quantitatively evaluated without pilot opinion (verifying that the ride comfort requirements of the pilot and crew are met)
- In a parallel investigation, the canonical systems can be flown while adjusting the control and guidance algorithms, to yield an ideal system structure that provides the best performance in a given mission, hence specializing the canonical system structure to a mission specification
- Finally, research in applying nonlinear system theory to flying qualities analysis should and must continue, in particular, the current research suggests that Volterra series methods promise some of the greatest near-term progress.

Note that these recommendations have been formed with consideration of the difficulties and high cost associated with pilot-in-the-loop simulations for calibrating the canonical system parameters. Finally, continued research in nonlinear system theory is warranted, not because of the shortfalls of the canonical systems theory, but because of the rapid progress being made in all facets of nonlinear system theory.

APPENDIX A
AFTI/F-16 SIX-DEGREE-OF-FREEDOM
SIMULATION OVERVIEW

The 6-DOF simulation used in the NFQ applied formulation implements a comprehensive AFTI/F-16 aircraft model. The 6-DOF simulation also provides automated linearization and eigenanalysis. The linearization directly provides linear system representations of the aircraft dynamics for use in the canonical system evaluator software. This appendix describes the functional features of the 6-DOF simulation and documents all the modeling equations necessary for the 6-DOF dynamics, AFTI/F-16 aerodynamics, and various other subsystems required to produce a faithful aircraft trajectory simulation. Section A.1 describes the overall structure and operation of the primary modules that perform the integration, linearization, eigenanalysis, and output functions. Section A.2 then gives a detailed account of each of the subsystem modeling modules. Finally, Section A.3 concludes the appendix with a description of the linearization and eigenanalysis procedures. Note that throughout this discussion a state-variable structure is emphasized, thus, facilitating the eigenanalysis and easy interface with the other NFQ analysis procedures (described in Appendix B).

A.1 OVERALL PROGRAM STRUCTURE

A.1.1 The Main Program

The 6-DOF simulation is organized into a hierarchy of subroutines in which the lowest level contains the direct implementation of subsystem functions. The central features of

the simulation are contained within a block of subroutines which are called by the MAIN program directly. The calling sequence is diagrammed in the upper half of Fig. A.1-1. Essential numerical algorithms are computed in the routines INTEG and EIGEN. Subroutine INTEG performs the numerical integration of the state derivatives, subroutine EIGEN directs the linearization and eigenanalysis. Subroutine OUTPUT provides the printing of intermediate variables and the storage of data for subsequent plotting. Subroutine UOIN reads time-spaced values for the aircraft control surfaces for flying preprogrammed maneuvers. The lower half of Fig. 2.1-1 diagrams the relationship of the module KINMAT to the individual subsystem modules; the description of this module can be found in Section A.2.2.

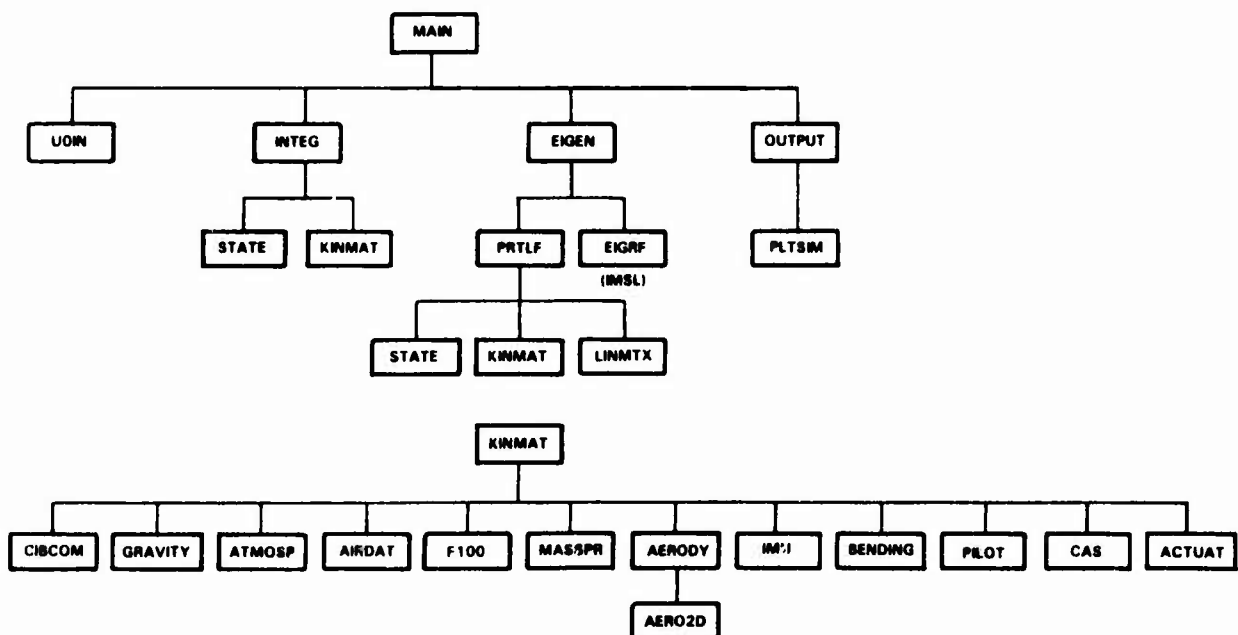


Figure A.1-1 Six-Degree-of-Freedom Simulation Structure

A flow chart of the MAIN program and its use of subroutines INTEG, EIGEN and OUTPUT is diagrammed in Fig. A.1-2. The major recursive computation is indicated with dash lines. This is the integration loop which calls INTEG continually until the number of integration steps has exceeded the maximum. During each pass through this loop, a test is performed to determine whether a call to EIGEN is needed. Similarly there is a variable, INTOUT, which is cycled to determine when calls to OUTPUT are made. These are typical of the supervisory functions performed by the MAIN program, with selectable parameters available in the input NAMELIST for specifying the specific operations.

A.1.2 Integration of the State Vector in INTEG

The subroutine INTEG, the core module of the 6-DOF simulation, performs the numerical integration of the nonlinear differential equations. The subroutine is primarily a numerical integration algorithm but it also organizes calls to two routines, KINMAT and STATE. KINMAT provides the state derivatives of the nonlinear dynamics after computation of the state at each successive time step. The subroutine STATE is a unique feature of the 6-DOF simulation which combines the state derivatives from each module (i.e., subroutine where they are calculated) and disseminates the newly integrated state to each module. Consequently, all time derivatives are combined into a single state vector and simultaneously integrated in INTEG. The new states which are the result of the numerical integration are returned to the respective modules for a new evaluation of the derivatives.

In the FORTRAN 77 programming language this is accomplished by having a common block associated with each subroutine which contains the states, the state derivative, and an integer

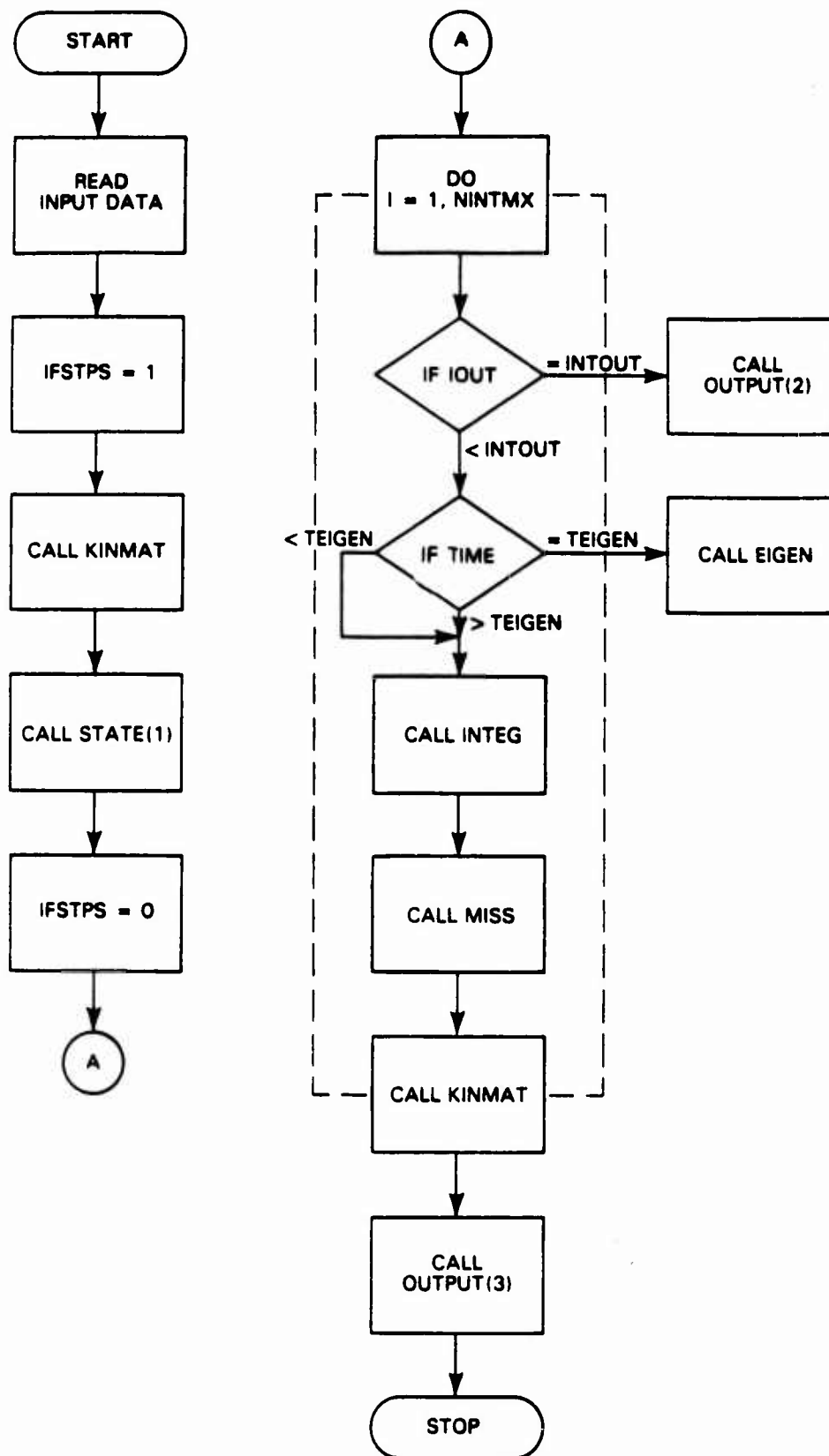


Figure A.1-2 Simulation Flow Chart (MAIN Program)

denoting the number of states for a particular aircraft subsystem. This option of specifying the number of states in any subroutine facilitates the rapid exchange of subroutines or subsystem models because the subroutine STATE concatenates only the number of states indicated by the state number in the associated common block. In addition to providing modularity and a flexible state vector, the operations performed in INTEG ensure that all the time derivatives are integrated in an identical algorithm and without time skewing. The unforeseen time delays or inconsistent roundoff errors associated with simulations which integrate portions of the model separately, are obviated in this approach.

The program flow chart is outlined in Fig. A.1-3. The recursive loop, which is executed four times, is characteristic of the fourth-order Runge-Kutta algorithm which is used for the numerical integration. Attributes and rationale for the Runge-Kutta algorithm can be found in Ref. 66. The 6-DOF simulation specifically employs a modification to the algorithm which bears the name Runge-Kutta-Gill. This modification provides two improvements: a form for the algorithm which minimizes the storage of successive values of the function, and a roundoff error control scheme. The derivation of this scheme can be found in the work by Gill in Ref. 67 or in an excellent tutorial presented in Ref. 66.

A.2 SIX-DEGREE-OF-FREEDOM EQUATIONS OF MOTION

A.2.1 The Equations of Motion and Coordinate Conventions

The six-degree-of-freedom equations of motion include all accelerations, velocities, rotational rates and rotational accelerations in three dimensions necessary for specifying the

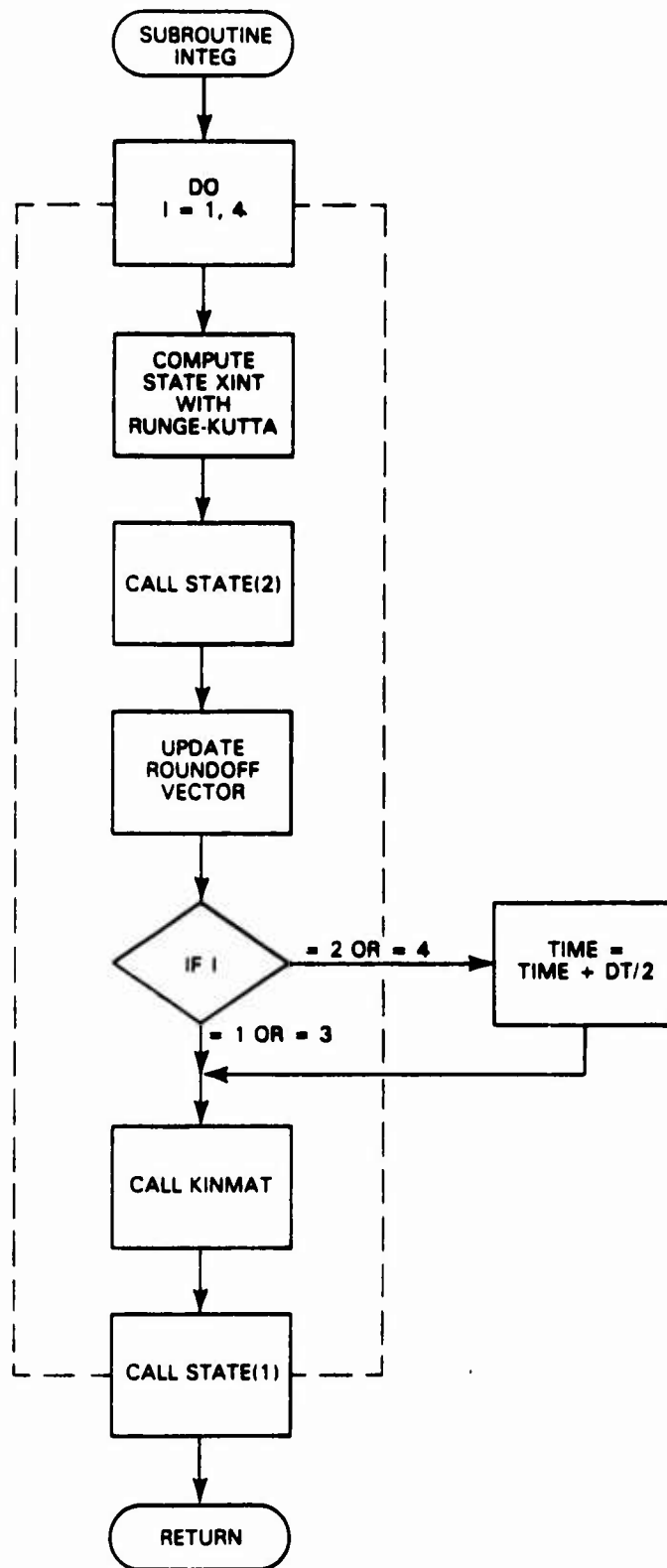


Figure A.1-3 Numerical Integration Flow Chart
(Subroutine INTEG)

trajectory of a free body. When modeling rigid-body dynamics in three dimensions, a variety of coordinate frames may be used. For the AFTI/F-16 6-DOF simulation the coordinate frames are an inertial frame, associated with a flat earth approximation, and a body axis frame (see Fig. A.2-1). Figure A.2-2 depicts the sign convention for the AFTI/F-16 control surface deflections. A direction cosine matrix is used to transform vectors from inertial to body axis (or vice versa with its transpose). The description of the equations of motion that follows is a state variable description, and hence affords convenient vector and matrix operations for coordinate transformations, linearization, and eigenanalysis.

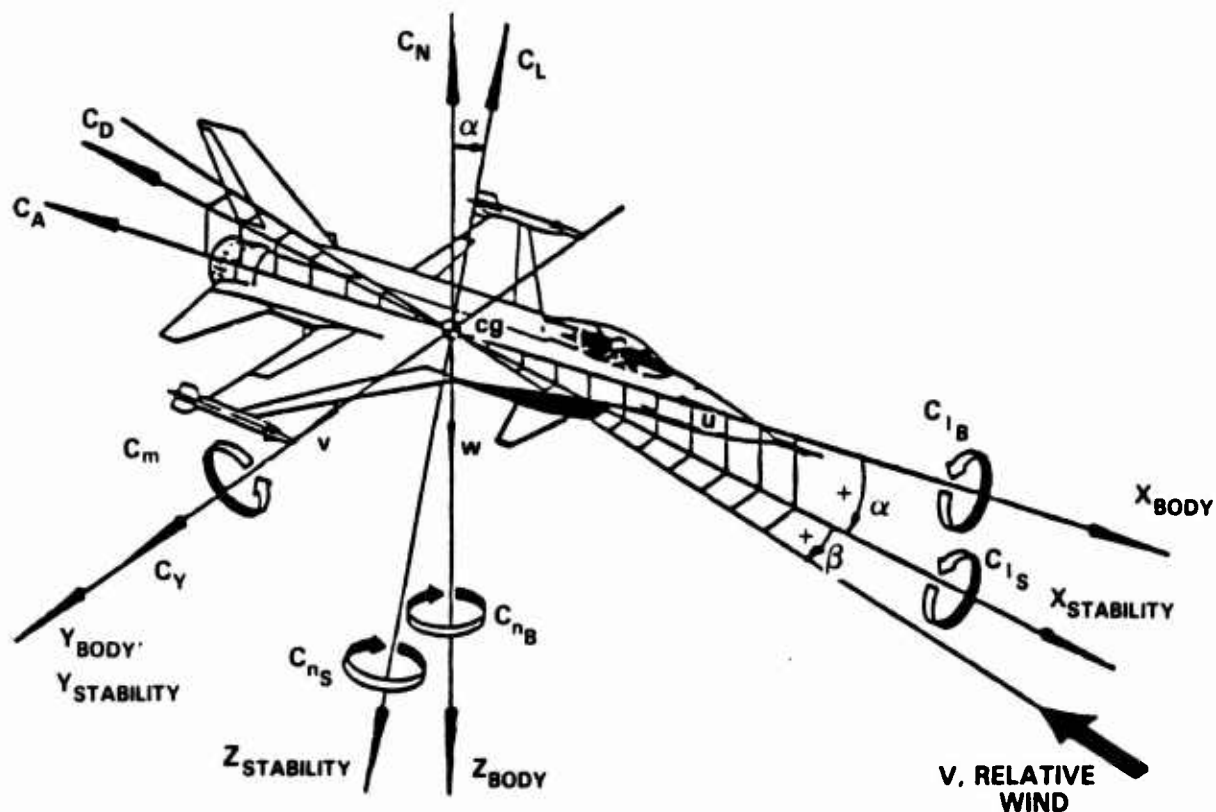


Figure A.2-1 Coordinate System Conventions

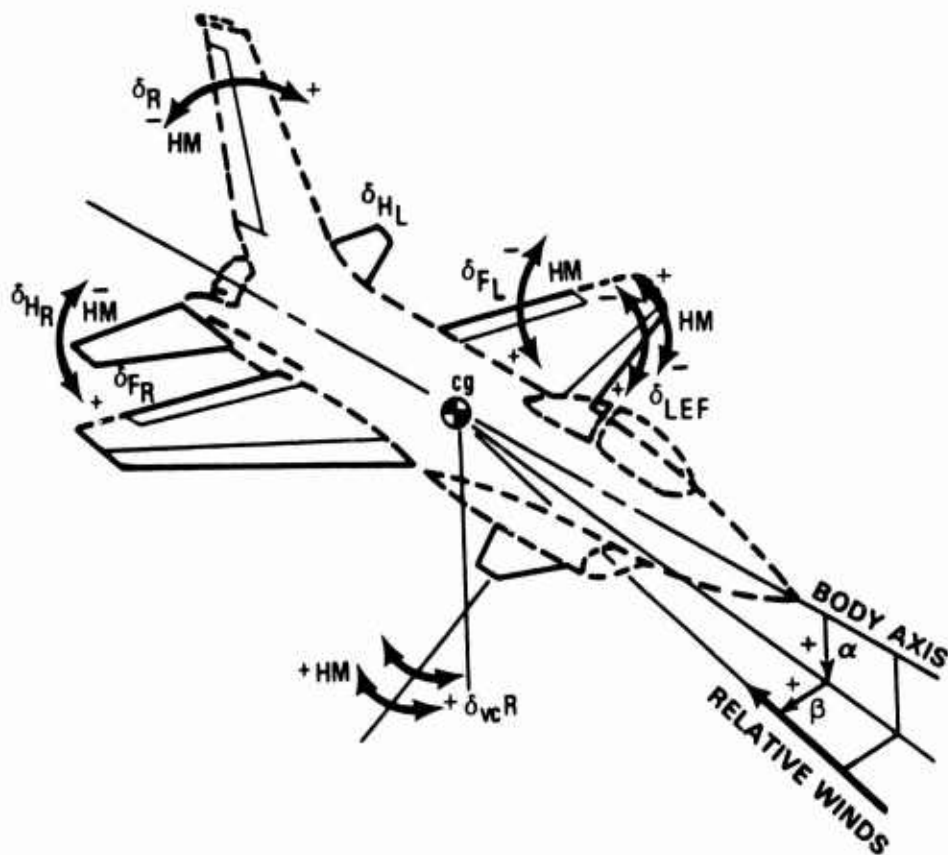


Figure A.2-2 Control Surface Sign Conventions

The state space model of the equations of motions consists of twelve states (see Table A.2-1), which are;

- Three aircraft translational velocity components in the body axis coordinate frame
- Three inertial position components defining the center of gravity (CG) position in the inertial coordinate frame
- Three rotation rate components of the body axes with respect to the inertial coordinate frame
- Three Euler angles which denote the angle between similar components of the body axes and inertial coordinate frames.

TABLE A.2-1
SYSTEM DYNAMIC STATES: THE 12 KINEMATIC STATES

STATE NUMBER	DEFINITION	MATH SYMBOL	UNITS
1	Velocity along body x-axis	v_x^B	ft/sec
2	Velocity along body y-axis	v_y^B	ft/sec
3	Velocity along body z-axis	v_z^B	ft/sec
4	Position along inertial x-axis	$r_x^I = x$	ft
5	Position along inertial y-axis (crossrange)	$r_y^I = y$	ft
6	Position along inertial z-axis (negative altitude)	$r_z^I = z$	ft
7	Body angular rate about body x-axis	$w_1 = p$	rad/sec
8	Body angular rate about body y-axis	$w_2 = q$	rad/sec
9	Body angular rate about body z-axis	$w_3 = r$	rad/sec
10	Body roll Euler angle	ϕ	rad
11	Body pitch Euler angle	θ	rad
12	Body yaw Euler angle	ψ	rad

These twelve states can be assembled into four vectors of three components each. These vectors are defined as:

$\underline{v}^B \triangleq$ Aircraft translational velocity with respect to inertial coordinate frame in the body axes coordinate frame

$\underline{r}^I \triangleq$ Aircraft (CG) position vector in the inertial coordinate frame

$\underline{w} \triangleq$ Aircraft rotation rates with respect to the inertial coordinate frame in the body axis coordinate frame

EANG \triangleq Vector of three Euler angles.

The state space equations for the twelve kinematic states are as follows. The time derivative of body-axis velocity is given by

$$\dot{\underline{v}}^B = \frac{\bar{q}S}{m} \underline{C}_f + \frac{\underline{f}_t}{m} + C_I^B \underline{g}^I - \underline{w} \times \underline{v}^B \quad (\text{A.2-1})$$

the time derivative of inertial position is given by

$$\dot{\underline{r}}^I = C_B^I \underline{v}^B \quad (\text{A.2-2})$$

the time derivative of rotation rate is given by

$$\dot{\underline{w}} = [I_N^{-1}] \left\{ \bar{q}S \hat{\underline{C}}_m - \bar{q}S (\underline{\Delta Cg} \times \underline{C}_f) + \underline{m}_T - (\underline{w} \times I_N \underline{w}) \right\} \quad (\text{A.2-3})$$

where

$$\hat{\underline{C}}_m = \begin{bmatrix} b & C_\ell \\ \bar{c} & C_m \\ b & C_n \end{bmatrix}$$

and finally the time derivative of the Euler angles,

$$\underline{\dot{E}ANG} = \begin{bmatrix} \dot{\phi} \\ \dot{\theta} \\ \dot{\psi} \end{bmatrix} = \begin{bmatrix} w_1 + (\sin \phi w_2 + \cos \phi w_3) \tan \theta \\ \cos \phi w_2 - \sin \phi w_3 \\ (\sin \phi w_2 + \cos \phi w_3)/\cos \theta \end{bmatrix} \quad (A.2-4)$$

The following quantities used in the six-degree-of-freedom equations are computed in the various modules called by KINMAT. The definitions are

\bar{q} = Dynamic Pressure

S = Aerodynamic Reference Area (wing plan area)

b = Lateral Reference Length (wing span)

\bar{c} = Longitudinal Reference Length (mean wing chord)

m = Mass

C_B^I = Direction Cosine Matrix (Table A.2-2)
 $= [C_I^B]^{-1}$ or $[C_I^B]^T$

I_N = Inertia tensor (see MASSPR module description)

\underline{C}_f = Aerodynamic force coefficients in body axes,
 C_x, C_y, C_z

$\hat{\underline{C}}_m$ = Aerodynamic moment coefficients, C_ℓ, C_m, C_n
times associated reference length

\underline{f}_T = Thrust vector in body axis

\underline{m}_T = Thrust moment vector

$\underline{\Delta Cg}$ = Vector from \underline{Cg} to aerodynamic reference point.

TABLE A.2-2
DIRECTION COSINE TRANSFORMATION
MATRIX ELEMENTS

i,j	C_B^I ij
1,1	$\cos \theta \cos \psi$
1,2	$\sin \phi \sin \theta \cos \psi - \cos \phi \sin \psi$
1,3	$\cos \phi \sin \theta \cos \psi + \sin \phi \sin \psi$
2,1	$\cos \theta \sin \psi$
2,2	$\sin \phi \sin \theta \sin \psi + \cos \phi \cos \psi$
2,3	$\cos \phi \sin \theta \sin \psi - \sin \phi \cos \psi$
3,1	$-\sin \theta$
3,2	$\sin \phi \cos \theta$
3,3	$\cos \phi \cos \theta$

The right side of Eq. A.2-1 includes the summation of all forces acting on the aircraft. The four terms on the right side of Eq. A.2-1 represent the following:

- Aerodynamic force effects in body axes
- Thrust force effects in body axes
- Projection of gravity onto body axes
- Centripetal accelerations (treated as apparent forces).

Equation A.2-2 defines the rate of change of the missile inertial position as the transformation of the body-referenced velocity \underline{v}^B . The right side of Eq. A.2-3 represents the effect of all moments acting on the airframe. The quantity

$[I_N]$ is the inertia matrix (see Eq. A.2-23); the following four terms are included within the braces of Eq. A.2-3, from left to right:

- Aerodynamic moments about the body-fixed aerodynamic reference point
- Aerodynamic moment translation to Cg location
- Thrust moment about the Cg
- Gyroscopic coupling terms (again, treated as apparent moments).

Equation A.2-4 represents the dynamics of the Euler angle states; a concise derivation of these equations can be found in Ref. 55, pp. 125-127.

A.2.2 The Module KINMAT

The subroutine KINMAT performs all the operations necessary for computing the twelve state derivatives of position, velocity, rotation rate and Euler angles. Equations A.2-1 to A.2-4 are evaluated in KINMAT. In addition, KINMAT is an executive routine which performs the function of calling all auxiliary and subsystem modules in the order necessary for proper closed-loop simulation (i.e., an aircraft containing an augmentation system which uses feedback). The calls to the various auxiliary modules are broken into two sequences so that KINMAT can compute specific force, which is required by the accelerometer model within the control augmentation system.

Figure A.2-3 is a flow chart for KINMAT. All those subroutines which were depicted in Fig. A.1-1 as being below KINMAT are explicitly called by KINMAT. Of the subroutines called, a portion are auxiliary modules necessary for simulating

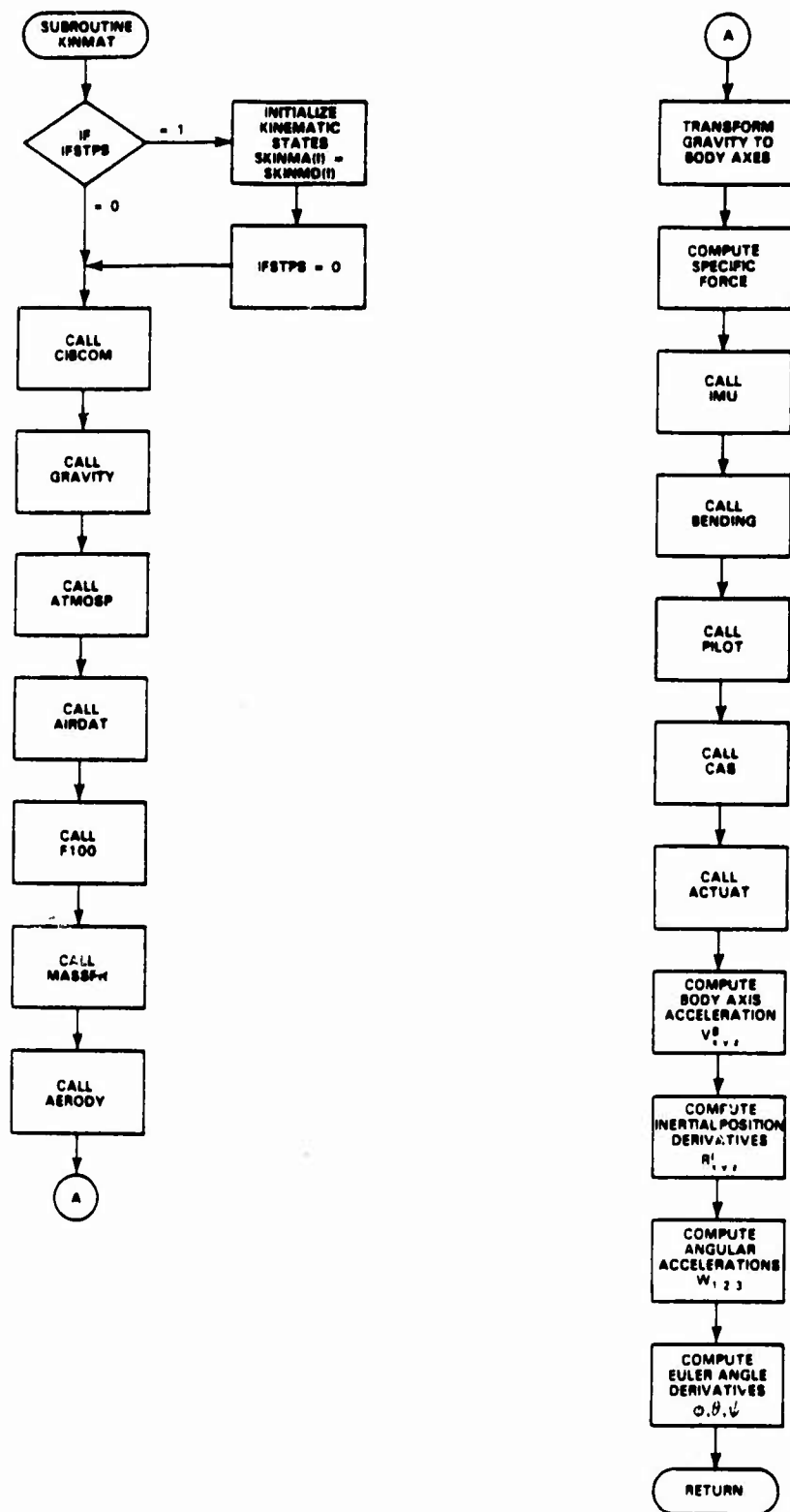


Figure A.2-3 6-DOF Equations of Motion
(Subroutine KINMAT)

an aerodynamic vehicle; these modules will be described in the following section. The remaining subroutines are subsystem models pertinent to simulating the AFTI/F-16 aircraft. These subsystem models include both intermediate variable computations and state dynamics. Common blocks are provided with each subroutine with the naming convention S_ _ _ _ where the blanks are the respective subroutine names. These specific common blocks are used for input/output of the states, state derivatives, and state dimension for each subsystem. By altering the state dimension parameter (from input data), direct modification to the number of subsystems simulated can be accomplished without altering the source code of KINMAT. This procedure provides a high degree of versatility and modularity to the simulation structure.

A.2.3 Auxiliary Modules for the Equations of Motion

The equations of motion for a general rigid body in space were described in the Subsection A.2.1. Additional computations and earth relative information are also necessary for the simulation of an aerodynamic vehicle in KINMAT. The essential modules (i.e., subroutines) in the 6DOF simulation are: CIBCOM, ATMOSP, GRAVITY, AIRDAT and MASSPR. A description of each of these modules will follow.

Module CIBCOM: Coordinate Transformation - The subroutine CIBCOM is used to compute the direction cosine matrix which is required for transforming vectors from the inertial to body coordinate frames or vice versa. The specific elements of the matrix are sine and cosine functions of the set of Euler angles (states 10, 11, and 12 in Table A.2-1) relating the coordinate frames. The subroutine accepts as input the Euler angle array, EANG(3), which is stored in the kinematic state common block, SKINMA. The subroutine state returns

the computed body-to-inertial transformation matrix C_B^I (defined in Table A.2-2) and its transpose, the inertial-to-body transformation matrix, C_I^B . The sines of Euler angles, θ and ψ , and the cosines of θ and ψ are returned as output as well. All of the output variables are passed via common block, OCIBCO, for later use in KINMAT and any additional routine which requires these Euler angle functions.

Module ATMOSP: Atmospheric Modeling - The subroutine, ATMOSP, provides a number of atmospheric variables as a function of altitude using the 1962, U.S. Standard Atmosphere (Ref. 56). The variables of interest are the atmospheric pressure, the air density, and the speed of sound. Furthermore, there is a provision to accept tables defining a wind velocity versus altitude profile from the input data stream.

The variables of interest (atmospheric pressure, air density, and speed of sound), are stored in tables as a function of altitude. Linear interpolation is performed to compute values of these variables for altitudes which are not stored in the tables. Consistent with this arrangement, if a need arises to input wind profiles, vector wind velocities would be supplied at those altitudes specified in the altitude table.

Module GRAVITY: Gravity Modeling - The subroutine GRAVITY computes gravitational acceleration as a function of altitude above a flat earth approximation. The flat earth approximation is the inertial system defined in Section A.2; hence, gravitational acceleration is a function of the third component or z-axis of that coordinate system. The specific expression in the software is

$$\text{grav}(3) = G_0 - (3.07 \times 10^{-6} h) \quad (\text{A.2-5})$$

where

$$G_0 = 32.1735 \text{ ft/sec}^2$$
$$h = -r_z^I \text{ in feet}$$

Note that the gravitational acceleration is a vector with the first and second components set to zero. The use of a full vector in computation of the vehicle specific acceleration provides the flexibility to include an expanded gravity model by simply altering the equations in subroutine GRAVITY.

Module AIRDAT: Wind Axis Computation - The subroutine AIRDAT consists of the equations which define the aerodynamic variables necessary for computing the aerodynamic forces and moments. The first in this series of equations defines the relative velocity vector \underline{v}_r , which represents the velocity (coordinatized in body axes) of the vehicle with respect to the air mass, where wind velocities are coordinatized in the earth inertial frame. Thus,

$$\underline{v}_r = \underline{v}^B - C_I^B \underline{v}_w^I \quad (\text{A.2-6})$$

where

C_I^B is the inertial to body frame transformation matrix

\underline{v}_w^I is the wind velocity in the inertial frame

\underline{v}^B is the aircraft velocity in the body axis frame.

The magnitude of \underline{v}_r is used in the Mach number computation, thus,

$$v_m = \sqrt{v_{r1}^2 + v_{r2}^2 + v_{r3}^2} \quad (\text{A.2-7})$$

$$\text{MACH} = v_m / v_s \quad (\text{A.2-8})$$

where v_s is the speed of sound, a function of altitude computed in ATMOSP.

The next parameter of interest is the dynamic pressure, \bar{q} . It is computed as

$$\bar{q} = \frac{1}{2} \rho v_m^2 \quad (\text{A.2-9})$$

where ρ is the air density, a function of altitude computed in ATMOSP.

The remaining equations define the aerodynamic angles, which identify the orientation of the body axis with respect to the relative velocity vector. The typical angles for single-plane-of-symmetry vehicles are the angle-of-attack (α) and the sideslip angle (β), defined as

$$\alpha = \tan^{-1} (v_{r3} / v_{r1}) \quad (\text{A.2-10})$$

$$\beta = \sin^{-1} (v_{r2} / v_m) \quad (\text{A.2-10})$$

Note that these definitions form valid Euler angles which can be used for transforming vectors from the wind axis coordinate frame to the body axis frame.

For reference, a cross index of Fortran variables to math symbols for the parameters computed in the auxiliary modules is provided in Table A.2-3. Units for each of these parameters are provided as well.

TABLE A.2-3
AUXILIARY VARIABLES AND THEIR RESPECTIVE
MATH AND COMPUTER SYMBOLS

VARIABLE	SUBROUTINE	MATH SYMBOL	COMPUTER LABEL	UNITS
Wind Velocity	ATMOSP	v_w	VWIND(I) I=1,3	ft/sec
Atmospheric Pressure	"	P	PATM	lbf/ft ²
Density of Air	"	ρ	RHO	slugs/ft ³
Speed of Sound	"	v_s	VS	ft/sec
Relative Velocity	AIRDAT	\underline{v}_r	VR(I)	ft/sec
Relative Velocity Magnitude	"	v_M	VM	ft/sec
Dynamic Pressure	"	\bar{q}	Q	slugs/ft·sec ²
Angle-of-Attack	"	α	ALPHA	degrees
Total Angle-of-Attack	"	α_T	ALPTOT	degrees
Sideslip Angle	"	β	BETA	degrees
Mass	MASSPR	m	RMASS	slugs
Center of Gravity Location	MASSPR	$\underline{C_g}$	CG(I)	feet
Center of Gravity to Aero Reference Point	"	$\underline{\Delta C_g}$	DELCG(I)	feet
Inertial Tensor	"	I_N	RIN(I,J) I=1,3 J=1,3	slug·ft ²
Inverse Inertial Tensor	"	I_N^{-1}	RININV(I,J) I=1,3 J=1,3	1/slug·ft ²
Gravity Vector	GRAVITY	\underline{g}	GRAV(I)	ft/sec ²
Inertial to Body Transformation Matrix	CIBCOM	C_B^I	CIB(I,J) I=1,3 J=1,3	--
Body to Inertial Transformation Matrix	"	C_I^B	CBI(I,J) I=1,3 J=1,3	--

A.2.4 Aircraft Specific Models: AERODY, PROPUL, MASSPR and CAS

The simulation model becomes specific to the AFTI/F-16 vehicle upon inclusion of real data for the subroutines PROPUL, MASSPR, AERODY, and CAS. Subroutines PROPUL and AERODY implement a series of linear table interpolations to determine propulsion and aerodynamic parameters as a function of parameters such as Mach number and angle of attack (α). Subroutine CAS provides a model for a Control Augmentation System, a mandatory addition to the AFTI/F-16 because of open loop instability. The CAS also aids in integrating the guidance commands (e.g., acceleration and roll) needed to produce the desired large amplitude maneuvers. The large number of dependent variables used in the table interpolations of AERODY and PROPUL precludes a detailed listing of the modeling data. The following description will present only the equations of the AFTI/F-16 aerodynamics model used in the NFQ 6-DOF simulation and the Pratt and Whitney F-100 engine model.

Module AERODY: Aerodynamic Coefficient Computation - The NFQ 6-DOF simulation contains a thorough set of 67 aerodynamic coefficients. These coefficients are functions of 1 to 5 independent variables.* Although the complete model, from which this subset is drawn, has 217 variable tables, (including propulsion and mass properties) the excluded modeling detail is not critical for the NFQ analysis. In particular, flexible body coefficients, landing gear, flight test, and stores effects were deemed unnecessary for the NFQ analysis 6-DOF simulation. In the presentation of the aerodynamic modeling equations, mathematical symbols with functional dependence indicated by multiple subscripts and table look-up

*Due to the large number of coefficients, a separate module AERO2D computes all two-dimensional coefficient interpolations.

dependence indicated by parentheses will be used to represent the various coefficients. The notation used in these equations is consistent with the General Dynamics AFTI/F-16 dynamics model definition.

The nomenclature for the independent variables is:

- α = angle of attack (degrees)
- α_T = tail angle of attack ($\alpha_T = \alpha + \delta_h$) (degrees)
- $\bar{\alpha}$ = equivalent rigid body deflection (degrees)
- β = sideslip angle (degrees)
- M = Mach number
- v_m = relative velocity magnitude (ft/sec)
- δ_H = horizontal tail deflection
 $\delta_H = 1/2(\delta_{H_{right}} + \delta_{H_{left}})$ (degrees)
- δ_{VC} = vertical canard deflection
 $\delta_{vc} = 1/2(\delta_{vc_{left}} - \delta_{vc_{right}})$ (degrees)
- δ_{SP} = snowplow, differential canard deflection
 $\delta_{sp} = 1/2(\delta_{vc_{left}} + \delta_{vc_{right}})$ (degrees)
- δ_{SB} = speed brake deflection (degrees)
- δ_R = rudder deflection (degrees)
- δ_{LEF} = leading edge flap deflection (degrees)
- δ_{TEF} = trailing edge flap deflection
 $\delta_{TEF} = 1/2(\delta_{TEF_{right}} + \delta_{TEF_{left}})$ (degrees)
- δ_{FA} = flaperon deflection, differential trailing edge flap
 $\delta_{FA} = 1/2(\delta_{TEF_{right}} - \delta_{TEF_{left}})$ (degrees)

$$\delta_{HA} = \text{aileron deflection, differential horizontal tail}$$

$$\delta_{HA} = 1/2(\delta_{H_{right}} - \delta_{H_{left}}) \text{ (degrees)}$$

The nondimensional lift equation is:

$$C_L = \left[C_{N_{WBV}}(\delta_{LEF}, \delta_{TEF}, \alpha, M) \right. \\
+ \Delta C_{N_{\delta_H}}(\delta_{LEF}, \delta_{TEF}, \alpha_T, M) \cos \delta_H \\
- \Delta C_{A_{\delta_H}}(\delta_{LEF}, \delta_{TEF}, \alpha_T, M) \sin \delta_H \left. \right] \cos \alpha \\
- \left[C_{A_{WBV}}(\delta_{LEF}, \delta_{TEF}, \bar{\alpha}, M) \right. \\
+ \Delta C_{N_{\delta_H}}(\delta_{LEF}, \delta_{TEF}, \alpha_T, M) \sin \delta_H \\
- \Delta C_{A_{\delta_H}}(\delta_{LEF}, \delta_{TEF}, \alpha_T, M) \cos \delta_H \left. \right] \sin \alpha \\
+ \Delta C_{L_{\delta_{VC}}}(\delta_{VC}, \beta, \alpha, M) + \frac{\delta_{SP}}{25.} \Delta C_{L_{\delta_{SP}}}(\beta, \alpha, M) \\
+ \left[\frac{\delta_{SB}}{60.} \right] \Delta C_{L_{\delta_{SB}}}(\alpha, M) + C_{L_{\delta_{FA}}}(\delta_{TEF}, \alpha, M) |\delta_{FA}| \\
+ C_{L_{\delta_r}}(\alpha, M) |\delta_R| + C_{L_q}(\alpha, M) \frac{Q \bar{c}}{2V_m} + C_{L_{\dot{\alpha}}}(\alpha, M) \frac{\dot{\alpha} \bar{c}}{2V_m} \\
+ \Delta C_{L_{\beta}}(\beta, \alpha, M) \quad (A.2-11)$$

The nondimensional drag equation is:

$$\begin{aligned}
C_D = & \left[C_{N_{WBV}}(\delta_{LEF}, \delta_{TEF}, \alpha, M) + \Delta C_{N_{\delta_H}}(\delta_{LEF}, \delta_{TEF}, \alpha_T, M) \cos \delta_H \right. \\
& \left. - \Delta C_{A_{\delta_H}}(\delta_{LEF}, \delta_{TEF}, \alpha_T, M) \sin \delta_H \right] \sin \alpha \\
& + \left[C_{A_{WBV}}(\delta_{LEF}, \delta_{TEF}, \alpha, M) \right. \\
& + \Delta C_{N_{\delta_H}}(\delta_{LEF}, \delta_{TEF}, \alpha_T, M) \sin \delta_H \\
& \left. + \Delta C_{A_{\delta_H}}(\delta_{LEF}, \delta_{TEF}, \alpha_T, M) \cos \delta_H \right] \cos \alpha \\
& + \Delta C_{D_{\delta_{vc}}}(\delta_{vc}, \beta, \alpha, M) + \left[\frac{\delta_{sp}}{25.} \right]^2 \Delta C_{D_{\delta_{sp}}}(\beta, \alpha, M) \\
& + \left[\frac{\delta_{SB}}{60.} \right]^2 \Delta C_{D_{\delta_{SB}}}(\alpha, M) + C_{D_{\delta_{FA}}}(\delta_{TEF}, \alpha, M) |\delta_{FA}| \\
& + \left[\frac{\delta_R}{20.} \right]^2 \Delta C_{D_{\delta_R}}(\alpha, M) + \Delta C_{D_{\beta}}(\beta, \alpha, M)
\end{aligned} \tag{A.2-12}$$

The nondimensional side force equation is

$$\begin{aligned}
C_y = & C_{y_{WBH}}(\delta_{LEF}, \delta_{TEF}, \beta, \alpha, M) + \Delta C_{y_{VT}}(\delta_{LEF}, \delta_{TEF}, \beta, \alpha, M) \\
& + \Delta C_{y_{\delta_{VC}}}(\delta_{VC}, \beta, \alpha, M) + \left[\frac{\delta_{SP}}{25.} \right] \Delta C_{y_{\delta_{SP}}}(\beta, \alpha, M) \\
& + \Delta C_{y_{\delta_R}}(\delta_R, \delta_{LEF}, \delta_{TEF}, \alpha, M) + C_{y_{\delta_{FA}}}(\delta_{FA}, \delta_{LEF}, \delta_{TEF}, \alpha, M) \\
& + 4 \left[\Delta C_{y_{\delta_{HA}}}(\delta_{FA}, \delta_{LEF}, \delta_{TEF}, \alpha, M) \right. \\
& \quad \left. - \Delta C_{y_{\delta_{FA}}}(\delta_{FA}, \delta_{LEF}, \delta_{TEF}, \alpha, M) \right] \left[\frac{\delta_{HA}}{\delta_{FA}} \right] \\
& + C_{y_p}(\alpha, M) \frac{pb}{2v_m} + C_{y_r}(\alpha, M) \frac{rb}{2v_m} \quad (A.2-13)
\end{aligned}$$

The nondimensional pitching moment equation is:

$$\begin{aligned}
C_m = & C_{m_{WBV}}(\delta_{LEF}, \delta_{TEF}, \alpha, M) + \Delta C_{m_{\delta_H}}(\delta_{LEF}, \delta_{TEF}, \alpha_T, M) \delta_H \\
& + \Delta C_{m_{(\delta_{VC}=0)}}(\alpha, M) + \Delta C_{m_{\delta_{VC}}}(\delta_{VC}, \beta, \alpha, M) \\
& + \left[\frac{\delta_{SP}}{25.} \right] \Delta C_{m_{\delta_{sp}}}(\beta, \alpha, M) + \left[\frac{\delta_{SB}}{60.} \right] \Delta C_{m_{\delta_{SB}}}(\alpha, M) \\
& + C_{m_{\delta_{FA}}}(\delta_{TEF}, \alpha, M) |\delta_{FA}| + C_{m_{\delta_R}}(\alpha, M) |\delta_R| \\
& + C_{m_q}(\alpha, M) \frac{q\bar{c}}{2v_m} + C_{m_{\dot{\alpha}}}(\alpha, M) \frac{\dot{\alpha}\bar{c}}{2v_m} + \Delta C_{m_{\beta}}(\beta, \alpha, M) \quad (A.2-14)
\end{aligned}$$

The nondimensional yawing moment equation:

$$\begin{aligned}
C_n = & C_{n_{WBH}}(\delta_{LEF}, \delta_{TEF}, \beta, \alpha, M) + \Delta C_{n_{VT}}(\delta_{LEF}, \delta_{TEF}, \beta, \alpha, M) \\
& + \Delta C_{n_{\delta_{VC}}}(\delta_{VC}, \beta, \alpha, M) + \left[\frac{\delta_{SP}}{25.} \right] \Delta C_{n_{\delta_{SP}}}(\beta, \alpha, M) \\
& + \Delta C_{n_{\delta_R}}(\delta_R, \delta_{LEF}, \delta_{TEF}, \alpha, M) + \Delta C_{n_{\delta_{FA}}}(\delta_{FA}, \delta_{LEF}, \delta_{TEF}, \alpha, M) \\
& + 4 \left[\Delta C_{n_{\delta_{HA}}}(\delta_{FA}, \delta_{LEF}, \delta_{TEF}, \alpha, M) \right. \\
& \quad \left. - \Delta C_{n_{\delta_{FA}}}(\delta_{FA}, \delta_{LEF}, \delta_{TEF}, \alpha, M) \right] \left[\frac{\delta_{HA}}{\delta_{FA}} \right] \\
& + C_{n_p} \frac{pb}{2v_m} + C_{n_r} \frac{rb}{2v_m}
\end{aligned} \tag{A.2-15}$$

Finally, the nondimensional rolling moment equation is:

$$\begin{aligned}
C_\ell = & C_{\ell_{WBH}}(\delta_{LEF}, \delta_{TEF}, \beta, \alpha, M) + \Delta C_{\ell_{VT}}(\delta_{LEF}, \delta_{TEF}, \beta, \alpha, M) \\
& + \Delta C_{\ell_{\delta_{VC}}}(\delta_{VC}, \beta, \alpha, M) + \left[\frac{\delta_{SP}}{25.} \right] \Delta C_{\ell_{\delta_{SP}}}(\beta, \alpha, M) \\
& + \Delta C_{\ell_{\delta_R}}(\delta_R, \delta_{LEF}, \delta_{TEF}, \alpha, M) + \Delta C_{\ell_{\delta_{FA}}}(\delta_{FA}, \delta_{LEF}, \delta_{TEF}, \alpha, M) \\
& + 4 \left[\Delta C_{\ell_{\delta_{HA}}}(\delta_{FA}, \delta_{LEF}, \delta_{TEF}, \alpha, M) \right. \\
& \quad \left. - \Delta C_{\ell_{\delta_{FA}}}(\delta_{FA}, \delta_{LEF}, \delta_{TEF}, \alpha, M) \right] \left[\frac{\delta_{HA}}{\delta_{FA}} \right] + C_{\ell_p} \frac{pb}{2v_m} + C_{\ell_r} \frac{rb}{2v_m}
\end{aligned} \tag{A.2-16}$$

Note that the flaperon and differential tail deflections are slaved together such that

$$\delta_{HA} = \frac{\delta_{FA}}{4}$$

For numerical computation, the quantity $\frac{\delta_{HA}}{\delta_{FA}}$ is set equal to zero when $\delta_{FA} \leq .1$ deg.

The final computations necessary are the transformation of the force and moment equations, A.2-11 to A.2-16, in wind axes to a body axis set, and the addition of moments due to the C.G. to aerodynamic reference point moment arm. The final body axis forces and moments are

$$C_{\ell_{BODY}} = C_{\ell} \cos \alpha - C_n \sin \alpha - C_y v_{arm} \frac{\bar{c}}{b} \quad (A.2-17)$$

$$C_{m_{BODY}} = C_m + C_x v_{arm} - C_z CG_{mac} \quad (A.2-18)$$

$$C_{n_{BODY}} = C_{\ell} \sin \alpha + C_n \cos \alpha + C_y x_{arm} \quad (A.2-19)$$

$$C_x = C_{\ell} \sin \alpha - C_D \cos \beta \cos \alpha \quad (A.2-20)$$

$$C_y = C_y \quad (A.2-21)$$

$$C_z = -(C_{\ell} \cos \alpha + C_D \cos \beta \sin \alpha) \quad (A.2-22)$$

The nondimensional force and moment coefficients in Eqs. A.2-17 to A.2-22 are dimensionalized in accordance with

the definitions presented early in the equations of motion, Eqs. A.2-1 to A.2-4.

A feature of the modeling in AERODY which must be noted is that surface deflection dependent terms (e.g., $\Delta C_{m\delta H}$) can be computed as a function of either control augmentation commands or actuator output. This feature, which can be selected at any time and permits the inclusion or exclusion of actuator dynamics from the trajectory simulation and the eigenanalysis (to be described in Section A.3). Excluding the actuator dynamics reduces the number of states, hence simplifying the interpretation of eigenvalues and permitting the use of a larger integration step size. The larger permissible step size occurs because the actuators typically represent the highest-frequency dynamics in the system.

Module PROPUL: F-100 Engine Model - The F-100 engine model contained in module PROPUL is drawn directly from Ref. 78. Linear interpolation of five thrust tables which are functions of Mach number provide the total thrust computation. The variable time-constant lag model discussed in Ref. 78 is selectable from an input flag to the 6-DOF simulation. When this model is not selected, thrust response to throttle settings is instantaneous.

Figure A.2-4 depicts a brief flowchart of the F-100 model including critical computations. The variables in Fig. A.2-4 are defined in Table A.2-4. Note that computations of TMAX and TMIL which are functions of altitude (i.e., a different table is used for above and below 36,089 feet) are not included in Fig. A.2-4.

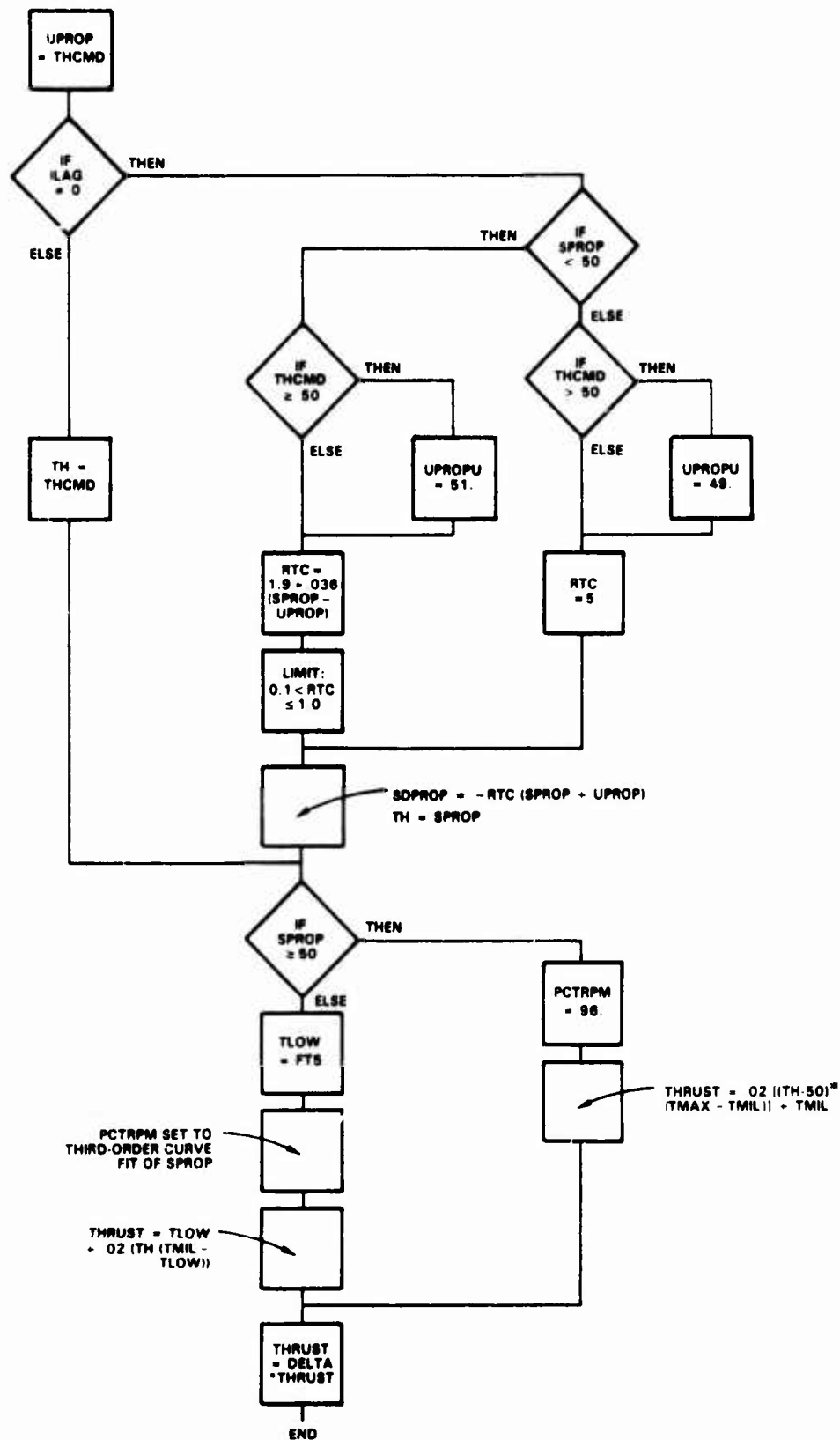


Figure A.2-4 F-100 Engine Model Flowchart and Computations

TABLE A.2-4
DEFINITIONS OF F-100 ENGINE MODEL VARIABLES

NAME	DESCRIPTION
DELTA	Ratio of altitude to sea level air pressure
FT5	Table of idle thrust at sea level versus Mach
ILAG	Dynamics flag: ILAG=1 enables first-order lag
PCTRPM	Percentage of full compressor rotational speed
RTC	Reciprocal of first-order lag time constant
SDPROP	Propulsion dynamic state derivative
SPROP	Propulsion dynamic state
THCMD	Thrust command (throttle setting 0 to 100)
THRUST	Engine thrust (pounds force)
TLOW	Interpolated value of idle thrust
TMAX	Thrust at full after-burner corrected for altitude
TMIL	Thrust at full military power corrected for altitude
UPROPU	Intermediate throttle setting variable

Module MASSPR: Mass Properties Model - The mass properties model in module MASSPR accounts for the mass, inertia, and center-of-gravity to aerodynamic reference point changes that occur as fuel is depleted within the aircraft. However, the propulsion model does not include mass flow rates as a function of throttle position or thrust. Consequently, the MASSPR module simply selects a set of mass, moment of inertia, cross product of inertia, and C.G. locations from a table as a function of a user supplied index. This procedure provides a

constant set of mass properties which do not change during a simulation trajectory.

One additional function of the mass properties module is to compute the inertia tensor and its inverse - for the AFTI/F-16 model the inertia tensor is

$$I_n = \begin{bmatrix} I_{xx} & 0 & -I_{zx} \\ 0 & I_{yy} & 0 \\ -I_{zx} & 0 & I_{zz} \end{bmatrix} \quad (A.2-23)$$

Note, computer variables and units for the mass properties module were previously listed in Table A.2-3.

Modules CAS and PILOT: Control Augmentation System and Pilot Models - The CAS and PILOT modules implement the final models necessary to simulate AFTI/F-16 large amplitude maneuvers. CAS implements a custom control augmentation system for stabilizing the aircraft longitudinal mode and to permit direct acceleration and roll attitude commands to the aircraft. Open-loop flap scheduling and programmed control surface deflections are also implemented within the CAS module. The PILOT module does not contain a pilot model; instead it contains guidance processing necessary to execute the desired large amplitude maneuvers.

A.3 STABILITY ANALYSIS ACROSS FLIGHT CONDITIONS

A particularly advantageous technique, which the state space implementation of the 6-DOF simulation affords, is the convenient linearization of the nonlinear equations. The

linear system matrix that can be derived from this linearization process readily provides the dynamic system eigenvalues (and therefore poles) via efficient eigenanalysis algorithms. With the availability of a convenient method for computing linear time-invariant characteristics of the aircraft system in a simulated trajectory, the simulation becomes an essential tool of the canonical systems, flying qualities analysis.

A.3.1 The Module PRTL

The computations necessary for linearizing the system equations are implemented in subroutine PRTL. Given the general nonlinear vector differential equation computed in the simulation,

$$\dot{\underline{x}} = \underline{f}(\underline{x}, \underline{u}, t) \quad (\text{A.3-1})$$

where

\underline{f} is a nonlinear vector function of time, \underline{x} the state vector, and \underline{u} the driving functions (controls)

PRTL computes the following linear vector matrix differential equation about a selected point in the aircraft trajectory,

$$\Delta \dot{\underline{x}} = \left. \frac{\partial \underline{f}}{\partial \underline{x}} \right|_{\underline{x}_0} \Delta \underline{x} + \left. \frac{\partial \underline{f}}{\partial \underline{u}} \right|_{\underline{u}_0} \Delta \underline{u} \quad (\text{A.3-2})$$

The partial derivative or Jacobian, $\frac{\partial \underline{f}}{\partial \underline{x}}$, can be represented by a matrix of constant coefficients for the time-invariant system. The subroutine PRTL computes the elements of the matrix, i.e.,

$\frac{\partial f_i}{\partial x_j}$ for i^{th} row, j^{th} column, with the central difference equation

$$\frac{\partial f_i}{\partial x_j} = \frac{f_i(x_{o_j} + \Delta x_j) - f_i(x_{o_j} - \Delta x_j)}{2\Delta x_j} \quad (\text{A.3-3})$$

where

x_{o_j} is the j^{th} state of the vector \underline{x} at the point x_{o_j} in the trajectory chosen for linearization

Δx_j is the perturbation value for the j^{th} state.

The second Jacobian in Eq. A.3-2, $\frac{\partial \underline{f}}{\partial \underline{u}}$ is also a matrix of constant coefficients which relates the external driving functions to the state derivative. The elements of the control effectiveness matrix are also computed with a central difference equation

$$\frac{\partial f_i}{\partial u_j} = \frac{f_i(u_{o_j} + \Delta u_j) - f_i(u_{o_j} - \Delta u_j)}{2\Delta u_j} \quad (\text{A.3-4})$$

where

u_{o_j} is the nominal control value of the j^{th} control at the time of interest

Δu_j is the perturbation applied to the j^{th} control.

Finally, the perturbation values, Δx_i and Δu_j are selectable on input; they must be judiciously selected so that the values truly represent small perturbations of the respective states or controls. For example, typical runs have control

perturbations of one degree of control surface deflection, translational velocity perturbations of 5 ft/sec, and Euler angle perturbations of 0.005 radians. Obviously these perturbations are units dependent and hence careful attention must be paid to their magnitudes. Furthermore, too small a perturbation will bury the changes in the state derivative, $\Delta \dot{x}$, below the least significant digit of the computer creating erroneous results.

A.3.2 The Module EIGEN

The subroutine EIGEN is the eigenanalysis executive routine. This routine performs the calls to PRTLTF and EIGRF. EIGRF is an International Mathematical and Statistical Library (IMSL) routine which actually extracts the eigenvalues from the system matrix computed in PRTLTF. Finally, upon return of the eigenvalues EIGEN computes the natural frequency and damping for each complex eigenvalue. A flow chart for this process is depicted in Figs. A.3-1 and A.3-2.

EIGRF performs its eigenanalysis by the QR algorithm. Essentially, this algorithm transforms the original input matrix to an upper triangular form. In an upper triangular matrix, the eigenvalues are equal to the diagonal elements of the matrix. These transformations are computed with additions and scalar multiplications of the rows of the system matrix and do not involve any powers of the coefficients, thereby avoiding the numerical difficulties inherent in raising numbers to a power. An excellent discussion of these algorithms can be found in Refs. 57-59.

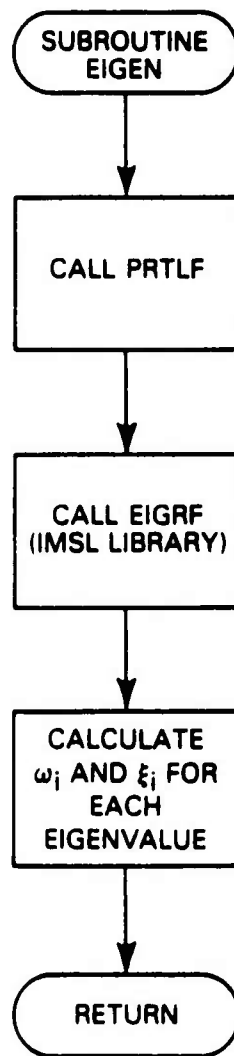


Figure A.3-1 Eigenanalysis Flow Chart: Part I
(Subroutine EIGEN)

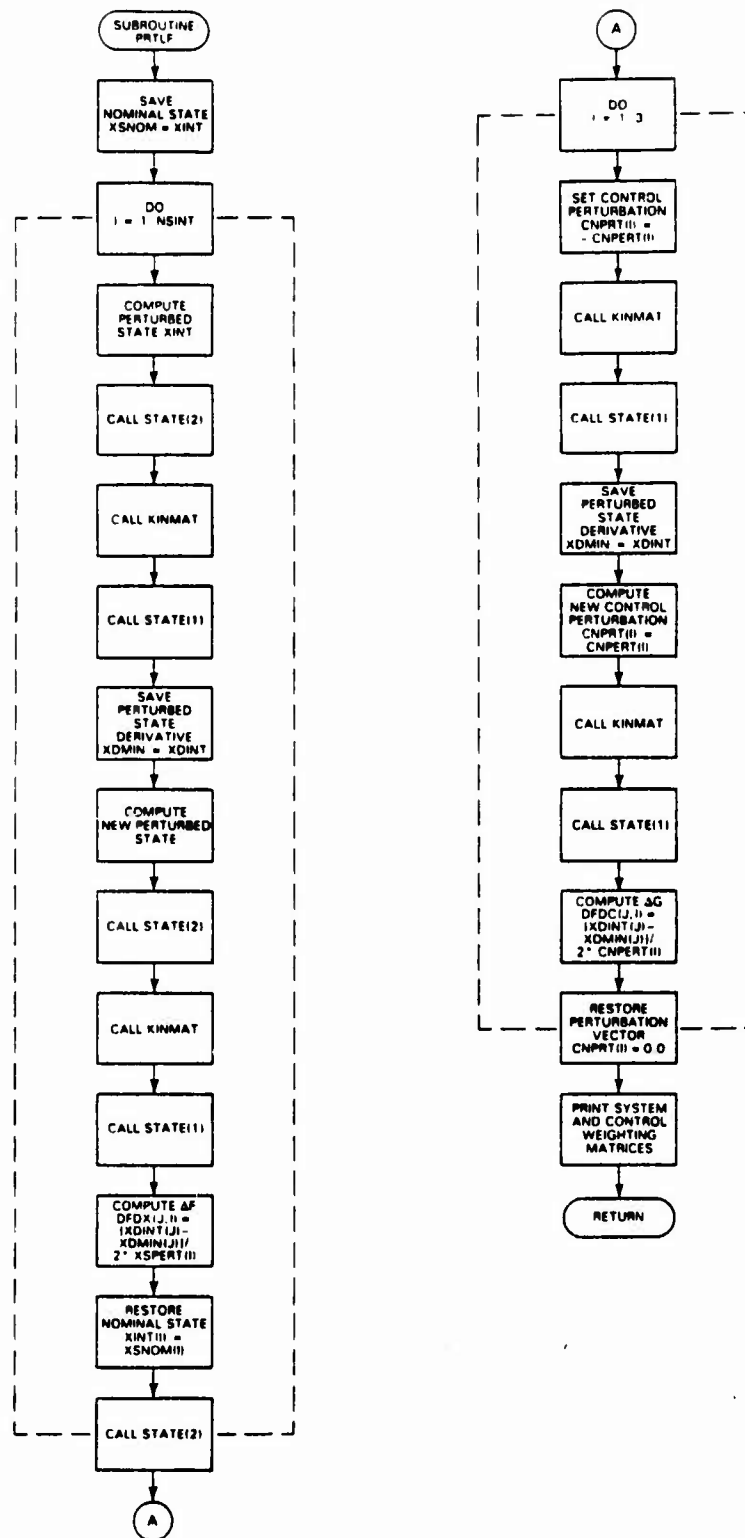


Figure A.3-2 Eigenanalysis Flow Chart: Part II
(Subroutine PRTLF)

APPENDIX B

CANONICAL SYSTEM EVALUATOR (CASE) SOFTWARE

The CASE software is a package of FORTRAN 77 procedures which solve the flying qualities evaluation methodology developed in the NFQ program. The software package, in addition to implementing a numerical solution of the methodology outlined in Section 3.4, integrates with the 6-DOF simulation software described in Appendix B and provides a simulation of the closest canonical system for verifying trajectory matches.

This appendix documents the software structure (calling sequence), numerical solution procedures, and general usage of the CASE software. The information provided herein constitutes a minimum level of documentation which can be used in executing, maintaining, and upgrading the software. However, this appendix is not intended as a comprehensive user's manual for the uninitiated user. Section B.1 describes the overall structure of and the modules which comprise the CASE software. Section B.2 documents the function of each primary module. Secondary modules, e.g., matrix multiply subroutine, are listed and described under auxiliary library procedures.

B.1 OVERALL PROGRAM STRUCTURE

The CASE software performs the functions necessary to numerically compute:

- The closest canonical system to a linearized state representation to the true aircraft dynamics, where a choice

of canonical system classes is available and the linearized system is provided by a numerical linearization within a 6-DOF simulation

- The relative controllability measure of the canonical system or the true linear time-varying system at selected points in an aircraft trajectory (including $[t_o, t_f]$)
- A linear time-varying simulation of the closest canonical system or the linearized true system over the reference trajectory through use of the true control surface deflections and initial state of the original 6-DOF simulation run.

The first two features are newly developed numerical solutions to the flying qualities methodology outlined in Section 3.4 (closest canonical system evaluation) and Section 4.3 (relative controllability theorem). The third feature of the CASE software is a numerical integration scheme employing a discrete representation of a linear time-varying system. The sampling interval is equivalent to the control surface deflection data intervals provided by the 6-DOF simulation. The three functions are interleaved, i.e., are performed independently to save execution-time memory requirements and simplify user control. The closest canonical system executes in the procedure EQUIVD. The linear simulation and relative controllability computation occur in the procedure LSIM.

Figure B.1-1 depicts the overall calling sequence of the primary procedures in the CASE software. Note the independent sequences for the EQUIVD and LSIM procedures. Although executed separately, LSIM requires a file of closest canonic system matrices generated by EQUIVD. Each of the modules depicted in Fig. B.1-1 will be separately described in subsequent sections.

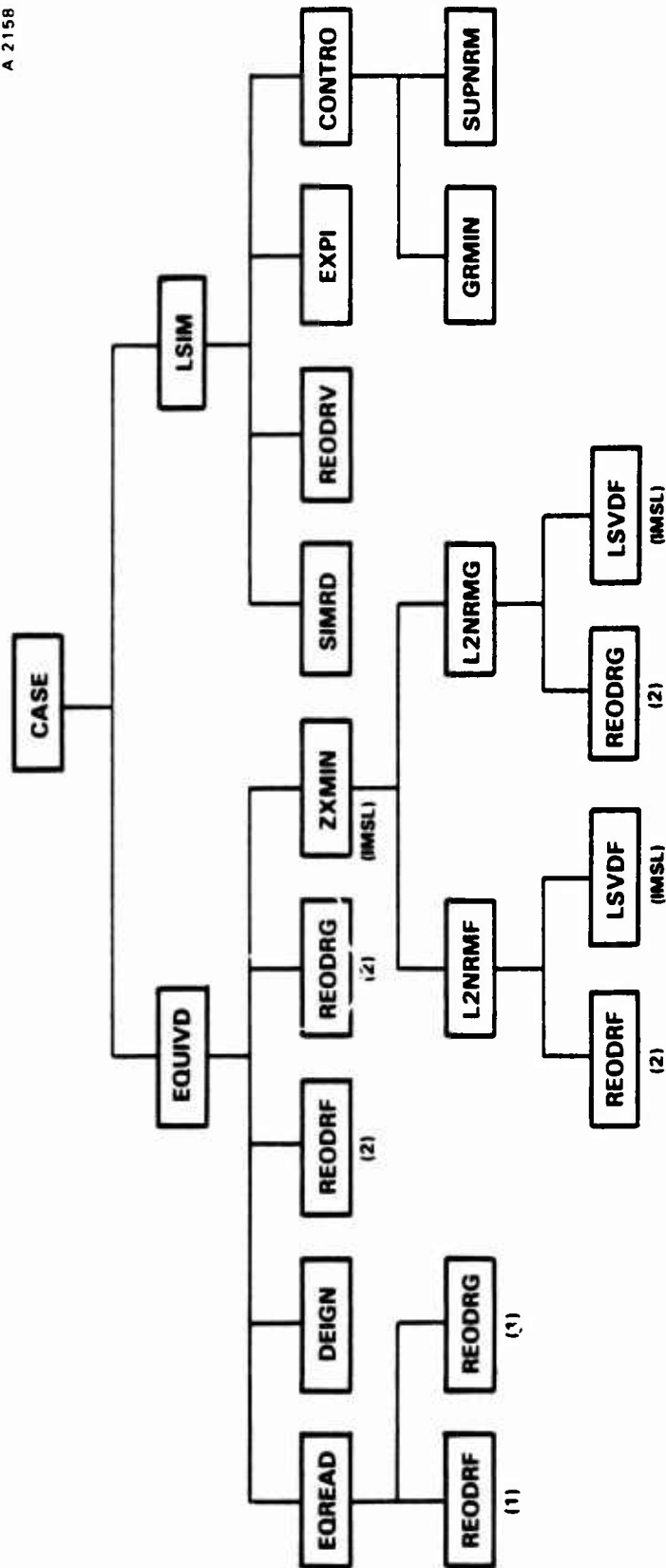


**Figure B.1-1 Canonical System Evaluator (CASE)
Software Structure**

B.2 MODULE DESCRIPTION: CLOSEST CANONICAL SYSTEM COMPUTATION

The following module descriptions include documentation of the equations to be solved, logical flow, and interface with other modules. Details of the subroutine arguments, array dimensions, or data types will not be presented in this appendix.

B.2.1 Module CASE

CASE is an executive routine that transfers execution to either the EQUIVD or LSIM procedures, no significant operations occur in this module. Current implementations of the CASE software permit direct entry into the EQUIVD and LSIM procedures, i.e., the CASE module is not executed. When used, CASE does rewind files that EQUIVD has used, e.g., the closest canonical system matrix file, prior to further use by the LSIM procedure.

B.2.2 Module EQUIVD

The module EQUIVD is the principal procedure for execution of the canonical system matching algorithm. This module organizes calls to the various modules which perform the reading and writing of user variables and true aircraft linearized dynamics, minimization of the L_2 norm of the difference between the true and canonical system matrices, and computation of the true and linearized dynamic system matrix eigenvalues. The procedure calls a minimization routine for separate evaluation of the closest canonical dynamics and control effectiveness matrices. Upon completion of each pair of optimizations, the final canonical system matrices are written to another file for subsequent use by LSIM. The procedure continues to loop through

pairs of canonical system matches until the end of file is encountered on the linearized system file created by the 6-DOF simulation. The loop is halted when the module EQREAD encounters an end-of-file condition.

B.2.3 Module EQREAD

The module EQREAD is used to read the file of linearized system dynamics created by the 6-DOF simulation and the user input parameters. The linearized system dynamics file contains data representing the state dimension NX , the control dimension NC , the linearization time, the $NX \times NX$ dynamics matrix, and the $NX \times NC$ control effectiveness matrix. The user input parameters include:

- ICLASS; the canonic system class to be used in a particular run, e.g., diagonal, longitudinal-lateral, etc
- NSIG; the number of significant digits desired in the final minimization of the difference between the true and canonic system, i.e., a closest canonical system has been obtained when the next step of the iterative minimization produces parameter values which agree to NSIG digits with values from the previous iteration
- MAXFN; the maximum number of function evaluations to be performed during minimization of the canonic-to-true system L_2 norm, this parameter is used to control overall execution time, 500 is adequate for obtaining a reasonable match
- IOPT; is a parameter that controls the initialization of the Hessian matrix (matrix of second partial derivatives) in the parameter optimization module ZXMIN. Additional details concerning the function of IOPT are in the ZXMIN module description

- IPRINT; an integer array of length five, the elements of which act as print control flags in the subroutines of the EQUIVD program, setting all members of IPRINT to one, provides full printing of intermediate variables for diagnostic purposes
- IORDER; an array of length NX which specifies the mapping of original state variable ordering in the 6-DOF simulation to a new state variable ordering consistent with the ICLASS specification; further details are in the descriptions of the REODRF and REODRG modules.

Although, each of the parameters has a default value, careful selection of the MAXFN, NSIG, ICLASS, and IORDER parameters is required if EQUIVD is to generate meaningful results. Furthermore, validity checks on each of the aforementioned parameters is minimal, and great care must be exercised when IORDER is specified (each ICLASS has an associated IORDER vector which is satisfactory for most cases).

B.2.4 Modules REODRF and REODRG

The modules REODRF and REODRG execute two essential functions of the canonical system matching procedure,

- The reordering of the state and control vectors from the 6-DOF simulation ordering to the ordering implicit in the canonical system class definitions
- Assignment of the canonical system class free parameters to the appropriate positions within the F and G matrices.

REODRF and REODRG perform the aforementioned function for the F and G system matrices respectively. Reordering of the state vector simply involves pre- and post-multiplying by

a matrix which contains all the locations necessary to interchange columns and rows. For example, the state vector $[x_1 \ x_2 \ x_3]$ is to be changed to the vector $[x_2 \ x_1 \ x_3]$, hence the transformation matrix is

$$T_x = \begin{bmatrix} 0 & 1 & 0 \\ 1 & 0 & 0 \\ 0 & 0 & 1 \end{bmatrix} \quad (\text{B.2-1})$$

an appropriate dynamics matrix would then be transformed as

$$F_{\text{new}} = T_x^T F_{\text{old}} T_x \quad (\text{B.2-2})$$

similarly the control effectiveness matrix is transformed with a pre- and post-multiplying where the post multiplying matrix is a $NC. \times NC.$ matrix for the control vector reordering, viz,

$$G_{\text{new}} = T_x^T G_{\text{old}} T_u \quad (\text{B.2-3})$$

The second function performed by REODRF and REODRG is the assignment of the parameter vector (of the minimization) to the appropriate matrix positions. Hence, if the canonic system is

$$F_c = \begin{bmatrix} f_1 & 0 & 0 \\ 0 & f_2 & 0 \\ 0 & 0 & f_3 \end{bmatrix} \quad (\text{B.2-4})$$

then the parameter vector

$$p = \begin{bmatrix} f_1 \\ f_2 \\ f_3 \end{bmatrix} \quad (\text{B.2-5})$$

must be reassigned to the canonical matrix at each iteration of p , i.e.,

$$F_c(1,1) = p(1) \quad (\text{B.2-6})$$

$$F_c(2,2) = p(2) \quad (\text{B.2-7})$$

$$F_c(3,3) = p(3) \quad (\text{B.2-8})$$

Forming F_c during each iteration of the minimization permits the computation of the matrix L_2 norm (maximum singular value) of the canonical system match ($F_{\text{true}} - F_c$).

B.2.5 Module DEIGN

Module DEIGN is used to compute the eigenvalues of the true and final canonical system dynamics matrix. Although not an essential part of the canonical system matching procedure, the eigenanalysis is useful when comparing the true and final canonical system matrices. The eigenanalysis is also used to verify that reordering was done properly, i.e., the eigenvalues for each dynamic system matrix read in by the CASE software must match the eigenvalues printed during the 6-DOF simulation run.

B.2.6 Module ZXMIN

Module ZXMIN performs the minimization of a cost function (in this case the L_2 norm of the difference between the true and canonical systems) with respect to a parameter vector without explicit calculation of the gradient of the cost with respect to the parameters. This subroutine is supplied through the International Mathematical and Statistical Library, detailed information can be found in Ref. 60.

The algorithm implemented in ZXMIN is a quasi-Newton method developed by R. Fletcher and documented in Ref. 61. Although it does not require a gradient calculation, ZXMIN does assume that the gradient $(\frac{\partial f}{\partial x_1} \dots \frac{\partial f}{\partial x_n})$ and the Hessian $(\frac{\partial^2 f}{\partial x_i \partial x_j})$ exist. The estimated gradient and Hessian for the function at the final parameter values are supplied by the subroutine upon completion. The gradient estimates are printed by the main routine EQUIVD.

B.2.7 Modules L2NRMF and L2NRMG

The modules L2NRMF and L2NRMG as their names imply, evaluate the L_2 norms of $F-F_c$ and $G-G_c$ respectively. Where F_c and G_c represent the canonical system matrices and F and G represent the true, linearized dynamics matrices. These subroutines are supplied as external functions to the minimization subroutine ZXMIN, which in turn calls L2NRMF or L2NRMG to evaluate the L_2 norm, which is the function to be minimized at each iteration of the minimization procedure.

Both modules contain a concise formulation for computing the L_2 norm. The first step requires that the minimization parameters be reassigned to the appropriate elements of F_c or G_c through a call to REODRF or REODRG. The result of $F-F_c$ or $G-G_c$ is then supplied to a singular value decomposition routine, LSVDF, which computes the m or n (minimum dimension) singular values. The routine then selects the maximum singular value which is the L_2 norm of the matrix difference, $F-F_c$ or $G-G_c$.

B.2.8 Module LSVDF

The module LSVDF performs the Singular Value Decomposition (SVD) of a $m \times n$ matrix, A . The SVD of a n -dimensional matrix A is defined as

$$A = U S V^T \quad (\text{B.2-9})$$

where U is a $m \times m$ unitary matrix, V is a $n \times n$ unitary matrix, and S is a quasi-diagonal real matrix of the form

$$S = \begin{bmatrix} s_1 & & 0 \\ & s_2 & \\ 0 & & s_n \\ - & - & - & - \\ & & 0 \end{bmatrix} \quad (\text{B.2-10})$$

when $m > n$ or

$$S = \begin{bmatrix} s_1 & & 0 & | & \\ & s_2 & & | & 0 \\ 0 & & s_m & | & \\ & & & | & \end{bmatrix} \quad (\text{B.2-11})$$

when $m < n$ or diagonal when $m = n$. The s_i are the singular values of the matrix A . LSVDF arranges them in descending magnitude such that s_1 is the maximum singular value. As in the case of ZXMIN, LSVDF is supplied through the IMSL, hence, further information regarding operation of subroutine and additional references on the singular value decomposition can be found in Ref. 60.

B.3 MODULE DESCRIPTIONS: RELATIVE CONTROLLABILITY AND LINEAR SIMULATION COMPUTATION

The following descriptions include the module LSIM and all subroutines called by LSIM. As in Section B.2, details concerning the subroutine arguments, array dimensions, or data types will not be presented.

B.3.1 Module LSIM

Module LSIM is the central procedure for performing the linear simulation and computation of the relative controllability index. The majority of computations necessary for the linear simulation occur in LSIM, relative controllability computations occur in a call to the module CONTRO. LSIM requires the definition of five files for input/output and storage of intermediate results. The file variable name, logical file numbers, and descriptions are listed in Table B.3-1.

TABLE B.3-1
LSIM INPUT/OUTPUT AND INTERMEDIATE FILES

VARIABLE NAME	DEFAULT VALUE	DESCRIPTION
LFSIM	8	6-DOF simulation trajectory data file
LFEQ	9	Matched canonical systems file from EQUIVD
LFGM	19	Temporary file for control matrix Γ
LFPHI	20	Temporary file for transition matrix Φ
LFLSIM	17	Output file of the linear simulation trajectory

The computation of the linear canonical system uses a piecewise time-invariant approximation to the continuously time-varying dynamics of the aircraft in accordance with the definitions in Chapter 4, Subsection 4.3.3. The canonical F and G matrices computed in EQUIVD are read from file LFEQ. Two sets of control sequences and the initial state are read from the 6-DOF simulation trajectory file LFSIM, i.e., $\underline{u}(t_0)$, $\underline{u}(t_1)$, ..., $\underline{u}(t_n)$ and $\underline{x}(t_0)$. The next state, $\underline{x}(t_1)$ is computed by propagating the discrete equivalent of the continuous matrices F and G. The specific equations are

$$\underline{x}(t_1) = \Phi(t_1, t_0) \underline{x}(t_0) + \Gamma(t_1, t_0) \underline{u}(t_0) \quad (\text{B.3-1})$$

where

$$\Phi(t_1, t_0) = e^{F(t_1 - t_0)} \quad (\text{B.3-2})$$

$$\Gamma(t_1, t_0) = \int_{t_0}^{t_1} e^{F\tau} d\tau G \quad (\text{B.3-3})$$

Computation of the matrix exponential Eq. B.3-2 and the integral in Eq. B.3-3 occur in module EXPI.

The computation of the state vector in Eq. B.3-1 occurs for every subsequent interval (t_k, t_{k+1}) until t_{k+1} exceeds the time at which a new set of canonic matrices are available. Equations B.3-2 and B.3-3 are then recomputed to supply a new $\Phi(t_{k+1}, t_k)$ and $\Gamma(t_{k+1}, t_k)$. The previous Φ and Γ are stored in LFPHI and LFGM for subsequent use in the relative controllability computations. At each time the state vector $\underline{x}(t_k)$ is stored in the file LFLSIM for subsequent plotting.

B.3.2 Module SIMRD

Module SIMRD performs the function of reading the 6-DOF simulation trajectory data in the file LSIM. The routine extracts the state and control vectors and their time-tag from the ensemble of 6-DOF simulation data. When running on IBM computers, this routine also converts the simulation data from single to double precision.

B.3.3 Module REODRV

Module REODRV reorders the state and control vectors read from the 6-DOF simulation file to conform with the state and control ordering associated with the canonical matrices in the LFEQ file. The particular reordering is selected by the user when the ICLASS variable is specified. REODRV contains a table reordering specification and class designations identical to those in REODRF and REODRG.

B.3.4 Module EXPI

The module EXPI implements an optimized algorithm for computing the matrix exponential, i.e., the right hand side of Eq. B.3-2. Numerical computation of the transition matrix is accomplished by directly computing a fixed number of terms of the power series,

$$e^{F\Delta t} = \sum_{n=0}^{\infty} \frac{(F\Delta t)^n}{n!} \quad (\text{B.3-4})$$

The number of terms to be computed is dependent upon the relative magnitudes of the interval Δt , and the matrix F . In general, if $F\Delta t$ is large compared to the floating-point precision of the computer in use a great many terms will be required for an accurate solution. To avoid this costly matrix expansion over many terms, the EXPI algorithm divides the interval, Δt , into 2^j sub-intervals such that j is the smallest integer satisfying

$$\frac{\|F\Delta t\|}{2^j} \leq \text{Maxnorm} \quad (\text{B.3-5})$$

where $||F\Delta t||$ is the L_∞ norm, the maximum row sum of the product $F\Delta t$.

Upon computing the sub-interval constant j , the algorithm then proceeds to compute the transition matrix over the sub-interval

$$\Delta t_{\text{sub}} = \frac{\Delta t}{j} \quad (\text{B.3-6})$$

This sub-interval should be small enough so that only three terms of the power series expansion are required. The semi-group property of the transition matrix

$$\phi(t_3, t_1) = \phi(t_3, t_2) \phi(t_2, t_1) \quad (\text{B.3-7})$$

can be used to compute the transition matrix for the original interval, viz,

$$\phi(j\Delta t_{\text{sub}}) = \phi^j(\Delta t_{\text{sub}}) \quad (\text{B.3-8})$$

EXPI also computes the integral of the transition matrix over the total interval, i.e.,

$$\Gamma = \int_0^{\Delta t} e^{F\tau} d\tau \quad (\text{B.3-9})$$

The definition of the matrix exponential in Eq. B.3-4 can be used to rewrite Eq. B.3-9 as

$$\Gamma(T) = \sum_{N=0}^{\infty} \frac{F^N \Delta t^{N+1}}{(N+1)!} \quad (\text{B.3-10})$$

which reduces to

$$\Gamma(T) = \Delta t I + \sum_{N=2}^{\infty} \frac{F^{N-1} \Delta t^N}{N!} \quad (\text{B.3-11})$$

$$\Gamma(T) = \Delta t \left(I + \sum_{N=2}^{\infty} \frac{F^{N-1} \Delta t^{N-1}}{N!} \right) \quad (\text{B.2-12})$$

$$\Gamma(T) = \Delta t \left(I + \sum_{N=2}^{\infty} \frac{\beta^{N-1}}{N!} \right) \quad (\text{B.3-13})$$

where

$$\beta = \Delta t \cdot F \quad (\text{B.3-14})$$

Equation B.3-13 is computed by subdividing Δt into 2^j sub-intervals as was the case with the transition matrix, Eqs. B.3-5 and B.3-6. However, the Γ 's for each subinterval cannot be multiplied to yield

$$\Gamma = \frac{\Delta t}{2^j} e^{F \Delta t_{\text{sub}}} \quad (\text{B.3-15})$$

$$\Gamma = \int_0^{\Delta t/2^j} e^{F \tau} d\tau \quad (\text{B.3-16})$$

Thus

$$\Gamma = \left(\sum_{k=j}^0 \int_0^{\Delta t/2^k} e^{F \tau} d\tau \right) \left(e^{F \Delta t/2^{k+1}} \right) \quad (\text{B.3-17})$$

which follows from

$$\begin{aligned} \Gamma = \int_0^{\Delta t} e^{F\tau} d\tau &= \int_0^{\Delta t/2} e^{F\tau} d\tau \\ &+ e^{F\Delta t/2} \int_0^{\Delta t/2} e^{F\tau} d\tau \end{aligned} \quad (\text{B.3-18})$$

Equation B.3-17 is computed recursively to yield the appropriate matrix Γ over the complete interval.

B.3.5 Module CONTRO

The module CONTRO is the central procedure for computing the relative controllability index, i.e., Eq. 4.3-12. Separate procedures are called by CONTRO to compute various elements of that equation. Namely, the grammian, reachability condition number, intrinsic drift factor, and the L_∞ norm of the transition and control effectiveness matrices.* CONTRO also includes control logic to perform the relative controllability over a subinterval of the trajectory data available. For example, a user can specify the computation of the relative controllability at each interval for which a canonical system has been computed or a single relative controllability index for an entire trajectory, t_0 to t_f , may be chosen.

B.3.6 Module GRMIN

Module GRMIN is used to compute the Grammian, reachability condition number, and the intrinsic drift factor for a specified interval of the simulation trajectory. The data

*Each of these terms is defined in Chapter 4, Section 4.3.

necessary for these computations is obtained from the files LFPHI and LFGM the files which respectively store the transition and discrete control matrices. Selection of the interval is controlled by number of matrix pairs read from LFPHI and LFGM.

The equations which have been implemented in GRMIN have been described in Subsection 4.3.3. Recall from Section 4.3, that once computation of the transition matrix is obtained, the linear canonical system is assumed to be a discrete time-varying system. Thus, the intrinsic grammian and reachability grammian are computed as

$$W(k_{t_o}, k_{t_f}) = \sum_{\ell=k_{t_o}}^{k_{t_f}-1} \phi(k_{t_f}, \ell+1) \Gamma(\ell) \Gamma^T(\ell) \phi^T(k_{t_f}, \ell+1) \quad (B.3-19)$$

and

$$W_I(k_{t_o}, k_{t_f}) = \sum_{\ell=k_o}^{k_{t_f}-1} \phi(k_{t_f}, \ell+1) \phi^T(k_{t_f}, \ell+1) \quad (B.3-20)$$

The eigenanalysis module DEIGN, previously described in Subsection B.2.5, is then used to compute the minimum and maximum eigenvalues of $W(k_{t_o}, k_{t_f})$ and $W_I(k_{t_o}, k_{t_f})$ to yield λ_S and λ_L and hence, χ_R and μ .

B.3.7 Module SUPNRM

The module SUPNRM is used to compute the supremum L_2 norm of the collection of transition and discrete control matrices stored on the files LFPHI and LFGM. Thus, the supremum

norm over the interval (t_o, t_f) of Φ and Γ are computed in accordance with Eqs. 4.3-42 and 4.3-43. The L_2 norm required at each available value of Φ and Γ is computed with the singular value decomposition, where the L_2 norm of a matrix is equivalent to maximum singular value of that matrix. Module LSVDF, previously described in Subsection B.2.8, computes the maximum singular value of each Φ and Γ .

APPENDIX C

REVIEW OF UNDERLYING MATHEMATICAL CONCEPTS

The purpose of this appendix is to provide a review of the underlying mathematical concepts that are essential for an understanding of the canonical system norms and the relative controllability theorem presented in Chapter 2 and Section 4.3. The concepts that require review are:

- Induced matrix norms
- Controllability for linear time-varying systems and derivation of the Grammian.

Section C.1 discusses induced matrix norms and Section C.2 presents basic linear time-varying controllability definitions.

C.1 INDUCED NORMS

The purpose of this section is to review the basic tenets and use of norms and induced norms for measuring the size of vectors and of linear operators/mappings. It is best to begin with a discussion of norms and then proceed to a discussion of induced norms of linear maps. More detailed discussions of norms in general can be found in Ref. 36 (Chapter 2), an engineering text, and even more rigorous discussion can be found in mathematics texts, such as Ref. 77, 45, and 41 in order of increasing difficulty.

C.1.1 Definition of Norms

A norm is effectively a mapping from some vector space X to a scalar which is an element of R_+ . Hence the function $\eta : X \rightarrow R_+$ (read η is a function that maps X into R_+) is a norm if and only if

- a) $\underline{x} \in X$ and $\underline{x} \neq \underline{0}$ implies that $\eta(\underline{x}) > 0^*$
- b) $\eta(\alpha \underline{x}) = |\alpha| \eta(\underline{x})$ for only α which is equal to a real number and any \underline{x} which is contained in X
- c) $\eta(\underline{x} + \underline{y}) \leq \eta(\underline{x}) + \eta(\underline{y})$ for \underline{x} and \underline{y} contained in X (also known as the triangle inequality).

In general a linear vector space can have many possible norms. The combination of a linear space X and a valid norm on that space η are a pair (X, η) and is called a normed space.

Throughout this report a vector space that is repeatedly used for describing the aircraft dynamics as a function of time is the space R^n . R^n is a space of n dimension vectors that consist of real numbers. Mathematically one says that $\underline{x} \in R^n$ which means $\underline{x} = (x_1, x_2 \dots x_n)$ with $x_i \in R$ (x_i equal to a real number) for all i . The most general norms on R^n are

$$\|\underline{x}\|_1 \triangleq \sum_{i=1}^n |x_i| \quad (C.1-1)$$

$$\|\underline{x}\|_p \triangleq \left(\sum_{i=1}^n |x_i|^p \right)^{1/p} \quad 1 \leq p < \infty \quad (C.1-2)$$

*The zero vector is indicated by $\underline{0}$.

$$||\underline{x}||_{\infty} \triangleq \max_i |x_i| \quad (C.1-3)$$

When the parameter p in the norm defined in Eq. C.1-2 is set equal to 2, the traditional root sum of squares vector magnitude results which is known as the Euclidean norm of the vector \underline{x} .

The space X need not be just the space of n -tuples (vectors) but can also be a space of functions (scalar or vector-valued). Any space x that is a vector space (i.e., satisfies the axioms of a vector space) can have a norm defined on it. Hence consider a space X of functions f that map real numbers into real numbers and f is locally integrable, i.e.,

$$X = \{f : \mathbb{R} \rightarrow \mathbb{R} \mid f \text{ is locally integrable}\} \quad (C.1-4)$$

Then a general set of norms for this function space are

$$||x||_1 \triangleq \int |x(t)| dt \quad (C.1-5)$$

$$||x||_p \triangleq \left(\int |x(t)|^p dt \right)^{1/2} \quad 1 \leq p < \infty \quad (C.1-6)$$

$$||x||_{\infty} \triangleq \operatorname{ess\,sup}_{t \in \mathbb{R}} |x(t)|^* \quad (C.1-7)$$

where $x(t) \in X$.

Note that since X is a vector space $x(t)$ is any function that satisfies the following axioms of a vector space

*ess sup reads the essential supremum where supremum is the least upper bound.

$$x + y = y + x \quad (C.1-8)$$

$$(x+y) + z = x + (y+z) \quad (C.1-9)$$

$$\begin{array}{l} \text{There is a null vector } \phi \text{ in } X \\ \text{such that } x + \phi = x \text{ for all } x \text{ in } X \end{array} \quad (C.10)$$

$$\alpha(x+y) = \alpha x + \alpha y \quad (C.1-11)$$

$$(\alpha+\beta)x = \alpha x + \beta x \quad (C.1-12)$$

$$(\alpha\beta)x = \alpha(\beta x) \quad (C.1-13)$$

$$0x = \phi, \quad 1x = x \quad (C.1-14)$$

It is easy to demonstrate that the collection of all real-valued continuous functions on some interval $[a,b]$ contained in R_+ form a vector space.

The set of function space norms defined in Eqs. C.1-5 to C.1-7 are also known as L_1 , L_p and L_∞ norms of the L_1 , L_p , L_∞ spaces. The norm in Eq. C.1-6 is the L_2 norm of the L_2 space when p equals 2. The L_2 norm is the norm repeatedly used in the discussions of the canonical systems matching technique (Section 3.1.2) and the relative controllability theorem (Section 4.3).

An analogous set of norms to those just defined for vectors and functions can be defined for $n \times n$ matrices. Let the vector space L consist of the of all $n \times n$ matrices with real number elements, $X = R^{n \times n}$. Then the following are norms on $R^{n \times n}$.

$$||A||_1 \triangleq \max_j \sum_{i=1}^n |a_{ij}| \quad (\text{column sums}) \quad (C.1-15)$$

$$||A||_2 \triangleq \max_i \left[\lambda_i(A^T A) \right]^{1/2} \quad (C.1-16)$$

$$||A||_\infty \triangleq \max_i \sum_{j=1}^n |a_{ij}| \text{ (row sums)} \quad (C.1-17)$$

where $\lambda_i(M)$ denotes the i -th eigenvalue of M . Equation C.1-16 is the Euclidean norm of a matrix and is equivalent to the maximum singular value of the matrix, hence the use of the singular value decomposition in the NFQ numerical procedures described in Section 4.3 and Appendix B.

C.1.2 Definition of Induced Norms

An induced norm describes a norm of a linear operator that is induced by the vector norm associated with the space from and to which the operator maps. For example an $n \times n$ matrix A can represent the linear mapping $A: \mathbb{R}^n \rightarrow \mathbb{R}^n$, hence given a vector $x \in \mathbb{R}^n$. The equation

$$y = Ax \quad (C.1-18)$$

maps x into y which is contained in \mathbb{R}^n .

A collection of all linear maps that map X into X will be represented by $\mathcal{L}(X, X)$. Let $||\cdot||$ be a norm on X and an operator $A \in \mathcal{L}(X, X)$. If we define a function $||\cdot||_i$ from a subset of $\mathcal{L}(X, X)$ into \mathbb{R}_+ , positive real scalars, by

$$||A||_i \triangleq \sup_{x \neq \phi} \frac{||Ax||}{||x||} \quad (C.1-19)$$

Then $||A||_i$ is called the induced norm of the map A or the norm of an operator induced by the vector norm $||\cdot||$.

If we consider the vector equation in Eq. C.1-18 the induced norm on the matrix A (which is a linear operator) is defined as

$$||A||_i = \max_{||\underline{x}|| \neq 0} \frac{||A\underline{x}||}{||\underline{x}||} \quad (C.1-20)$$

if this induced norm is with respect to the Euclidean vector norm, then

$$||A||_i = \max_{||\underline{x}||_2 \neq 0} \frac{||A\underline{x}||_2}{||\underline{x}||_2} \quad (C.1-21)$$

which can be proved to be

$$||A||_i = ||A||_2 \quad (C.1-22)$$

where the Euclidean norm of the matrix A was defined in Eq. C.1-16. Note if A maps a function x(t) into a function y(t), i.e.,

$$x(t) = Ay(t) \quad (C.1-23)$$

then the induced norm of the matrix is the L_2 norm and is defined by

$$||A||_{L_2} = \max_i \sqrt{\lambda_i(A^T A)} \quad (C.1-24)$$

where the operator A is a constant $n \times n$ matrix. The L_2 induced norm defined in Eq. C.1-24 is the induced used in calculating the relative controllability index as described in Section 4.3.

C.2 DEFINITION OF THE CONTROLLABILITY GRAMMIAN

The purpose of this section is to review the definition of controllability (reachability) and the derivation of the controllability Grammian for linear systems. Bear in mind that the generalization of the concepts described in this section to nonlinear systems is the objective of Section 4.2.1. The linear system controllability concepts, however, are heavily used in the derivation of the relative nonlinear controllability theorem presented in Section 4.3.

The derivation of the controllability Grammian begins with the definition of reachability. The definition that follows is a restatement of the linear system reachability definitions contained in Section 4.2.1. Given the n-dimensional linear system

$$\dot{\underline{x}}(t) = F(t) \underline{x}(t) + G(t) \underline{u}(t) \quad (C.2-1)$$

The system in Eq. C.2-1 is said to be completely reachable if the set of reachable states $\Omega(\underline{x}_0)$ equals the entire state space, i.e.,

$$\Omega(\underline{x}_0) = R^n \quad \forall \underline{x}_0 \quad (C.2-2)$$

where a reachable state, a state contained in the set $\Omega(\underline{x}_0)$, is any state for which there is an input $\underline{u}(t)$ that can drive the system from $\underline{x}_0(t)$ to $\underline{x}(t)$. Complete controllability is simply a specialization of reachability to include the zero vector in the set of reachable sets. Specifically, a system is completely controllable if and only if $\underline{x} = 0 \in \Omega(\underline{x}_0)$ for all \underline{x}_0 .

The distinction between controllability and reachability is important for discrete time systems where a system

may be reachable but not controllable or vice versa. However, as stated in Section 4.2.1, reachability and controllability are equivalent for continuous-time systems.

The controllability Grammian arises in an attempt to devise a test for complete reachability/complete controllability. Furthermore, there are familiar tests for controllability which do not involve the Grammian matrix introduced in Section 4.3. Take heed, however, that these other tests apply only to time-invariant systems. A quick review will clarify this point. Given the n -dimensional linear time-invariant system

$$\dot{\underline{x}}(t) = \underline{F}\underline{x} + \underline{G}\underline{u} \quad (\text{C.2-3})$$

where \underline{F} is an $n \times n$ constant matrix and \underline{G} is a $n \times m$ constant matrix. The system in Eq. C.2-3 is said to be completely controllable if the matrix

$$\underline{C} = [\underline{A} : \underline{A}\underline{b} : \dots : \underline{A}^{n-1}\underline{b}] \quad (\text{C.2-4})$$

is of rank n . If $m=1$, i.e., a single-input system then \underline{C} will be a square matrix, thus, the test requires that \underline{C} be non-singular, i.e., invertible. This test however, is only valid for constant \underline{F} and \underline{G} and is meaningless for a system in which either \underline{F} or \underline{G} is time-varying.

Derivation of a controllability test whether for time-invariant or time-varying systems, involves an inspection of the solution of the differential equations in time. A linear time-varying system of the form

$$\dot{\underline{x}}(t) = \underline{F}(t) \underline{x}(t) + \underline{G}(t) \underline{u}(t) \quad (\text{C.2-5})$$

has a solution described by the variation of constants formula (see Ref. 44)

$$\underline{x}(t) = \Phi(t_0, t) \underline{x}(t_0) + \int_{t_0}^t [\Phi(t_0, \tau) B(\tau) \underline{u}(\tau)] d\tau \quad (C.2-6)$$

where $\Phi(t_0, t)$ is the transition matrix for the system and is defined as

$$\Phi(t, t_0) = I + \int_{t_0}^t d\sigma_1 F(\sigma_1) + \int_{t_0}^t d\sigma_1 F(\sigma_1) \int_{t_0}^{\sigma_1} d\sigma_2 F(\sigma_2) + \dots \quad (C.2-7)$$

The expression for solution of the transition matrix is known as the Peano-Baker series. In general, it is difficult to compute the series in Eq. C.2-7 and thus, numerical integration of the differential equation is usually preferred. Equation C.2-7 does simplify if the dynamics matrix satisfies the condition

$$F(\tau) F(\sigma) = F(\sigma) F(\tau) \quad \forall \tau, \sigma \quad (C.2-8)$$

then the transition matrix becomes

$$\Phi(t, t_0) = e^{\int_{t_0}^t F(\sigma) d\sigma} \quad (C.2-9)$$

An examination of the controllability definition and the variation of constants formula Eq. C.2-6, reveals that a test for controllability, i.e., that a finite energy input $u(\cdot)$ can bring the state to zero a time t_f , requires a test

on the integral expression of Eq. C.2-6. Ultimately it will be shown that the system Eq. C.2-5 is completely controllable if and only if the rows of $\phi(t_0, \cdot) G(\cdot)$ are linearly independent on $[t_0, t_f]$. Although it will be rigorously demonstrated that the previous statement must be true, intuitively one can sense that if the product $\phi(t_0, \cdot) G(\cdot)$ does not contain n linearly independent rows, i.e., full rank, then the integral expression on the right hand side of Eq. C.2-6 does not affect all the states. In other words $u(\cdot)$ may not influence one or more states.

A general and well known test for linear independence of a set of functions $\{f_i(\cdot), i = 1, \dots, n\}$ is that their Grammian matrix

$$G = [G_{ij}] \quad (C.2-10)$$

$$G_{ij} = \int_{t_0}^{t_f} f_i(\tau) f_j(\tau) d\tau \quad (C.2-11)$$

be nonsingular. Consequently, if we apply the Grammian test to our controllability condition then the controllability Grammian becomes

$$W(t_0, t_f) = \int_{t_0}^{t_f} \phi(t_0, \tau) G(\tau) G^T(\tau) \phi^T(t_0, \tau) d\tau \quad (C.2-12)$$

and for the system in Eq. C.2-5 to be completely controllable it is necessary and sufficient that $W(t_0, t_f)$ be nonsingular. We will now demonstrate how the two conditions (1) $\phi(t_0, \cdot) G(\cdot)$ have n linear independent rows and (2) $W(t_0, t_f)$ nonsingular arise.

Recall that for complete controllability it is necessary that there exists a control $\underline{u}(\cdot)$ that for any condition drives the state to zero. Hence Eq. C.2-6 can be set to zero if

$$0 = \underline{x}(t_f) = \phi(t_f, t_0) \underline{x}(t_0) + \int_{t_0}^{t_f} \phi(t_f, \tau) G(\tau) \underline{u}(\tau) d\tau \quad (\text{C.2-13})$$

or

$$-\phi(t_f, t_0) \underline{x}(t_0) = \int_{t_0}^{t_f} \phi(t_f, \tau) G(\tau) \underline{u}(\tau) d\tau \quad (\text{C.2-14})$$

which can be rewritten as

$$-\underline{x}(t_0) = \int_{t_0}^{t_f} \phi(t_f, \tau) \phi^{-1}(t_f, t_0) G(\tau) \underline{u}(\tau) d\tau \quad (\text{C.2-15})$$

which becomes

$$-\underline{x}(t_0) = \int_{t_0}^{t_f} L(\tau) \underline{u}(\tau) d\tau \quad (\text{C.2-16})$$

where $L(\tau) = \phi(t_0, \tau) G(\tau)$ Eq. C.2-16 is the result of the following two properties of state transition matrices

$$\phi(t, t_0) = \phi^{-1}(t_0, t) \quad (\text{C.2-17})$$

$$\phi(t_1, t_2) = \phi(t_1, t_3) \phi(t_3, t_2) \quad (\text{C.2-18})$$

(Eq. C.2-18 is known as the semigroup property).

Equation C.2-16, an integral equation, must be solved for the unknown function $u(\cdot)$. If we approximate the integral in Eq. C.2-16 with a summation

$$-\underline{x}(t_0) = \sum_{i=1}^{N-1} L(\tau_i) \underline{u}(\tau_i) \Delta \quad (C.2-19)$$

where

$$\tau_i = t_0 + i\Delta \quad (C.2-20)$$

$$i = 0, \dots, N \quad (C.2-21)$$

$$N\Delta = t_f - t_0 \quad (C.2-22)$$

$$L(\tau_i) = \Phi(t_0, \tau_i) G(\tau_i) \quad (C.2-23)$$

then

$$-\underline{x}(t_0) = \mathcal{L} \mathcal{U} \quad (C.2-24)$$

where

$$\mathcal{U} = [u(\tau_0), \dots, u(\tau_{N-1})]^T \quad (C.2-25)$$

the collection of $u(\cdot)$ functions that satisfy Eq. C.2-16 and

$$\mathcal{L} = [L(\tau_0)\Delta \dots L(\tau_{N-1})\Delta] \quad (n \times n \text{ matrix}) \quad (C.2-26)$$

the collection of $L(\cdot)$ functions that satisfy Eq. C.2-16. Equation C.2-24 is a system of linear equations with more unknowns than equations, i.e., undetermined. However, it can be demonstrated that there can be a solution \mathcal{U} if and only if $-\underline{x}(t_0)$ is contained in the range space of \mathcal{L} , i.e., $-\underline{x}(t_0)$ is a linear combination of the columns of \mathcal{L} . Since $-\underline{x}(t_0)$ is a

n-dimensional vector then \mathcal{L} must have at least n linearly independent columns. Thus \mathcal{L} must be full rank or $L(\tau)$ must be full rank, i.e., have n linearly independent rows, which is condition (1) for controllability.

A particular solution of Eq. C.2-24 is

$$\underline{u}^* = -\mathcal{L}^{-1}(\mathcal{L}\mathcal{L}^T)^{-1} \underline{x}(t_0) \quad (C.2-27)$$

where invertibility of $\mathcal{L}\mathcal{L}^T$ can be verified using Sylvester's equality. Combining Eqs. C.2-19 and C.2-27 yields

$$\mathcal{L}\mathcal{L}^T = \sum_{i=0}^{N-1} L(\tau_i)L^T(\tau_i)\Delta^2 \quad (C.2-28)$$

$$= \Delta \sum_{i=0}^{N-1} \phi(t_0, \tau_i)G(\tau_i)G^T(\tau_i)\phi^T(t_0, \tau_i)\Delta \quad (C.2-29)$$

and thus

$$u_*(\tau_i) = -G^T(\tau_i)\phi^T(t_0, \tau_i)\Delta(\mathcal{L}\mathcal{L}^T)^{-1} \underline{x}(t_0) \quad (C.2-30)$$

which becomes

$$u_*(\tau_i) = -G^T(\tau_i)\phi^T(t_0, \tau_i) \left[\sum_{i=0}^{N-1} \phi(t_0, \tau_i)G(\tau_i)G^T(\tau_i)\phi^T(t_0, \tau_i)\Delta \right]^{-1} \quad (C.2-31)$$

Consequently, if limits are applied to Eq. C.2-31, it approaches the continuous equation, with the components in brackets becoming the Grammian integral. The limits to be applied are

$$\begin{aligned}
\Delta &\rightarrow 0 \\
N &\rightarrow \infty \\
N\Delta &= t_f - t_o
\end{aligned}
\tag{C.2-32}$$

and

$$\tau_i = \tau \tag{C.2-33}$$

which yields

$$u_*(\tau) = -G^T(\tau)\phi^T(t_o, \tau)W^{-1}(t_o, t_f)\underline{x}(t_o) \tag{C.2-34}$$

Equation C.2-34 is a general equation for finding a control $u(\cdot)$ that drives the system to $\underline{x}(t_f) = \underline{0}$ from any $\underline{x}(t_o)$. Hence, if such a $u(\cdot)$ exists, i.e., the system is completely controllable, then Eq. C.2-34 must apply which requires a non-singular controllability Grammian.

REFERENCES

1. Gentry, T.A., "Guidance for the use of Equivalent Systems with MIL-F-8785C", 1982 AIAA Atmospheric Flight Mechanics Conference (San Diego), Paper No. 82-1355.
2. Moorhouse, D.J., "The History and Future of U.S. Military Flying Qualities Specifications," AIAA 17th Aerospace Sciences Meeting (New Orleans), Paper No. 79-0402.
3. Bischoff, D.E., "The Definition of Short-Period Flying Qualities Characteristics via Equivalent Systems," AIAA Journal of Aircraft, Vol. 20, No. 6, June 1983.
4. Fuller, S.G., and Moorhouse, J.D., "Perspectives of the Flying Qualities Specification," 1982 AIAA Atmospheric Flight Mechanics Conference (San Diego), Paper No. 82-1354.
5. Hodgkinson, J., Wood, J.R., and Hoh, R.H., "An Alternate Method of Specifying Bandwidth for Flying Qualities," 1982 AIAA Guidance and Control Conference (San Diego), Paper No. 82-1609.
6. Bischoff, D.E., and Palmer, R.E., "Investigation of Low Order Lateral Directional Transfer Function Models for Augmented Aircraft," 1982 AIAA Guidance and Control Conference (San Diego), Paper No. 82-1610.
7. Hodgkinson, J., and LaManna, W.J., "Equivalent System Approaches to Handling Qualities Analysis and Design Problems," 1977 AIAA Guidance and Control Conference (Hollywood, FL), Paper No. 77-1122 (Also MCAIR-77-016).
8. Hodgkinson, J., Berger, R.L., and Bear, R.C., "Analysis of High Order Aircraft/Flight Control System Dynamics Using an Equivalent System Approach," MCAIR 76-009 Presented as Seventh Annual Pittsburgh Conference on Modeling and Simulation, April 1976.
9. Hodgkinson, J., LaManna, W.J., and Heyde, J.L., "Handling Qualities of Aircraft with Stability and Control Augmentation Systems - A Fundamental Approach," The Aeronautical Journal, February 1976.

REFERENCES (Continued)

10. Hoh, R.H., et al., "Development of Handling Quality Criteria for Aircraft with Independent Control of Six Degrees-of-Freedom," AFWAL-TR-81-3027, April 1981.
11. Black, G.T., and Moorhouse, D.J., "Flying Qualities Design Requirements for Sidestick Controllers," Air Force Flight Dynamics Laboratory, Report No. AFFDL-TR-79-3126.
12. Stapleford, R.L., et al., "Analysis of Several Handling Quality Topics Pertinent to Advanced Manned Aircraft," Air Force Flight Dynamics Laboratory, Report No. AFFDL-TR-67-2.
13. Desoer, C.A., and Vidyasagar, M., Feedback Systems: Input-Output Properties, Academic Press, New York, 1975.
14. Luenberger, D.G., Optimization by Vector Space Methods, Wiley, New York, 1969.
15. Brockett, R.W., Finite Dimensional Linear Systems, Wiley, New York, 1970.
16. Mees, A.I., Dynamics of Feedback Systems, Wiley, 1981.
17. Holtzman, J.M., Nonlinear System Theory: A Functional Analysis Approach, Prentice-Hall, 1970.
18. Rugh, W.J., Nonlinear System Theory: The Volterra/Wiener Approach, Johns Hopkins Univ. Press, Baltimore, 1981.
19. Casti, J.L., "Recent Developments and Future Perspectives in Nonlinear System Theory," SIAM Review, Vol. 24, No. 2, July 1982, pp. 301-331.
20. Crouch, P.E., "Geometric Structures in Systems Theory," IEE Proceedings, Vol. 128, pt. D, No. 5, September 1981, pp. 242-252.
21. Thom, R., "System's Versus Morphological Approach in General System Theory,"
22. Dacka, C., "On the Controllability of a Class of Nonlinear Systems," IEEE Trans. Aut. Contr., AC-25, No. 2, April 1980, pp. 263-266.

REFERENCES (Continued)

23. Vidyasagar, M., "A Controllability Condition for Non-linear Systems," IEEE Trans. Aut. Contr. AC-17, No. 4, August 1972, pp. 569-570.
24. Mirza, K., and Womack, B.F., "On the Controllability of a Class of Nonlinear Systems," IEEE Trans. Aut. Contr., Vol. AC-17, No. 4, August 1972, pp. 531-535.
25. Sastry, S.S., and Desoer, C.A., "The Robustness or Controllability and Observability of Linear Time-Varying Systems," IEEE Trans. Aut. Contr., Vol. AC-27, No. 4, August 1982, pp. 933-939.
26. Sastry, S.S., and Desoer, C.A., "The Robustness of Controllability and Observability of Linear Time-Varying Systems with Applications to the Emergency Control of Power Systems," Univ. California, Berkeley, ERL Memo M79/74, October 1979.
27. Hermann, R., and Krener, A.J., "Nonlinear Controllability and Observability," IEEE Trans. Aut. Contr., Vol. AC-22, No. 2, October 1977.
28. Van Der Schaft, A.J., "Observability and Controllability for Smooth Nonlinear Systems," SIAM Journal of Control and Optimizaiton, Vol. 20, No. 3, May 1982, pp. 338-353.
29. Hunt, L.R., "Sufficient Conditions for Controllability," IEEE Trans. on Circuits and Systems, Vol. CAS-29, No. 5, May 1982, pp. 285-288.
30. Nijmeijer, H., "Controllability Distributions for Non-linear Control Systems," Systems and Control Letters, Vol. 2, No. 2, August 1982, pp. 122-129.
31. Sussmann and Jurdjevic, V., "Controllability of Nonlinear Systems," Journal of Differential Equations, Vol. 12 (1972), pp. 95-116.
32. Gauthier, J.P., and Barnard, G., "An Openess Condition for the Controllability of Nonlinear Systems," SIAM Journal of Control and Optimization, Vol. 20, No. 6, November 1982, pp. 808-814.
33. Sandberg, I.W., "Expansions for Nonlinear Systems," The Bell System Technical Journal, Vol. 61, No. 2, February 1982.

REFERENCES (Continued)

34. Sandberg, I.W., "Volterra Expansions for Time-Varying Nonlinear Systems," The Bell System Technical Journal, Vol. 61, No. 2, February 1982.
35. Sandberg, I.W., "Series Expansions for Nonlinear Systems," CH1681-6/82/0000-0110, 1982, IEEE.
36. Brockett, R.W., "Volterra Series and Geometric Control Theory," Automatica, Vol. 12, pp. 167-176.
37. Crouch, P.E., "Dynamical Realizations of Finite Volterra Series," SIAM J. Control and Optimization, Vol. 19, No. 2, March 1981, pp. 177-203.
38. Lawrence, P.J., "Estimation of the Volterra Functional Series of a Nonlinear System Using Frequency-Response Data," IEE Proceedings, Vol. 128, Part D, No. 5, September 1981.
39. Sandberg, I.W., "On Volterra Expansions for Time-Varying Nonlinear Systems," IEEE Trans. on Circuits and Systems, Vol. CAS-30, No. 2, February 1983, pp. 61-67.
40. Sandberg, I.W., "Volterra-like Expansions for Solutions of Nonlinear Integral Equations and Nonlinear Differential Equations," IEEE Transactions on Circuits and Systems, Vol. CAS-30, No. 2, February 1983, pp. 68-77.
41. Harper, T.R., and Rugh, W.J., "Structural Features of Factorable Volterra Systems," IEEE Trans. on Automatic Control, Vol. AC-21, No. 6, December 1976, pp. 822-832.
42. Lomnabbi, M., "A New Symbolic Calculus for the Response of Nonlinear Systems," Systems and Control Letters, Vol. 2, No. 3, October 1982, pp. 154-162.
43. Porter, W.A., "An Overview of Polynomic System Theory," IEEE Proceedings, Vol. 64, No. 1, January 1976, pp. 18-23.
44. Shamaly, A., Chistensen, G.S., and El-Hawory, M.E., "Functional Optimization of Systems with Polynomial Nonlinearities," Proceedings 20th Midwest Symposium on Circuits and Systems, August 1977, pp. 794-803.
45. Shamaly, A., Christensen, G.S., and El-Hawory, M.E., "A Transformation for Necessary Optimality Conditions for Systems with Polynomial Nonlinearities," IEEE Trans. on Aut. Contr., Vol. AC-24, No. 6, December 1976, pp. 983-985.

REFERENCES (Continued)

46. Crouch, P.E., "Polynomic Systems Theory: A Review," IEE Proceedings, Vol. 127, Pt. D, No. 5, September 1980, pp. 220-228.
47. Barrelet, J.F., "Banach-Space Theory of Analytic Systems," IEE Proceedings, Vol. 128, Pt. D, No. 5, September 1981, pp. 188-194.
48. Monoco, S., and Normond-Cyrot, D., "On the Immersion of a Discrete-Time Polynomial Analytic System into a Polynomial Affine One," Systems and Control Letters, Vol. 3, No. 2, July 1983, pp. 83-90.
49. Bruni, C., DiPillo, G, and Koch, G., "Bilinear Systems: An Appealing Class of 'Nearly Linear' Systems in Theory and Applications," IEEE Transactions on Automatic Control, Vol. AC-19, No. 4, August 1974, pp. 334-348.
50. Isidori, A., Krener, A.J., Gori-Giorgi, C., and Monoco, S., "Nonlinear Decoupling Via Feedback: A Differential Geometric Approach," IEEE Trans. Aut. Contr., Vol. AC-26, No. 2, April 1981, pp. 331-
51. Singh, S.N., "Generalized Decoupled-Control Synthesis for Invertible Nonlinear Systems," IEE Proceedings, Vol. 128, Pt. D, No. 4, July 1981.
52. Nijmeijer, H., and Van Der Schaft, A., "Controlled Invariance by Static Output Feedback for Nonlinear Systems," Systems and Control Letters, Vol. 2, No. 1, July 1982, pp. 39-47.
53. Isidori, A., and Krener, A.J., "On Feedback Equivalence of Nonlinear Systems," Systems and Control Letters, Vol. 2, No. 2, August 1982, pp. 119-121.
54. Nijmeijer, H., "Invertibility of Affine Nonlinear Control Systems: A Geometric Approach," Systems and Control Letters, Vol. 2, No. 3, October 1982, pp. 163-168.
55. Rudin, W., Real and Complex Analysis, McGraw-Hill, 1966.
56. Singer, I.M., and Thorpe, J.A., Lecture Notes on Elementary Topology and Geometry, Springer-Verlag, 1967.
57. Brockett, R.W., "Lie Theory and Control Systems Defined on Spheres," SIAM Journal of Applied Mathematics, September 1973.

REFERENCES (Continued)

58. Krall, A.M., Linear Methods of Applied Analysis, Addison-Wesley, 1973.
59. Baillieul, J., "Geometric Methods for Nonlinear Optimal Control Problems," Journal of Optimization Theory and Applications, Vol. 25, 1978, pp. 519-548.
60. Baillieul, J., "Controllability and Observability of Polynomial Dynamical Systems," Nonlinear Analysis: Theory, Methods, and Applications, Vol. 5, No. 5, pp. 543-552.
61. McFarlane, A.G.J., (Ed.), Frequency Response Methods in Control Systems, IEEE Press Selected Reprint Series, New York, 1979.
62. LaSalle, J., and Lefschetz, S., Stability by Lyapunov's Direct Method with Applications, Academic Press, 1961.
63. Bryson, A.E., and Ho, Y.C., Applied Optimal Control, Hemisphere, Washington, D.C., 1975.
64. Smart, D.R., Fixed Point Theorems, Cambridge University Press, 1976.
65. Granas, A., "The Theory of Compact Vector Fields and Some of its Applications," Rozprawy Matematyczne, Vol. 30, 1962.
66. Ralston, A., and Wilf, H.S., Mathematical Methods for Digital Computers, Wiley, New York, 1960, pp. 110-120.
67. Gill, S., "A Process for the Step-by-Step Integration of Differential Equations in an Automatic Digital Computing Machine," Proceedings Cambridge Philosophical Society, Vol. 47, 1951, pp. 96-108.
68. Etkin, B., Dynamics of Atmospheric Flight, Wiley, New York, 1972.
69. U.S. Standard Atmosphere, 1962, Bureau of Documents, Government Printing Office, Washington, D.C.
70. Smith, B.T., et al, Matrix Eigensystem Routines -- Eispack Guide, Springer Verlag, New York, 1974.

REFERENCES (Continued)

71. Peters, G., and Wilkinson, J.H., "Eigenvectors of Real Complex Matrices by LR and QR Triangularizations," Numerische Mathematik, Vol. 16, No. 3, 1970, pp. 181-204.
72. Jennings, A., Matrix Computation for Engineers and Scientists, Wiley, New York, 1977.
73. IMSL, International Mathematical and Statistical Library Users Manual, Edition 7, 1970 Revised.
74. Fletcher, R., "FORTRAN Subroutines for Minimization by Quasi-Newton Methods," Report R7125 AERE, Harwell, England, June 1972.
75. Stengel, R.F., "Equilibrium Response of Flight Control Systems," AUTOMATICA, Vol. 18, No. 3, May 1982.
76. Onstott, E.D., and Faulkner, W.H., "Discrete Maneuver Pilot Models for Flying Qualities Evaluation," AIAA Journal of Guidance and Control, Vol. 1, No. 2, March-April 1977.
77. Gelb, A. (editor), Applied Optimal Estimation, MIT Press, Cambridge, MA, 1974.
78. Floyd, R.M., "F-100 Engine Model," Memo for the Record, 24 July 1979.

GLOSSARY

G.1 GENERAL SYMBOLS

\triangleq	$A \triangleq B$	A is by definition B
\rightarrow	$a \rightarrow b$	as a approaches b
\downarrow	$a \downarrow b$	as a approaches b from above
\forall		for all; for every

G.2 SET NOTATION

\in	$a \in B$	a is an element of B; a belongs to B
\subseteq	$A \subseteq B$	A is a subset of B; A is contained in or equal to B
\subset	$A \subset B$	A is a proper subset of B; A is contained in but not equal to B
\cup	$A \cup B$	Union of Set A with Set B
\cap	$A \cap B$	Intersection of Set A and Set B
\Rightarrow	$p \Rightarrow q$	p implies q
\Leftarrow	$p \Leftarrow q$	q implies p
\Leftrightarrow	$p \Leftrightarrow q$	p implies and is implied by q; p if and only if q

G.3 LINEAR ALGEBRA

R	field of real numbers
R^n	vector space of dimension n
R_+	space of functions on the interval $[0, \infty]$

\underline{x}	x is a vector
$\underline{0}_n$	zero vector of dimension n
$ \underline{x} $	vector norm
$ A $	norm of matrix induced by associated vector norm
A^*	complex conjugate transpose of A
\underline{x}^T, A^T	transpose of \underline{x} and A
\sup	the supremum; the least upper bound
\inf	the infimum; the greatest lower bound
$\Omega(\underline{x}_0)$	set of states \underline{x} reachable from \underline{x}_0
$O_\varepsilon(\cdot)$	neighborhood of (\cdot) ; a number less than or equal to $\varepsilon \cdot $
C^∞	space of smooth complex functions; all derivatives of order 1 to ∞ exist
C^ω	space of analytic functions
$\underline{P}(\cdot)$ or $\underline{Q}(\cdot)$	vector polynomial function of (\cdot)
A_i	i th row of the matrix A
A_j	j th row of the matrix A